

# POLITECNICO DI TORINO

Master of Science in Automotive Engineering



Master Thesis Project

## Influence of cooled and uncooled EGR on performance and emissions of 3.0L PCCI diesel engine

### **Academic Supervisors**

Prof. Stefano D'Ambrosio

Ing. Roberto Finesso

### **Candidate**

Roberto Martinelli

Academic Year 2018-2019



# Abstract

This thesis work is the result of a 7 months engine testing and calibration activity performed at the ICEAL (Internal Combustion Engine Advanced Laboratory) inside the Energy Department (DENERG) of Politecnico di Torino. The experimental study was headed by ICE PhD students research team, with the supervision of Prof. Stefano D'Ambrosio, and it involved test bench investigation of an industrial diesel engine provided by FPT Industrial (F1C) with a modified design for PCCI (Premixed Charge Compression Ignition) advanced combustion mode. The aim of this activity is to gain insight on the influence of the utilization of cooled and uncooled EGR strategies on performance and pollutant emissions characteristics of the above-cited engine, with focus on the attainable benefits that hot EGR could produce on the common shortcomings of PCCI combustion.

The first chapter addresses conventional combustion in diesel engine, describing its peculiar features as well as the evolution of its conceptual combustion model conceived in recent times. Pollutant emissions formation mechanisms in CI (compression ignition) engines are presented in the second chapter, inside which diesel combustion noise is also introduced. The third chapter is devoted to the central theme of the thesis, i.e., EGR (Exhaust Gas Recirculation), which is typically defined as an engine in-cylinder emissions control technology implemented in diesel engines for nitrogen oxides abatement. The chapter goes through the definition of EGR working principles, its effect on other pollutant emissions, EGR system configurations and the need for EGR cooling, with focus on conventional diesel applications. Then, being this writings concentrated on premixed charge compression ignition (PCCI) combustion strategy, advanced diesel combustion or low temperature combustion (LTC) modes are described in chapter four. Among the various advanced combustion approaches, PCCI could be defined as an early injection low temperature combustion which is achieved by means of an advanced start of injection (SOI) and heavy EGR level, resulting in simultaneous low soot and low  $NO_x$  pollutant emissions level due to lengthening of the ignition delay and the decrease of in-cylinder peak temperature. Despite that, increase in CO and HC emissions as well as fuel consumption and combustion noise level are encountered, determining the necessity to mitigate such penalties. The testing campaign have been performed on AVL dynamic engine test bench situated inside Politecnico di Torino ICE advanced laboratory. The engine dyno was equipped with AVL AMAi60 emission analyzer for HC,CO, $CO_2$  and  $NO_x$  measurement, while fuel consumption and smoke emissions were collected with KMA 4000 and AVL 415S smokemeter, respectively, as described in chapter five.

The core of the activity regarded steady state testing on two engine key points: 1400x1.1 (rpm x bar) and 2000x2.3, calibrated in cooled EGR configuration during previous experimental studies. Hot EGR configuration was implemented by substituting the EGR cooled with an ad-hoc manufactured steel tube. Tests were executed on both engine EGR layouts by performing EGR quantity sweep varying exhaust back pressure flap opening with EGR valve set on wide-open position. Moreover, the engine was tested by implementing single and double stage injection strategies in either EGR configurations. Results are shown and discussed in terms of intake charge characteristics such as temperature, pressure and relative air fuel ratio, pollutant emissions levels, fuel consumption, combustion noise and DOC hydrocarbon conversion efficiency. From the analysis of the gathered data, hot EGR double injection approach emerged to improve HC and CO emissions in a more significant way with minor penalties in terms of noise and fuel consumption for engine working point 2000x2.3, whereas this was not the case for 1400x1.1. In addition to that, hot EGR proved to bring relevant benefits on DOC operation, leading for point 2000x2.3 to conversion efficiency of about 95% from the 20% value encountered for the cooled EGR case, regardless of the injection strategy. However, no such improvement on DOC conversion performance was seen for the other engine key point.

# Contents

<b>Introduction</b>	<b>1</b>
<b>1 Conventional combustion in CI engines</b>	<b>5</b>
1.1 Main features . . . . .	5
1.2 Combustion process stages . . . . .	7
1.3 Combustion conceptual model . . . . .	10
1.3.1 Old combustion model . . . . .	10
1.3.2 Dec's combustion model . . . . .	11
<b>2 Pollutant emissions in diesel engines</b>	<b>18</b>
2.1 Mechanisms of formation . . . . .	18
2.1.1 Nitrogen oxides . . . . .	20
2.1.2 Particulate matter . . . . .	23
2.1.3 Carbon monoxide . . . . .	28
2.1.4 Unburned hydrocarbons . . . . .	30
2.2 Diesel combustion noise . . . . .	33
<b>3 Exhaust gas recirculation</b>	<b>35</b>
3.1 Definition . . . . .	35
3.2 Working principles . . . . .	36
3.3 Effects on emissions and performance . . . . .	37
3.4 Calculation methods . . . . .	39
3.5 EGR configurations . . . . .	40
3.6 EGR cooling and EGR coolers . . . . .	43
<b>4 Advanced diesel combustion modes</b>	<b>45</b>
4.1 Generalities . . . . .	45
4.2 HCCI combustion . . . . .	47
4.3 Diesel LTC . . . . .	50
4.3.1 LTC strategies . . . . .	50
4.3.2 LTC conceptual model . . . . .	53

<b>5</b>	<b>Experimental set-up</b>	<b>59</b>
5.1	F1C PCCI engine . . . . .	59
5.1.1	Engine layout . . . . .	59
5.1.2	Engine instrumentation . . . . .	62
5.2	Test bench . . . . .	66
5.2.1	Monitoring and acquisition systems . . . . .	66
5.2.2	The dynamometer . . . . .	67
5.2.3	The cooling system . . . . .	68
5.2.4	Fuel consumption measuring system . . . . .	69
5.2.5	Emissions analyzer . . . . .	70
5.2.6	PM measurement . . . . .	73
<b>6</b>	<b>Cooled and uncooled EGR</b>	<b>76</b>
6.1	Generalities . . . . .	76
6.2	Methodology . . . . .	79
6.3	Results and discussions . . . . .	80
6.3.1	Intake charge analysis . . . . .	80
6.3.2	Performance and combustion features . . . . .	83
6.3.3	Engine-out emissions . . . . .	92
6.3.4	Trade-offs . . . . .	99
6.3.5	DOC conversion efficiency . . . . .	104
	<b>Conclusion</b>	<b>108</b>
	<b>Bibliography</b>	<b>110</b>

# List of Figures

1	EU emission standards limits for steady-state (a) and transient (b) engine test cycles for heavy-duty diesel engine applications. . . . .	2
2	Kamimoto-Bae diagram or $\phi - T$ (equivalence ratio - temperature) plot representing a fuel parcel path during conventional and advanced combustion processes [3]. . . . .	3
1.1	In-cylinder pressure trace for firing and motored engine, net heat release rate and the fuel mass fraction burned as a function of crank angle for DI supercharged diesel engine [6]. . . . .	7
1.2	Typical DI multispray diesel engine net heat release rate diagram [4]. . . . .	8
1.3	Schematic of the mid-plane of a combusting diesel jet representing the "old" view of diesel combustion, prior to laser-sheet imaging studies [10]. . . . .	11
1.4	Left: Optical-access diesel engine showing the laser sheet along the fuel jet axis. Right: Geometry and optical configuration of the combustion chamber from top and side view [10]. . . . .	12
1.5	Schematics displaying a temporal sequence of how DI diesel combustion develops from the start of injection until the early part of mixed controlled burn [15]. . . . .	15
1.6	Conceptual model of DI diesel combustion with further characteristics concerning pollutants distribution along the combustion plume prior the end of fuel injection [15]. . . . .	17
2.1	Schematic of pollutant formation during premixed and mixing-controlled combustion stages in DI diesel engine with swirl [5]. . . . .	20
2.2	Nitrogen dioxide share as a function of engine load and engine speed in diesel engine [4]. . . . .	22
2.3	Temperature and chemistry of a typical DI diesel engine's combustion plume [15]. . . . .	23
2.4	Relative $NO_x$ concentration throughout the combustion process [15]. . . . .	23
2.5	Components of diesel particulate matter: nucleation mode and accumulation mode particles [5]. . . . .	24
2.6	Normalized mass and number distribution of PM as a function of the aerodynamic diameter of the particles [17]. . . . .	25

2.7	Particle composition typical of heavy-duty diesel engines under transient test cycle operating conditions [18]. . . . .	26
2.8	<i>Left:</i> Soot formation mechanisms paths from aromatic and aliphatic HC compounds. <i>Right:</i> Soot particles substructure [5]. . . . .	27
2.9	Schematic of primary processes for production of diesel particulates [5]. . . . .	27
2.10	SI engine CO emissions for eleven different fuels as a function of relative air/fuel ratio $\lambda$ [4]. . . . .	29
2.11	Kinetically predicted CO emissions compared to experimental measurements and equilibrium curves at TC combustion and exhaust conditions versus air/fuel ratio [5]. . . . .	29
2.12	Combustion plume development and composition during premixed (a) and mixing-controlled combustion (b) phases in DI diesel engine with swirl [5]. . . . .	31
3.1	Schematic representation of an EGR system for diesel engines [22]. . . . .	35
3.2	Relative $NO_x$ reduction due to the three different effects of EGR as a function of the replaced inlet charge mass percentage [7]; . . . . .	37
3.3	Comparison between injection timing retard and EGR as strategies to achieve $NO_x$ reduction and corresponding brake specific fuel consumption and PM emission penalties [7]; . . . . .	38
3.4	Effect of exhaust recirculation system on particulate matter emissions [29]; . . . . .	38
3.5	Inlet charge oxygen and carbon dioxide concentration as a function of EGR rate [22]; . . . . .	39
3.6	Schematic representation of a high pressure loop (HPL) or short route EGR system [22]. . . . .	41
3.7	Schematic representation of a low pressure loop (LPL) or long route EGR system [22]. . . . .	42
3.8	Schematic representation of an EGR heat exchanger [28]. . . . .	44
4.1	Kamimoto-Bae diagram or $\phi$ -temperature diagram showing ranges of mixture composition and temperature for $NO_x$ and soot formation as well as conventional combustion path and regions for HCCI and LTC combustion modes [32]. . . . .	46
4.2	Schematics representing combustion process attributes in conventional gasoline and diesel fueled engines, and homogeneous charge compression ignition engine [31]. . . . .	47
4.3	Emissions patterns for both low load early-injection and late-injection LTC operation in a heavy-duty engine application as a function of intake oxygen concentration and start of injection [33]. . . . .	51
4.4	Apparent heat release rate, in-cylinder pressure and needle-lift or injection profile for low-load conventional diesel combustion and low-load early direct-injection low temperature combustion [33]. . . . .	55

4.5	Schematics describing low temperature combustion conceptual model for low-load, single injection, EGR diluted, partially premixed, heavy-duty direct injection diesel engine [33]. . . . .	57
5.1	Perspective view of F1C conventional diesel engine design [34]; . . . . .	60
5.2	(a): Schematic representing the engine installations at the test bench [39], (b): Picture of test bench installation of F1C PCCI engine; . . . . .	61
5.3	(a): F1C EURO VI engine EGR cooler (left side) and F1C PCCI engine EGR cooler (right side), (b): Picture of F1C PCCI engine EGR cooler installation; . . . . .	62
5.4	Schematic of engine instrumentation concerning temperature and pressure sensors; . . . . .	63
5.5	AVL transient dynamometer installed in ICEAL; . . . . .	67
5.6	Engine cooling system . . . . .	69
5.7	AVL KMA 4000 fuel consumption measuring system; . . . . .	69
5.8	AVL AMA i60 emissions analyzer; . . . . .	70
5.9	Chemiluminescence detector schematic for $NO_x$ measurements [7]; . . . . .	71
5.10	Schematic of a non-dispersive infrared analyzer for CO and $CO_2$ measurement [7]; . . . . .	72
5.11	Schematic of a paramagnetic analyzer for molecular oxygen measurement [7]; . . . . .	73
5.12	AVL 415S smokemeter; . . . . .	74
5.13	AVL 439 opacimeter; . . . . .	75
6.1	(a): EGR rate as a function of EGR flap opening , (b): EGR temperature at EGR cooler outlet as a function of EGR rate; . . . . .	81
6.2	(a): Intake charge temperature as a function of EGR rate, (b): Intake charge pressure as a function of EGR rate; . . . . .	82
6.3	Relative air-to-fuel ratio as a function of EGR rate; . . . . .	83
6.4	Engine working point 1400x1.1, Single injection: (a) Normalized brake specific fuel consumption as a function of EGR rate, (b) Noise level variation as a function of EGR rate, (c) Apparent heat release rate versus crank angle position for low and high EGR content, (d) Mean in-cylinder pressure versus crank angle position for low and high EGR content; . . . . .	85
6.5	Engine working point 2000x2.3, Single injection: (a) Normalized brake specific fuel consumption as a function of EGR rate, (b) Noise level variation as a function of EGR rate, (c) Apparent heat release rate versus crank angle position for low and high EGR content, (d) Mean in-cylinder pressure versus crank angle position for low and high EGR content; . . . . .	87

6.6	Engine working point 1400x1.1, Double injection: (a) Normalized brake specific fuel consumption as a function of EGR rate, (b) Noise level variation as a function of EGR rate, (c) Apparent heat release rate versus crank angle position for low and high EGR content, (d) Mean in-cylinder pressure versus crank angle position for low and high EGR content; . . . . .	89
6.7	Engine working point 2000x2.3, Double injection:(a) Normalized brake specific fuel consumption as a function of EGR rate, (b) Noise level variation as a function of EGR rate, (c) Apparent heat release rate versus crank angle position for low and high EGR content, (d) Mean in-cylinder pressure versus crank angle position for low and high EGR content; . . . . .	91
6.8	Engine working point 1400x1.1, Single injection: (a) Normalized soot emissions as a function of EGR rate, (b) Normalized $NO_x$ emissions as a function of EGR rate, (c) Normalized HC emissions as a function of EGR rate, (d) Normalized CO emissions as a function of EGR rate; . . . . .	93
6.9	Engine working point 2000x2.3, Single injection: (a) Normalized soot emissions as a function of EGR rate, (b) Normalized $NO_x$ emissions as a function of EGR rate, (c) Normalized HC emissions as a function of EGR rate, (d) Normalized CO emissions as a function of EGR rate; . . . . .	95
6.10	Engine working point 1400x1.1, Double injection: (a) Normalized soot emissions as a function of EGR rate, (b) Normalized $NO_x$ emissions as a function of EGR rate, (c) Normalized HC emissions as a function of EGR rate, (d) Normalized CO emissions as a function of EGR rate; . . . . .	96
6.11	Engine working point 2000x2.3, Double injection: (a) Normalized soot emissions as a function of EGR rate, (b) Normalized $NO_x$ emissions as a function of EGR rate, (c) Normalized HC emissions as a function of EGR rate, (d) Normalized CO emissions as a function of EGR rate; . . . . .	98
6.12	Engine working point 1400x1.1, Single-Double injection, EGR trade-off curves: (a) Normalized brake specific fuel consumption versus normalized $NO_x$ emissions, (b) Normalized soot emissions versus normalized $NO_x$ emissions, (c) Normalized CO emissions versus normalized $NO_x$ emissions, (d) Normalized HC emissions versus normalized $NO_x$ emissions; . . . . .	100
6.13	Engine working point 1400x1.1, Single-Double injection, EGR trade-off curve: Noise level variation versus normalized $NO_x$ emissions; . . . . .	101
6.14	Engine working point 1400x1.1, Single-Double injection, Optimal trade-off points: (a) Apparent heat release rate versus crank angle position for optimal EGR quantity, (b) Mean in-cylinder pressure versus crank angle position for optimal EGR quantity; . . . . .	101

6.15	Engine working point 2000x2.3, Single-Double injection, EGR trade-off curves: (a) Normalized brake specific fuel consumption versus normalized $NO_x$ emissions, (b) Normalized soot emissions versus normalized $NO_x$ emissions, (c) Normalized CO emissions versus normalized $NO_x$ emissions, (d) Normalized HC emissions versus normalized $NO_x$ emissions; . . . . .	102
6.16	Engine working point 2000x2.3, Single-Double injection, EGR trade-off curve: Noise level variation versus normalized $NO_x$ emissions; . . . . .	103
6.17	Engine working point 2000x2.3, Single-Double injection, Optimal trade-off points: (a) Apparent heat release rate versus crank angle position for optimal EGR quantity, (b) Mean in-cylinder pressure versus crank angle position for optimal EGR quantity; . . . . .	103
6.18	(a): Engine-out exhaust gas temperature (cylinder 4) as a function of EGR rate, (b): Exhaust gas temperature before and after diesel oxidation catalyst as a function of EGR rate at 1400x1.1; . . . . .	105
6.19	(a): Exhaust gas temperature before and after diesel oxidation catalyst as a function of EGR rate at 2000x2.3, (b): Diesel oxidation catalyst HC conversion efficiency as a function of EGR rate; . . . . .	106
6.20	(a): Engine-out exhaust gas temperature (cylinder 4) as a function of EGR rate, (b): Exhaust gas temperature before and after diesel oxidation catalyst as a function of EGR rate at 1400x1.1; . . . . .	106
6.21	(a): Exhaust gas temperature before and after diesel oxidation catalyst as a function of EGR rate at 2000x2.3, (b): Diesel oxidation catalyst HC conversion efficiency as a function of EGR rate; . . . . .	107

# List of Tables

5.1	Kistler 6058A pressure sensor technical data . . . . .	65
5.2	Kistler 4007C pressure sensor technical data . . . . .	65
5.3	Kistler 4049BDS pressure sensor technical data . . . . .	65
5.4	AVL APA 100 dynamometer technical data . . . . .	68
6.1	Engine ECU parameters for the two key points . . . . .	79

# Acknowledgments

Ringrazio il mio grande Amore, per avermi sempre sostenuto e sopportato in questi anni pieni di gioie e traguardi ma anche di ostacoli e difficoltà per Noi. A volte penso che non sarei mai potuto arrivare fino a questo punto se non avessi incontrato lei, perché la verità è che ha cambiato il mio modo di vedere le cose e mi ha incosciamente guidato lungo questo percorso duro e tortuoso che bisogna affrontare da soli, non lasciando mai il mio fianco e riempiendomi sempre di amore. Anche se Lei non lo sa o non vuole riconoscerlo, mi ha dato e mi sta dando molto, più di quello che ogni ragazzo possa immaginare e desiderare. Ringrazio i miei Genitori, per tutti i sacrifici che hanno fatto per me, per avermi dato l'opportunità di studiare dando qualcosa a me e togliendo qualcosa a se stessi. Sono quello che sono grazie a loro e non finirò mai di ringraziarli. Ringrazio mia sorella e mia nonna per avermi supportato non solo con i loro incoraggiamenti ed il loro affetto ma con tanti fatti concreti che sono stati determinanti lungo il mio percorso di studi ed anche per la mia crescita personale. Ringrazio tutti i miei amici, dai quali in questi anni ho potuto imparare davvero tanto ed i quali, nonostante la lontananza ed a volte il poco tempo insieme, non hanno mai smesso di volermi bene e di farmi sentire il loro affetto. Infine, e non meno importante, ringrazio Dio per ascoltare le mie preghiere ed essermi sempre vicino aiutandomi ad affrontare le difficoltà della vita.

# Introduction

Over the last two decades, light-duty and heavy-duty vehicles equipped with diesel engines became more and more widespread, particularly for the European market. This internal combustion engine typology is characterized by a combustion process whose peculiar features allow higher thermal efficiency, lower fuel consumption and so  $CO_2$ , with respect to gasoline ICEs (Internal combustion Engines). Furthermore, diesel engines guarantee higher durability, higher reliability, reduced pumping losses and lower fuel price compared to gasoline applications, facts which all together favored a large adoption of these engines from both manufacturers and customers point of view. Despite of these advantages, diesel ICEs are afflicted by high particulate matter (PM) and nitrogen oxides ( $NO_x$ ) pollutant emissions, making diesel transport sector the largest contributor (about 40%) to the total ambient concentrations of  $NO_x$  in Europe [1]. As a consequence, even if the dieselization of some markets brought benefits in terms of carbon dioxide emissions, the ever stringent emission regulations regarding pollutants render increasingly difficult for car manufacturers meeting emission limits, especially for  $NO_x$  and PM, as shown in figure 1 for on-road heavy-duty engines. In addition to that, the introduction of new test driving procedure and cycle (Worldwide harmonized Light-duty Test Procedure - WLTP) more representative of real-driving conditions for light-duty, and the introduction of Real-Driving Emissions (RDE) tests using PEMS (Portable Emissions Measurement Systems) for both light and on-road heavy-duty (In-Service Conformity Testing), ask for huge efforts for the development of diesel engine and their after-treatment system (ATS). Currently available ATS technologies is capable of complying with Euro VI emission standards, however, its design complexity results in huge costs in terms of reasearch, development and maintenance, as well as difficulties in engine-vehicle packaging, factors which have to be accounted for in a long term perspective. Regarding soot emissions, the adoption of the Diesel Particulate Filter (DPF) after-treatment device is able to provide engine-out PM abatement with an efficiency up to 99,5 %. They basically operates as mechanical filter blocking solid particles in the gas stream thanks to their typical wall-flow substrate pattern. The soot accumulated inside these traps has to be periodically removed, or better burn out, requiring high exhaust temperature level and so specific regeneration strategies to be conceived, very often leading to fuel consumption penalties. As far as diesel  $NO_x$  abatement is concerned, two main after-treatment systems are currently at disposal: lean-burn  $NO_x$  absorbers or even called lean  $NO_x$  traps or LNTs and selective catalytic converters (SCR).

Stage	Date	Test	CO	HC	NOx	PM	PN	Smoke
			g/kWh					1/kWh
Euro I	1992, $\leq$ 85 kW	ECE R-49	4.5	1.1	8.0	0.612		
	1992, > 85 kW		4.5	1.1	8.0	0.36		
Euro II	1996.10		4.0	1.1	7.0	0.25		
	1998.10		4.0	1.1	7.0	0.15		
Euro III	1999.10 EEV only	ESC & ELR	1.5	0.25	2.0	0.02		0.15
	2000.10		2.1	0.66	5.0	0.10 <sup>a</sup>		0.8
Euro IV	2005.10		1.5	0.46	3.5	0.02		0.5
Euro V	2008.10		1.5	0.46	2.0	0.02		0.5
Euro VI	2013.01	WHSC	1.5	0.13	0.40	0.01	8.0×10 <sup>11</sup>	

<sup>a</sup> PM = 0.13 g/kWh for engines < 0.75 dm<sup>3</sup> swept volume per cylinder and a rated power speed > 3000 min<sup>-1</sup>

(a)

Stage	Date	Test	CO	NMHC	CH <sub>4</sub> <sup>a</sup>	NOx	PM <sup>b</sup>	PN
			g/kWh					1/kWh
Euro III	1999.10 EEV only	ETC	3.0	0.40	0.65	2.0	0.02	
	2000.10		5.45	0.78	1.6	5.0	0.16 <sup>c</sup>	
Euro IV	2005.10		4.0	0.55	1.1	3.5	0.03	
Euro V	2008.10		4.0	0.55	1.1	2.0	0.03	
Euro VI	2013.01	WHTC	4.0	0.16 <sup>d</sup>	0.5	0.46	0.01	6.0×10 <sup>11e</sup>

<sup>a</sup> for gas engines only (Euro III-V: NG only; Euro VI: NG + LPG)

<sup>b</sup> not applicable for gas fueled engines at the Euro III-IV stages

<sup>c</sup> PM = 0.21 g/kWh for engines < 0.75 dm<sup>3</sup> swept volume per cylinder and a rated power speed > 3000 min<sup>-1</sup>

<sup>d</sup> THC for diesel (CI) engines

<sup>e</sup> PN limit for PI engines applies for Euro VI-B and later [4374]

(b)

Figure 1: EU emission standards limits for steady-state (a) and transient (b) engine test cycles for heavy-duty diesel engine applications.

In the former, nitrogen oxides are chemically bound and stored by the catalyst under lean-burn engine operating conditions. When the  $NO_x$  trap is saturated, its regeneration is needed by implementing short period fuel-rich operation which allows nitrogen oxides desorption and subsequently reduction of the latter in  $N_2$  and  $O_2$ . Again this regeneration mode is detrimental for engine fuel consumption which is typically increased in a range of 2-4% depending on the application. When SCR after-treatment technology is employed, a catalyst together with the injection of an external reducing agent is used to reduce nitrogen oxides into molecular nitrogen and water. The catalytic medium utilized is also referred to as Diesel Exhaust Fluid (DEF), and it usually involves an aqueous urea solution which contains ammonia ( $NH_3$ ), stored in separate tank to be periodically refilled. In both LNTs and SCR cases, the major shortcomings regards the high costs, the packaging, and the complex control strategies to be implemented. Although, the current emission legislation requires the adoption of ATS systems on light and heavy-duty vehicles, the actual combustion engine technologies permits to also reduce  $NO_x$  engine-out emissions by adjusting the combustion process or by reshaping the combustion chamber, i.e., at engine calibration level or engine design level, respectively.

These in-cylinder emission control actions could guarantee low nitrogen oxides level through a combination of aggressive use of exhaust gas recirculation (EGR), boost and swirl level alteration, injection timing and pressure variation, multiple injection, compression ratio reduction and piston bowl reshaping. The most of these in-cylinder techniques lead to penalties in terms of unburned hydrocarbon, particulate matter emissions and fuel consumption. As a results of that, it is common for conventional diesel engines to investigate the  $NO_x$ /PM trade-off or the  $NO_x$ -bsfc trade-off. Considering EGR, this is an emission control technologies adopted in diesel engine to lower combustion flame peak and average temperature and diminish the charge oxygen concentration, by replacing part of the induced intake charge with a portion of the engine exhaust gas. The latter factors, temperature and oxygen concentration, are associated to the production of  $NO_x$  which is then inhibited. The recirculation of exhaust gas back into the intake manifold has also a positive effect on diesel combustion noise, because of the reduced heat release rate (HRR) which results in restrained pressure rate rise and peak firing pressure values, i.e., lower combustion noise level. Nevertheless, the application of EGR causes penalties in terms of engine emissions and performance, such as soot, carbon monoxide (CO), unburned hydrocarbons and degradation of brake specific fuel consumption. Moreover, EGR can negatively affect the quality of the lubricant oil and engine durability because of the increased wear between piston rings and cylinder liner.

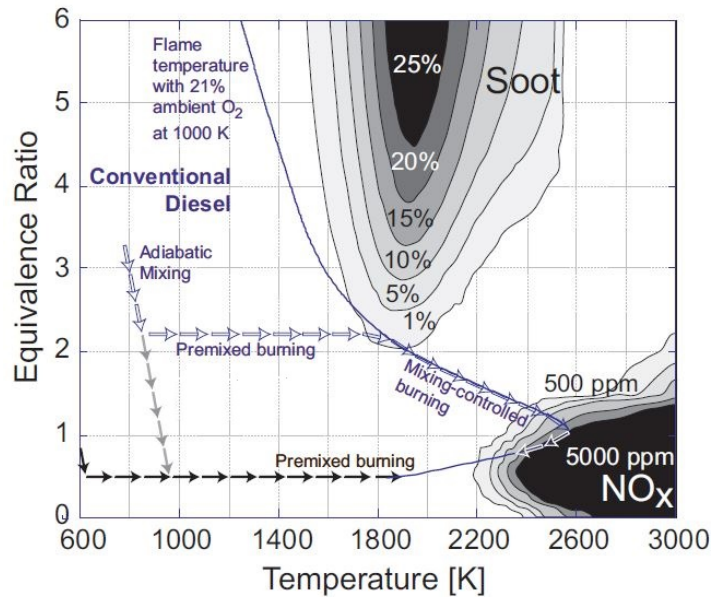


Figure 2: Kamimoto-Bae diagram or  $\phi-T$  (equivalence ratio - temperature) plot representing a fuel parcel path during conventional and advanced combustion processes [3].

With the aim of simultaneous abatement of both PM and  $NO_x$ , advanced combustion concepts [2], generally referred to as Low Temperature Combustions (LTC), have been emerging focusing the attention on lowering the combustion peak temperature and guarantee a larger degree of charge homogeneity with respect to conventional diesel combustion .

In the latter combustion process, considering direct injection engine, the fuel is injected during the last part of the compression stroke, then it atomizes, evaporates and mixes with the intake charge. When sufficiently high temperatures are reached the fuel auto-ignites and burns under premixed conditions. The term "premixed" refers to the portion of fuel which mixes during the time interval between the start of injection and the start of combustion (SOC), even called ignition delay period, that burns almost instantaneously when combustion begins. The fuel that does not participate to this phase burns under diffusive combustion, i.e., a combustion in which the rate of injection and the consequent mixing with air controls the speed of the oxidation process. The potential benefits of LTC, with respect to conventional combustion, concerns the exploitation of diluted mixtures, realized either with a large excess of air or with moderate to high EGR quantities, to obtain a combustion in which the fuel burns in premixed conditions. As a result of the increased homogeneity of the mixture, the presence of locally fuel rich and high temperature areas is prevented, which permits to achieve a combustion process where formation of  $NO_x$  and PM is largely precluded as shown in the  $\phi-T$  plot in figure 2. Several LTC strategies have been presented in literature with different names, acronyms and techniques, nonetheless, they resort to the previously discussed principles to achieve low temperature combustion conditions. HCCI (Homogeneous Charge Compression Ignition) is an advanced combustion mode in which fuel is inducted in the combustion chamber prior the start of compression stroke, thus having enough time to obtain an overall lean and homogeneous mixture. However, this conditions results in a decoupling between the injection timing and ignition event, which is then governed by reaction chemical kinetics, making combustion phasing control complicated. The characteristic needed for low temperature combustion can also be attained by realizing a not completely homogeneous combustion in which a lower degree of premixing is achieved by either direct early or late fuel injection with respect to TDC (top dead centre) and taking advantage of the effect of dilution of EGR to permit long premixing time. This low temperature combustion mode is usually referred to as Premixed Charge Compression Ignition (PCCI). In this case, the coupling between fuel injection and SOC is stronger and combustion phasing control can be reached by properly setting EGR rate and injection timing, according to the considered engine load and speed. PCCI shares the same advantages and disadvantages of LTC modes, therefore, the simultaneous abatement of  $NO_x$  and soot emissions can be achieved, while deterioration of unburned HC and CO emissions is typically experienced. Another downside common to PCCI is the limited load range over which the engine can operate due to the worsening of combustion noise level and the high in-cylinder pressure level. Many research studies have been performed in order to attenuate the main limits of PCCI combustion by either acting on calibration parameters such as fuel injection pressure, split injection or design action, i.e., piston bowl modification, injector choice and compression ratio variation. This writing aims to understand the influence that the adoption of uncooled EGR, with respect to the largely explored cooled approach, could have on mitigating the previously discussed shortcomings of PCCI and low temperature combustion processes.

# Chapter 1

## Conventional combustion in CI engines

In the following chapter, the basic characteristics regarding diesel engines (even called Compression-Ignition engines) conventional combustion process and its conceptual modelling are described. The term conventional refers to the fact that the main combustion features, which will be subsequently depicted, are the starting knowledge needed for the design and development of this internal combustion engines typology.

### 1.1 Main features

Diesel engine combustion involves the use of high reactivity, low volatility fuels, such as diesel, which are constituted by a mix of hydrocarbons that can be represented by the cetane,  $C_{16}H_{34}$ , with long straight chain molecule in which the preliminary reaction of the oxidation process proceed rather quickly in high pressure and temperature conditions. As a results, the fuel is injected by the injection system into the combustion chamber toward the end of the compression stroke, just before the desired start of combustion event. Indeed, the injection cannot take place too early during the compression stroke, since the fuel mixing with air and its compression would results in its auto-ignition during the compression stroke.

Therefore, the liquid fuel is usually injected as high velocity spray (jet velocity can reach values even beyond 100 m/s depending on the injection pressure and injector hole diameter) into the compressed air of the cylinder, as one or more jets through the injector orifices. Due to the high aerodynamic resistance encountered in those conditions, the fuel jet atomizes into small drops (fuel break up phenomenon) and penetrates into the combustion chamber, where it successively vaporizes and mixes with the high-temperature high-pressure cylinder air (typical pressure and temperature for natural aspirated CI engine, at the start of the injection event, are of about 900 K and 50 bar).

Since the pressure and temperature are above the fuel's ignition point, combustion of portions of the formed mixture starts spontaneously without the need of any external positive ignition system, with a delay period with respect to the beginning of injection event of few crank angle degrees (or few millisecond). Afterwards, the consequent compression of the unburned charge shortens both the ignition delay of this part of the mixture which is forming and the

evaporation time of the remaining liquid fuel.

Basically, the whole fuel injected goes through the following process:

- Atomization;
- Evaporation;
- Mixing with air;
- Combustion;

Moreover, it must be pointed out that, the remaining air in the cylinder continues to mix with burning gases and combustion products throughout the combustion and expansion processes.

Some primary considerations regarding the combustion process previously described on the engine operation are:

- Due to the CI engine injection feature, namely, injection is triggered just before the wanted start of combustion, there is no knock limit as for spark-ignition engine where the premixed air-fuel mixture in the end gas region might ignite spontaneously giving rise to the typical noise defining the knock phenomenon. As a result, CI engines can be designed with higher compression ratio than SI engines, providing advantages in terms of thermodynamic efficiency but requiring a more robust engine structure to withstand the higher peak firing pressure;
- Injection timing is used to control combustion timing, therefore the ignition delay, i.e., the period between the start of injection and start of combustion must be short, not only to control the beginning of the ignition, but also to limit the peak pressure, the exhaust emissions and the engine combustion noise;
- Torque control of diesel engine is performed by varying the amount of fuel injected per cycle with the intake air flow substantially unchanged, therefore these engine can operate unthrottled. As a consequence pumping work losses are reduced relative to SI engine, giving a better mechanical efficiency at part-load operating condition;
- Considering the type of regulation we operate on these engines, as the load increases the fuel injected per cycle increases as well, raising the problem of proper air exploitation due to reduced degree of mixing between air and fuel with respect to SI engine. As a results of this, diesel engines operate with an overall lean mixture, in order to prevent an excessive production of black smoke (or soot) or even the occurrence of misfire in some working conditions;
- One of the major problematic in the diesel engines is the achievement of a sufficient rapid mixing between the injected fuel and cylinder air in order to complete the combustion event with a proper crank angle interval close to the top-dead center so as to obtain a high fuel conversion efficiency. As a consequence of this, CI combustion chamber design and fuel injection system requirements [6] result to be different depending on the engine size, in order to provide the desired fuel-air mixing rate;

- Differently from SI engines, the combustion process in diesel engine does not speed up as the engine revolution speed increases [7]. Indeed, the time needed for evaporation, mixing and ignition delay (differently from the fuel burning rate) does not scale down with the increasing speed of the engine and the corresponding reduction of available time for combustion to occur in a defined crank angle interval. As a consequence, these engines cannot be run beyond a certain limit revolution speed (typically not higher than 5000 rpm);

Finally, compression-ignition combustion process is described by [4] as follows: "*it is an unsteady, heterogeneous, three dimensional combustion process*". The above definition wants to underline the level of complexity involved in the study of this process. Nowadays, thanks to refined diagnostic techniques, a satisfactory conceptual understanding of diesel combustion is reached, as we will see in section 1.3, while a quantitative description of this process depends on the characteristic of the fuel, on the design of the engine's combustion chamber and fuel injection system, and on the engine's operating condition. Therefore, being diesel combustion affected by all these factors, CI engines performance and emissions results to be dependent on them as well.

## 1.2 Combustion process stages

For a preliminary analysis of the combustion development, we can consider figure 1.1, where the in-cylinder pressure trace for firing and motored engine, the net heat release rate  $\frac{dQ_{ch}}{dt}$  due to combustion and the fuel mass fraction burned are reported.

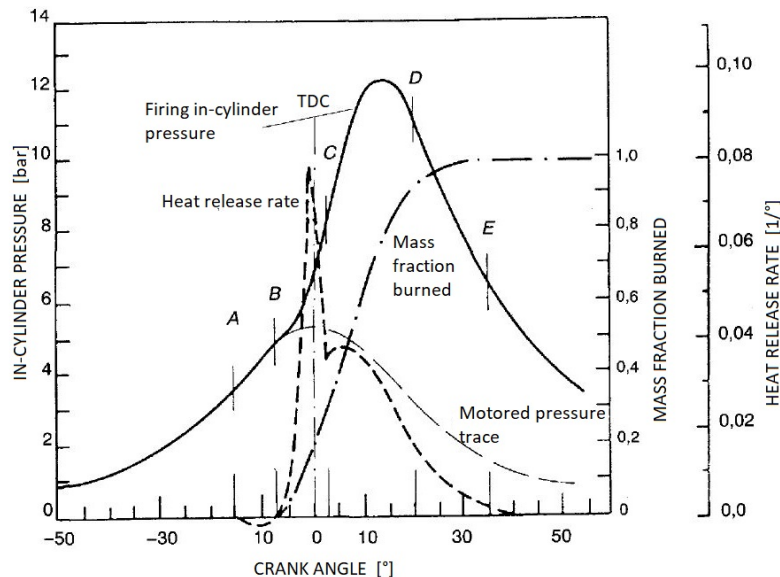


Figure 1.1: In-cylinder pressure trace for firing and motored engine, net heat release rate and the fuel mass fraction burned as a function of crank angle for DI supercharged diesel engine [6].

The in-cylinder pressure is an information which is always available when an engine is installed on a test bench, while the net heat release rate and the mass fraction burned can be evaluated by employing pressure-based diagnostic models which exploit the application of the energy conservation equation on the combustion chamber control volume during the instants of combustion [8]. For sake of completeness, the definition of net heat release rate is here presented:

$$\frac{dQ_{net}}{dt} = \frac{dQ_{ch}}{dt} - \frac{dQ_{ht}}{dt} = \frac{\gamma}{\gamma-1} p \frac{dV}{d\theta} + \frac{1}{\gamma-1} V \frac{dp}{d\theta} \quad (1.1)$$

where:

- $Q_{ch}$  is the chemical heat released by the combustion; [J]
- $Q_{ht}$  is the heat exchanged by the gas bulk inside the cylinder through the wall during combustion phase; [J]
- $\gamma$  is the isentropic coefficient; [-]
- $p$  is the in-cylinder pressure; [Pa]
- $V$  is the piston displaced volume; [ $m^3$ ]

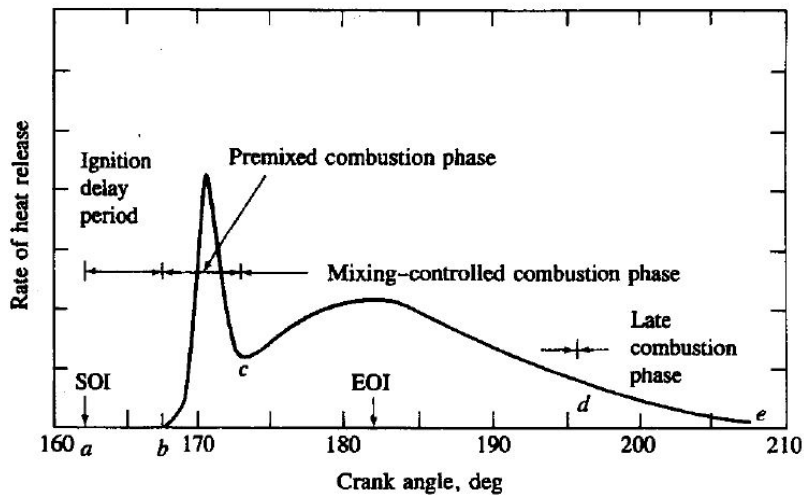


Figure 1.2: Typical DI multispray diesel engine net heat release rate diagram [4].

Looking at figures 1.1 and 1.2, the overall CI combustion process can be divided into 4 main stages both in terms of pressure and heat release rate:

**Ignition delay (a-b or A-B)** The ignition delay is the time between the SOI (start of injection) and the SOC (start of combustion), so it begins when the fuel starts to penetrate into the combustion chamber and it ends when the combustion is detected. The latter can be determined from the sudden change in slope on the  $p(\theta)$  curve, or from the net heat release rate analysis, or by means of luminosity detection with optical

diagnostic set-up. During this phase, the heat release rate, shortly after the injection, assumes negative values due to heat transfer to the walls (which is not negligible in this period), and the heating and the evaporation of the injected fuel. This delay is caused by physical process such as fuel atomization, its evaporation and the mixing with air and chemical process which involves the pre-reactions occurring before the start of combustion (radical pool reactions)[6]. As a result of this non-instantaneous ignition, a significant amount of fuel can cumulate inside the combustion chamber, fact which will affect the characteristics of the next stage of combustion as well as the overall process, influencing efficiency and combustion duration, and the resulting exhaust emissions and combustion noise.

**Premixed or rapid combustion phase (b-c or B-C)** In this stage, the fuel accumulated during the previous stage, which has already mixed with air, burns almost instantaneously all at once. Indeed, when combustion starts, the consequent temperature increase speed up both physical and chemical processes, leading to rapid burning phase of the ready-to-burn mixture. This results in a sharp pressure rise which excites the engine structure causing vibrations and the associated engine noise. Similarly to the pressure, the HRR (Heat Release Rate) features a steep rise reaching a peak, meaning, this phase is characterized from a high burning rate which lasts for few crank angle degrees. The higher the amount of fuel injected during the ignition delay, the more intense the premixed phase, which on one side is beneficial for the engine thermodynamic efficiency (the fuel burns at almost constant volume), but on the other is deleterious for combustion noise and pollutant emissions as explained in detail in chapter 2.

**Mixing-controlled combustion phase (c-d or C-D)** The third stage of combustion starts once all the fuel cumulated in the ignition delay has been burned during the premixed phase. This stage is referred to as diffusive or mixing-controlled combustion, since the burning rate or the heat release rate is now controlled by the speed at which fresh mixture becomes available and so mainly by the air-fuel vapor mixing process. The HRR may reach a second peak of lower intensity than that of the premixed phase, and it starts decreasing as the combustion proceeds. Typically, this period is characterized by the achievement of the peak combustion temperature and pressure, and the injected fuel does not only mix with air but also with burned gases, conditions which again affect pollutants formation.

**Late combustion phase (d-e or D-E)** Typically, the last stage of combustion can be temporally positioned after the end of injection and prior the opening of the exhaust valve, therefore well into the expansion stroke. The existing and decreasing trend of the heat release rate can be explained by several motives, such as the combustion of a small fraction of fuel which has not burned yet as well as the energy release of soot (solid aggregate compounds) and fuel-rich combustion products.

These concluding burn-out processes are featured by a lower burning rate since the expansion reduces the in-cylinder temperature which exponentially affects the kinetic of the reactions, however, this stage of combustion still promotes a more complete fuel oxidation and less-dissociated combustion products.

### 1.3 Combustion conceptual model

A conceptual combustion model represents an organized qualitative description of how the combustion process proceeds in compression-ignition engines. Such element provides an insight about the main phenomena characterizing the different stages of combustion and the emission-formation mechanisms, hence, resulting of primary importance for interpreting experimental measurements, develop numerical model and provide engineers with a guide in the challenge to enhance CI engine efficiency and reduce their engine-out emissions. A detailed and thorough model concerning direct-injection modern-diesel-engine was introduced in the late 90s, thanks to the work of John E. Dec and his co-workers at the Sandia National Laboratories [10]. Indeed, the advent of advanced laser diagnostic techniques permit to perform detailed in-situ measurements inside of a reacting diesel fuel jet. An earlier phenomenological description of diesel combustion was already conceived, however, because of the lack of suitable diagnostic technologies, limited information and measurements were available, leading to conceptualize the CI combustion process similarly to other steady spray flames [9].

#### 1.3.1 Old combustion model

The first depiction of diesel spray combustion was based on zones of varying fuel air mixture from the center to the edge of the spray, in particular, from a cold very fuel-rich liquid core, the concentration of fuel drop off with a Gaussian-like trend toward the jet periphery. The zone of combustion was thought to be at a certain distance from the center of the plume where an appropriate air/fuel mixture was formed. Main characteristics regarding the old description of combustion were:

- The liquid phase penetrated well out from the injector with fuel droplets being present up to or within the combustion zone;
- Autoignition and premixed burn were thought to take place only in few points around the jet periphery which were at nearly stoichiometric conditions;
- After premixed burn, combustion occurred solely in a diffusion flame confined to the peripheral region of the jet;
- Soot formation was generally assumed to occur mainly on the fuel-rich side of the diffusion flame, as shown in figure 1.3, where the temperature were sufficiently high (at least above 1300 K to promote fuel pyrolysis reactions). Moreover, the initial premixed burn was believed to not influence the soot production since it took place around the jet periphery, region with nearly stoichiometric air/fuel ratio;

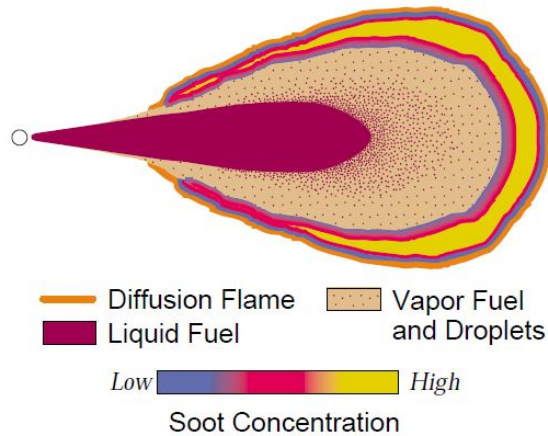


Figure 1.3: Schematic of the mid-plane of a combusting diesel jet representing the "old" view of diesel combustion, prior to laser-sheet imaging studies [10].

The laser-sheet imaging studies performed later proved these considerations to be not reliable and provided a deeper knowledge about liquid and vapor zones, fuel/air mixing, autoignition, reaction zones and soot distributions.

### 1.3.2 Dec's combustion model

The new conceptual model of diesel combustion was the result of combined individual studies performed by John E. Dec and his co-workers which allowed them to reach a thorough understanding of the evolution of a reacting diesel fuel jet.

The experimental set-up adopted in those studies consisted of single cylinder, four stroke, direct-injection diesel engine, shown in figure 1.4, which was derived by one series production heavy-duty engine of Cummins company. The engine was designed with a piston-crown window to obtain a view of the combustion chamber (lower image) and a cylinder head window which replaced one of the exhaust valves to gather images of the squish region and the outer portion of the combustion bowl (upper view). Other windows situated in the upper part of the cylinder wall were necessary to realize planar laser imaging diagnostic, therefore, allowing the laser sheet to enter the cylinder along the fuel jet axis or horizontally. Proper intake charge conditioning was performed in order to reproduce the same working conditions between the standard engine and the experimental one, in particular aiming to reproduce the same peak pressure under motored conditions [11].

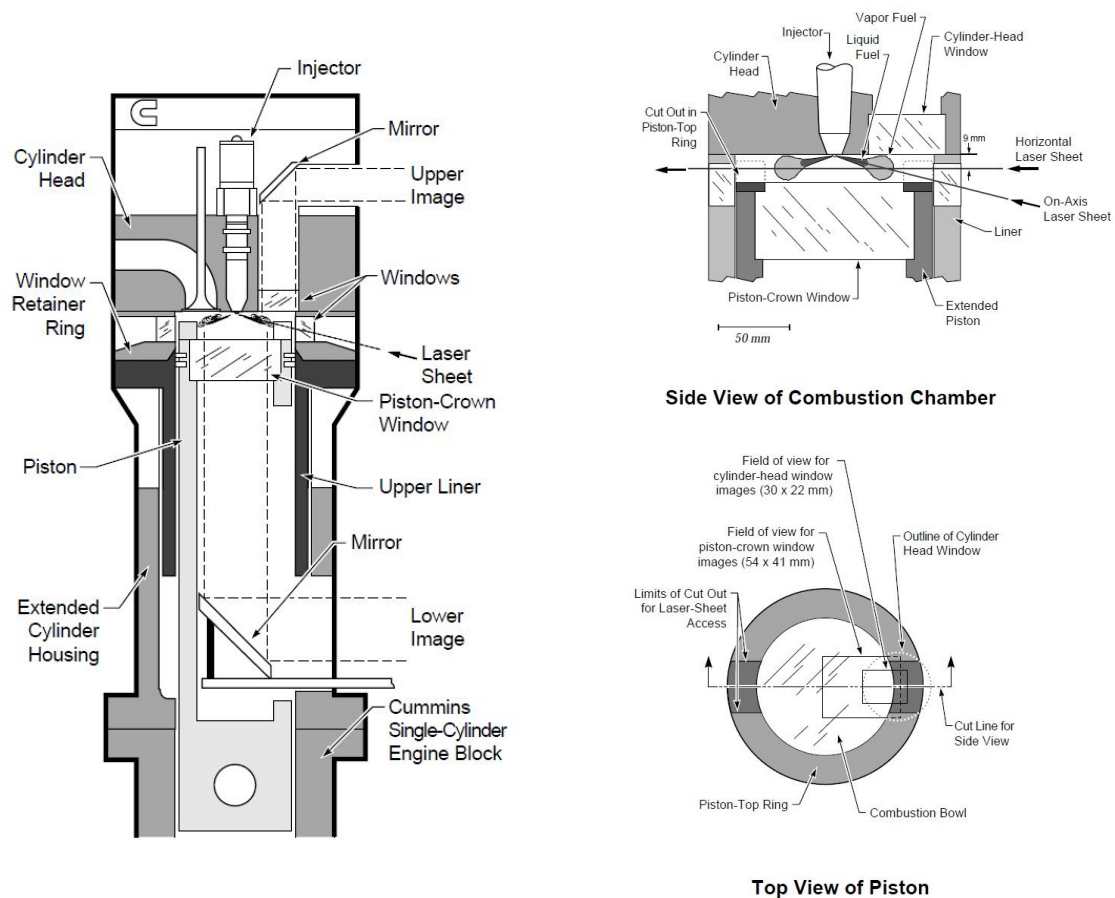


Figure 1.4: Left: Optical-access diesel engine showing the laser sheet along the fuel jet axis. Right: Geometry and optical configuration of the combustion chamber from top and side view [10].

The above set-up together with multiple laser-based imaging techniques permitted to gather data on diesel combustion and emission formation processes which include: liquid-phase fuel distributions, quantitative vapor-fuel/air mixture images, relative soot concentrations, relative soot particle size distributions, images of the diffusion flame structure, and natural-chemiluminescence images of the autoignition. More in detail, the laser techniques employed to perform the previous investigations were:

- Elastic scatter was utilized to study the liquid fuel penetration and its features during injection [12];
- Autoignition event and diffusion flame early formation were investigated by means of planar laser-induced fluorescence (PLIF) [13], technique which was also used to identify the presence of PAHs (polycyclic aromatic hydrocarbons);
- Air/fuel-vapor mixture images were acquired through planar laser Rayleigh scatter (PLRS) [14];

- Soot formation and its evolution in concentration and distribution along the reacting fuel jet was examined combining elastic scatter and laser-induced incandescence (LII) [12];

The information from individual imaging measurements coupled with heat release rate data were combined by Dec and co-workers in a series of schematics, as shown in figure 1.5, representing idealized cross-sectional slices through the mid-plane of the jet, on which interaction with the piston-bowl wall and plume to plume interaction due to swirl motion were neglected. This temporal and conceptual representation of how DI diesel combustion occurs was performed from the start of injection, through the premixed burn and into the first part of mixing-controlled burn (prior the end of injection) under defined engine working conditions [10]. As a consequence of that, this conceptual description offers a thorough qualitative description of the combustion process in modern DI diesel engines, while quantitative information are valid only for the case being considered because they depend on the specific engine design and on its operating condition.

**Initial Jet Development (0.0° - 4.5° ASI)** Firstly a liquid fuel jet enters the combustion chamber (1.0° ASI), then the fuel atomizes and air is entrained within the jet. The dark brown region represent the liquid fuel jet portion, hence, the maximum extent of the liquid fuel droplets or equally where the last droplet of liquid fuel vaporizes. At 2.0° ASI, a vapor-fuel region builds up adjacent to the side of the jet beyond the liquid droplets and starts to grow in thickness. Then, the liquid reaches its maximum penetration (3.0°), since the entrainment of hot air has been capable of vaporizing all the fuel at this distance from the injector tip. Up to 4.5°, the gas phase of the jet has been penetrating the combustion chamber beyond the liquid phase, and its leading portion contains a relative uniform fuel/air mixture with equivalence ratio in the range of about 2 to 4;

**Autoignition (3.0° - 5.0° ASI)** The temporal and spatial position of autoignition is not well determined. Chemiluminescence due to the presence of OH radicals might begin as early as 3.0° ASI, as shown in 1.3, and by 4.5° ASI most of the chemiluminescence comes from the well developed vapor-fuel/air mixture region in the leading portion of the jet. The presence of OH radicals before the rapid heat release rise is caused by the occurrence of pre-reactions between fuel and oxygen which results in production of radicals (radical pull). Once a certain concentration is achieved all over the fuel vapor region, fuel breakdown or chain branching reactions and PAHs formation occur at 5.0° ASI (thermal explosion), marking in some way the start of "thermal combustion" (HRR rise);

**First Part of Premixed Burn Spike (4.0° - 6.5° ASI)** At 4.0° the HRR curve starts rising up and by 4.5° ASI a sharp increase occurs when the leading portion of the jet is highly chemiluminescent, however without significant fuel breakdown.

Then, at 5.0° ASI where the equivalence ratio range from 2 to 4, the fuel breaks down and relevant amount of PAHs almost uniformly form across the jet cross section in the leading region. This time instant correspond to the rapid rise in the heat release rate, therefore, highlighting that the premixed burn spike involves the combustion of this fuel-rich mixture. By 6.0° ASI, soot is formed as small particles and can be found at location which vary from cycle to cycle in the cross section of the downstream portion of the fuel jet. PAHs are considered "soot precursors", because during premixed burn an environment with high temperature and low oxygen content (rich mixture conditions) promotes chemical processes of hydrogen abstraction and carbon addition between them and other HCs resulting in soot particle formation. Then, by 6.5° soot is present throughout the leading portion of the fuel jet due to the previous and other formation mechanisms;

**Onset of the Diffusion Flame (5.5° - 6.5° ASI)** Between 5.5° and 6.5° ASI, at the jet periphery within the products of the fuel-rich premixed burn (which also contains significant quantity of unconsumed fuel) and the surrounding air, a diffusion flame forms. At 6.5° ASI, it completely encircles the downstream portion of the jet extending back toward the injector until just upstream of the tip of the liquid fuel portion. At the same angle, soot particles grow in size in a thin peripheral layer of the combustion plume due to some effects of the diffusion flame, which conversely does not influence the soot concentration;

**Last Part of Premixed Burn Spike (7.0° - 9.0° ASI)** At 7.0° ASI, the premixed burn is still ongoing and the jet keeps growing and penetrating the combustion chamber. Considering soot concentration, it continues to increase in the cross section of the sooting region, featuring the highest concentration toward the leading edge of the combustion plume where the head vortex is forming. The latter fact can be seen considering the 8.0° ASI schematic where a red zone near the jet tip is depicted. Moreover, this location is characterized by the largest soot particles, even larger than those formed along the jet periphery due to diffusion flame. Between 8.0° ASI and 9.0° ASI, the last premixed air is consumed leading to the end of the premixed burn and the start of a pure mixing-controlled burn;

**First Part of Mixing-Controlled Burn (9.0° ASI to end of injection)** As the mixing-controlled combustion takes over the premixed burn, the overall jet morphology do not change significantly, probably due to the coexistence of premixed burn and diffusive burn leading not to an abrupt combustion transition. Moreover, as it can be seen in the 10° ASI schematic, the jet is still penetrating further and soot concentration and particles size are increasing following the same pattern seen previously. An identical jet appearance and soot distribution can be witnessed up to the end of injection, while soot concentration and particle size continue to increase in the well-formed head vortex;

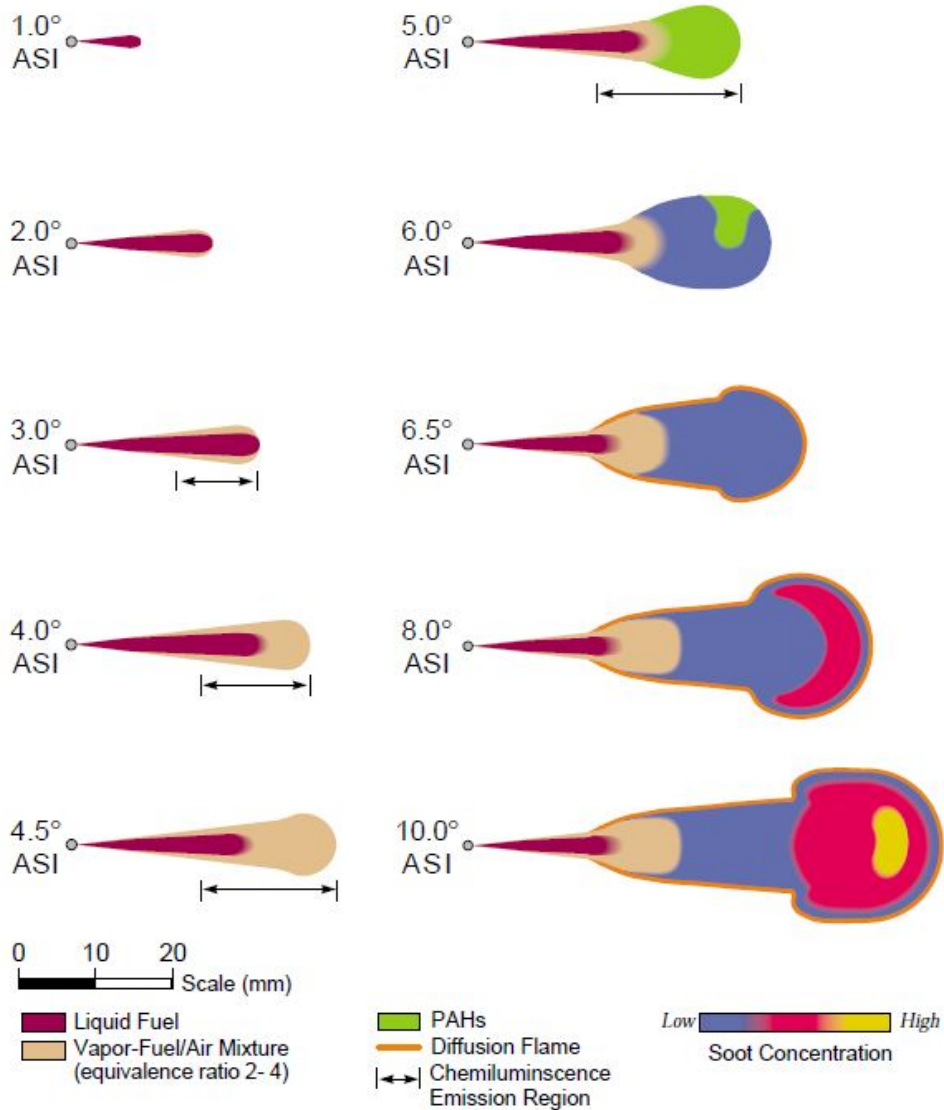
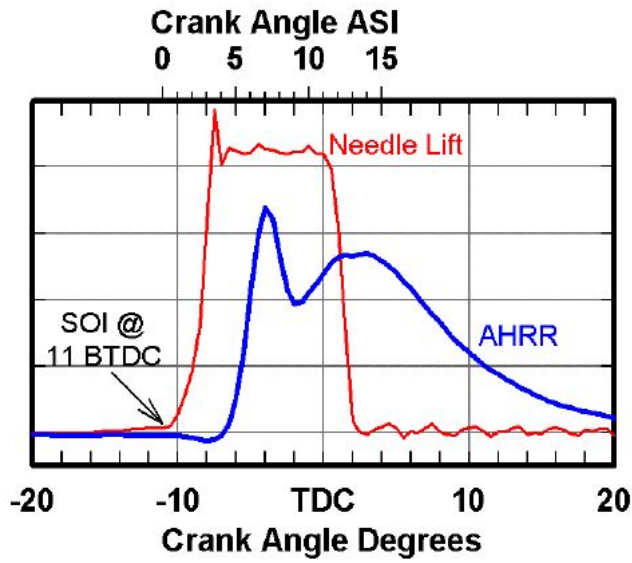


Figure 1.5: Schematics displaying a temporal sequence of how DI diesel combustion develops from the start of injection until the early part of mixed controlled burn [15].

**Mixing-Controlled Burn** Figure 1.6 represents the schematic concerning the mixing-controlled burn up until the end of injection. This picture of the combustion plume temporally follows the sequence at  $10^\circ$  ASI with which it shares multiple similarities except that the jet is bigger, soot concentration is even larger in the head vortex as well as the particles size, and the jet boundaries are drawn with ragged appearance to imply the turbulent nature of a real diesel jet. The soot particle pattern is the one seen from  $8.0^\circ$  ASI to  $10^\circ$  ASI, i.e., small particles are present at a certain distance from the injector tip downstream the vapor fuel/air mixture then its concentration and particle size increase down the jet to the head vortex where the largest particles and concentration are found. Soot formation, between the tip of the liquid fuel and the point where soot itself appears, is still ongoing even after the last part of premixed-burn until the end of injection. This fact is not justified neither by fuel pyrolysis due to hot cylinder air (1000 K) nor by heating of the jet core due to transport phenomena of diffusion flame hot products. Indeed, the production of small soot particle similar to those produced by the initial premixed burn are caused by the presence of a standing fuel-rich premixed flame, which also supports the distribution of soot seen by imaging. As a result, the presence of a standing premixed flame during the mixing controlled burn and considering the previous premixed-burn combustion means that all the injected fuel undergoes a *two-stage combustion process* both for premixed and mixing controlled burn. Moreover, the diffusion-flame combustion occurs between the products of the fuel-rich premixed combustion and air, instead of a more common pure-fuel/air diffusion flame;

Figure 1.6 contains additional thermal and chemical information about the burning fuel plume accordingly with the time period depicted. Indeed, the developed conceptual model is capable to give an insight on pollutant emissions which for diesel engine regards mostly soot and NOx or better NO. Those findings were initially proposed in [10] and successively investigated and confirmed in [15]. Together with the already discussed soot formation, concentration and distribution along the jet, a further knowledge about its oxidation is shown. In particular, the latter process occurs at diffusion flame level where high OH radicals concentration and oxygen presence can be found, and OH radical attack (primary method) and oxygen attack (secondary mechanism) are the main responsible for soot transformation in complete combustion products ( $CO_2$  and  $H_2O$ ). Theoretically, all the soot produced from the rich premixed flame could be oxidized by the diffusion flame, however, upon the closing of the injector fuel velocity decrease significantly, atomization and mixing are poor, factors which leads to a significant amount of soot formation which do not reach the diffusion flame resulting in one of the contribution to tailpipe soot emissions. Analogously to soot oxidation, the sheath diffusion flame surrounding the plume results to be the location where high temperature and oxygen contents conditions are ideal for thermal NO production mechanism (see chapter 2). High NO production rate is then present only at the jet periphery on the lean side of the diffusion flame, as indicated by the green color. Nevertheless, it must be pointed out that the bulk of NO production does not occur in that region, since the signifi-

cant NO production happens after the time period represented, therefore in the last part of the mixing-controlled burn or due to postflame phenomena after the end of combustion in hot-gas regions.

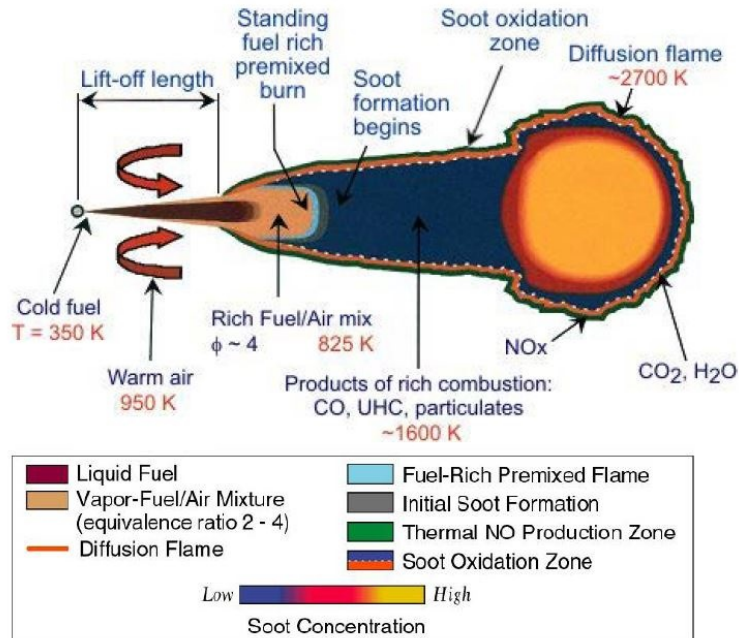


Figure 1.6: Conceptual model of DI diesel combustion with further characteristics concerning pollutants distribution along the combustion plume prior the end of fuel injection [15].

Finally, comparing the "old" and "new" description of the combustion model, the following main phenomenological differences can be stated:

- Autoignition occurs under fuel-rich conditions with an equivalence ratio ranging from 2 to 4 and not in near-stoichiometric condition as previously believed. Therefore, the premixed burn spike is responsible for the initial soot formation;
- The actual liquid fuel penetration length is shown to be relatively short and all the fuel in the main combustion zone is vapor phase, in contrast with the old description. As a result, the penetration of the liquid fuel jet is stopped by the evaporation process and not by combustion event;
- Soot presence is found on the whole jet cross section, conversely to the old model where soot was supposed to be contained in a shell-like region near the diffusion flame around the jet periphery;
- Even if the diffusion flame appear around the jet periphery as in the old description of diesel combustion, throughout the mixing-controlled combustion phase, a premixed fuel-rich flame is taking place within the combustion plume prior the diffusive flame, so that all the fuel undergoes a double stage combustion;

## Chapter 2

# Pollutant emissions in diesel engines

The next chapter will describe the formation mechanisms concerning the in-cylinder production of pollutants in diesel engines. The main design and calibration actions aimed to control and reduce these noxious emissions will not be here addressed as well as after-treatment systems. Finally, another relevant content associated with the compression-ignition combustion, i.e. diesel combustion noise, will be discussed.

### 2.1 Mechanisms of formation

Considering the ideal combustion process of a hydrocarbon fuel, the only products of this oxidation reaction are carbon dioxide  $CO_2$ , water  $H_2O$ , molecular nitrogen  $N_2$ , which does not theoretically take part to any reaction, and molecular oxygen  $O_2$  in case of lean mixtures. However, in the real combustion process, primary pollutants, i.e., chemical species affecting human health which are produced directly inside the combustion chamber, are produced. Therefore, the pollutants contained in the exhaust gases of both spark-ignition and CI engines are mainly oxides of nitrogen such as nitric oxide (NO) and nitrogen dioxide ( $NO_2$ ), also referred collectively to as  $NO_x$ , carbon monoxide (CO) and unreacted or partially unreacted hydrocarbons (HC). Moreover, for fuel with a content higher than 10 ppm (by weight) of sulfur (upper limit for sulfur-free fuel), other pollutant species of main concern result from sulfur oxidation in sulfur dioxide ( $SO_2$ ) and trioxide ( $SO_3$ ). In addition to the previous gaseous emissions, in case of diesel and direct injection gasoline engine, liquid and solid particulate emissions, even called Particulate Matter (PM), are present in the exhaust stream. Generally, the concentration of these pollutants depends on the engine typology, its design and operating conditions, however, as an average they can be considered to represent 1% (by volume) of the total exhaust gases. The definition of the emission level is strictly related to the detailed knowledge of the chemical mechanisms involved in pollutant formation as well as the kinetics of these processes. Furthermore, the formation and destruction of some pollutants species such as carbon monoxide, unburned hydrocarbons and particulates are directly related to the principal fuel combustion process, highlighting the importance of a relevant understanding of the combustion chemistry. On the other hand, concerning nitrogen oxides

and sulfur oxides, they are not directly involved in the combustion process, but the chemical reactions which lead to their formation occur because of an environment generated by the reactions of combustion. Hence, the formation and destruction of these latter pollutants are still correlated with the combustion event. As far as conventional CI engines are concerned, order of magnitude regarding noxious engine-out emissions are of about:

- $NO_x$ , 500 to 1000 ppm or 10 g/kg fuel or even higher;
- Particulate matter, between 0.1-0.2% of the burned fuel mass;
- CO, lower than 1% (by volume) or 15 g/kg fuel;
- HC, less than 1000 ppm or 10 g/kg fuel ;
- Low  $SO_x$  emissions, due to the adoption of sulfur-free fuels;

As described in chapter 1, diesel combustion is a heterogeneous process, either in space or in time, meaning that pollutant formation processes are heavily related on the fuel distribution and how that distribution changes over time due to mixing. Differently from gasoline engine in which an almost two homogeneous zones can be identified from composition and thermodynamic point of view (burned gas and unburned gas zones), in CI engine fuel is injected into the cylinder slightly before start of combustion, therefore a homogeneous mixture formation is never reached. As a matter of fact, reactants concentration varies from point to point into the combustion chamber resulting in values of equivalence ratio  $\phi$  ranging from 0 to inf. The latter fact tells us, once more, that even if diesel engines run with an overall lean mixture, locally we have pure air region, pure fuel region, rich mixture and lean mixture zones whose presence obviously affects pollutant formation.

Considering figure 2.1, in which various part of a fuel jet in a direct-injection engine are depicted, the formation of NO, unburned HC, and soot (solid fraction of PM) during premixed and mixing-controlled phase are reported. As shown with the conceptual model of diesel combustion, nitric oxide forms with relevant rates in the diffusion flame zone around the jet periphery where high temperature and close-to-stoichiometric conditions are present, while, within the combustion plume, where product of rich combustion are present,  $NO_x$  formation rate is less significant. Soot forms inside the fuel rich zone within the jet, where sufficiently high temperature is provided from the ongoing premixed flame, and then it oxidizes in the diffusion flame region. Unburned hydrocarbons presence at the exhaust is due to different phenomena such as flame quenching, both at the walls and where excessive air dilution permits neither start nor completion of the combustion process, and processes where slow or incorrect mixing occurs. CO emissions are of minor concern in diesel engine because they always operate with a large excess of air which promote the oxidation reaction to  $CO_2$ . The details regarding the above formation mechanisms will be addressed in the next subsections.

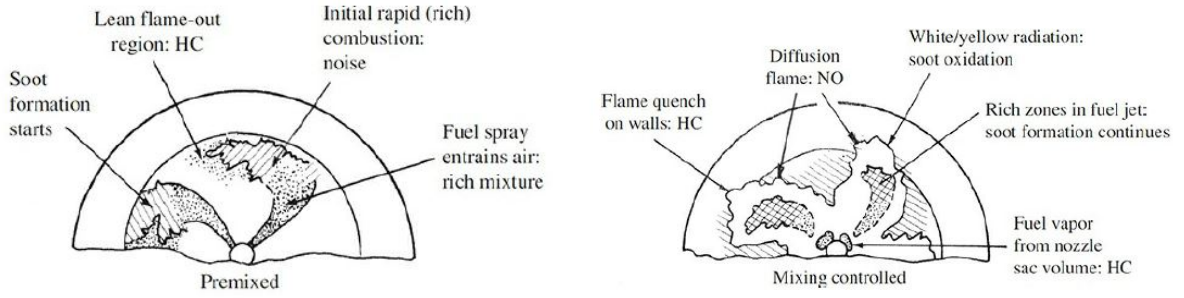


Figure 2.1: Schematic of pollutant formation during premixed and mixing-controlled combustion stages in DI diesel engine with swirl [5].

### 2.1.1 Nitrogen oxides

Being nitrogen oxidation reactions indirectly related to the combustion process, the same mechanisms of formation for NO and  $NO_2$  apply for both spark ignition and compression ignition engine. The substantial difference between the two engine typologies consist on the instant of time, during the fuel oxidation process, and the locations, within the combustion chamber, in which  $NO_x$  production occur. Diesel nitrogen oxides breakdown is of about 70% - 90% nitric oxide (NO) and 10% - 30% nitrogen dioxide ( $NO_2$ ), with more significant presence of the latter chemical specie with respect to SI engines.

#### NO formation

NO forms as a by-product of the combustion process due to nitrogen oxidation which is triggered above the temperature threshold of 1850 K. The corresponding production (and destruction) mechanism is also referred to as *thermal  $NO_x$  production mechanism* or considering the three main reactions involved in the conversion of  $N_2$  into NO, as *extended Zeldovich mechanism*, which is reported below.



Reaction 2.1 is characterized by a high activation energy which results in a high sensitivity to temperature. As a consequence, this mechanism features significant importance where the temperature is sufficiently high to permit the reaction to be initiated and where enough oxygen concentration is present. These conditions are those typical of the diffusion flame zone of a conventional burning diesel spray, where temperatures around 2700 K and near-to-stoichiometric air/fuel ratios are found. The NO production rate ( $\frac{d[NO]}{dt}$ ) is exponentially dependent on temperature, therefore the higher the latter quantity, the larger the

contribution of NO to  $NO_x$  emissions, which, in turn, means that the sudden and abrupt cooling occurring during the expansion stroke prevents any reverse reaction to reduce the nitric oxide concentration which basically freezes before the exhaust process begins.

Another process of formation of NO which is typically less significant of the thermal one, but it can have some relative importance especially at low temperature (or extremely diluted mixtures), is the so called *prompt mechanism*, which reference reaction is:



This production process involves the interaction between molecular nitrogen and CH radicals and it is characterized by a low sensitivity to temperature since the activation energy is low and it is extremely fast where concentration of HC radicals are abundant. The chemical reaction gives rise to hydrogen cyanide (HCN) and the high unstable nitrogen atom which can both form NO reacting with oxygen.

### **NO<sub>2</sub> formation**

Despite the dominant presence of nitric oxide, diesel engine exhaust features a notable amount of nitrogen dioxide, which is again formed at diffusion flame level by the conversion of NO, as shown in 2.5.



Then, unless flame quenching phenomena caused by mixing with cooler mixture take place, the  $NO_2$  previously formed is successively converted in NO via the following reaction:



Figure 2.2 denotes the exhaust gases share of  $NO_2$  as a function of engine load (bmep) and engine speed with the aim to underline the higher content of this specific pollutant in diesel engines with respect to spark ignition ones where it usually retains 1% of the total nitrogen oxide emissions. Considering the diesel fuel jet burning process and the main findings from optical investigation about NOx formation [16], no noticeable nitrogen oxidation process takes place during premixed fuel rich burning which is justified by the low oxygen concentration ( $\phi \approx 4$ ) and low temperatures of this regions, as shown in figure 2.3. The first presence of nitric oxide is witnessed within a thin layer at the jet periphery where the diffusion flame is established, providing the right condition in terms of temperature ( $\approx 2700$  K) and oxygen availability (close-to-stoichiometric air/fuel ratio) to have the highest NO formation rate.

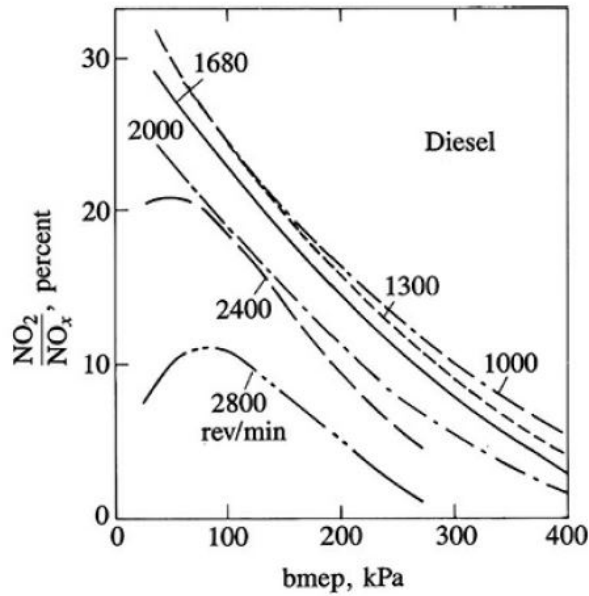


Figure 2.2: Nitrogen dioxide share as a function of engine load and engine speed in diesel engine [4].

The presence of nitrogen oxides outside the sooting region of the jet appear to last up to the end of the injection event and through the early burn-out of the mixing controlled phase until the jet structure vanishes. Although, the major heat release phase ends and the jet structure disappears, NO formation continues in the hot post-combustion gases, as depicted in figure 2.4 where the end of combustion event and the cumulative concentration of  $NO_x$  are reported. Further data analysis from Dec and his co-workers [15] supported the results, on location and timing of nitrogen oxides formation, concerning the previous investigation which can be summarized as follow:

- Rapid  $NO_x$  formation begins well after the start of heat release, i.e., when the sheath diffusion flame appears at the jet periphery, contradicting the past belief that the premixed combustion phase was one of the cause of  $NO_x$  formation.
- The principal source of nitrogen oxides formation is indeed the mixing-controlled diffusion-flame burning process, where NO forms on the lean side of the flame;
- Nitric oxide production continue even after end of combustion due to post-flame phenomena, prior the sudden cooling due to expansion and mixing with cool gas region.
- The split amount of  $NO_x$  formed in the two different conditions (mixing-controlled and post-combustion production) depends on the engine working conditions.

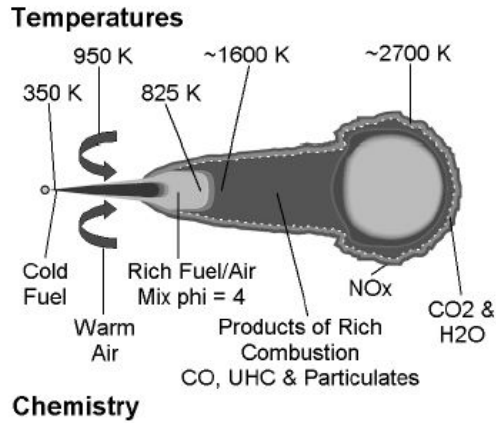


Figure 2.3: Temperature and chemistry of a typical DI diesel engine's combustion plume [15].

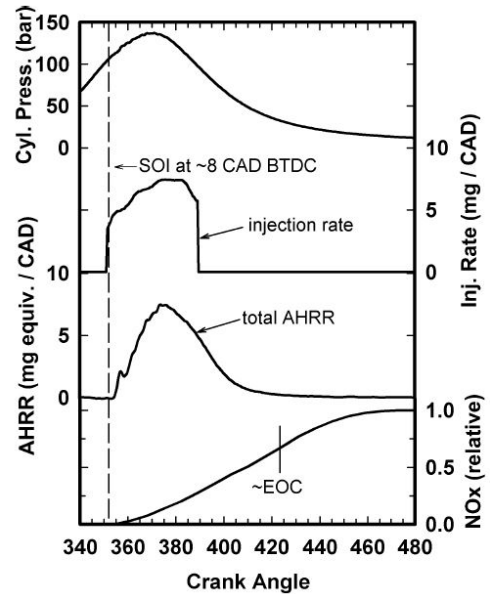


Figure 2.4: Relative  $NO_x$  concentration throughout the combustion process [15].

### 2.1.2 Particulate matter

Particulate Matter is a general term used to denote a complex aerosol system, which is mainly constituted by elemental carbonaceous material (soot particles) which agglomerates and absorb other species (principally organic compounds coming from the fuel and lubricant oil) forming structure with complicate physical and chemical properties. The definition of particulate matter resort to the sampling method used to determine the amount of particulates emitted by a vehicle in the atmosphere, therefore changes in the particulate collection procedure and system results in different composition and structure. The mass measuring procedure involves the air dilution of the vehicle's exhaust gases, in order to cool down the exhaust stream before filtering through sampling filters where the particles are collected. The purpose of this laboratory dilution process is to represent the physical and chemical processes at which PM are exposed when emitted in the atmosphere from the vehicle's exhaust system. Most of the standards and regulations worldwide prescribe dilution ratios in the range of 3:1 - 20:1 so as to reach a sampling temperature not higher than 52 °C. Obviously, any change in the previous physical conditions under which the measurement is performed determines significant variation in size and composition of the emitted species as well as the use of different filters results in diverse particles collection. Being fiberglass filters able to capture solid particles as well as liquid droplets condensed during the dilution process, and accounting for the sampling procedure, PM can be defined as *any matter (solid and condensate liquid material) present in the diluted and cooled exhaust stream of an internal combustion engines, which is trapped on a sampling filter medium at 52° C.*

Diesel particulates are characterized by a bimodal size distribution constituted by a blend of nuclei mode and accumulation mode particles, as shown in figure 2.5. The first group is composed by the smaller-size particles with diameters ranging from 0.007 to 0.04  $\mu\text{m}$  and they usually are also referred to as nanoparticles, though the latter term indicates more properly all the particles featuring a diameter lower than 50 nm. Nuclei mode particles are primarily constituted by volatile compounds which consist of liquid hydrocarbon droplets and hydrated sulfuric acid nuclei ( $\text{H}_2\text{O}-\text{H}_2\text{SO}_4$ ) condensed due to the cooling and mixing along the exhaust system and in the atmosphere, and by a small amount of individual spherules of solid material such as carbon or metallic ash from lube oil additives. Their volatile part is very unstable and its concentration strongly depends on dilution parameters. Accumulation mode particles are formed by larger-size particles which are the results of agglomeration process of primary carbon spherules (soot) and other solid material (metallic ash, cylinder wear metals, etc) mixed with adsorbed or condensed heavy HCs and other condensation vapors (sulfate particles). Their diameters are between 0.04 and 1  $\mu\text{m}$  with high concentration between 0.1 and 0.2  $\mu\text{m}$ .

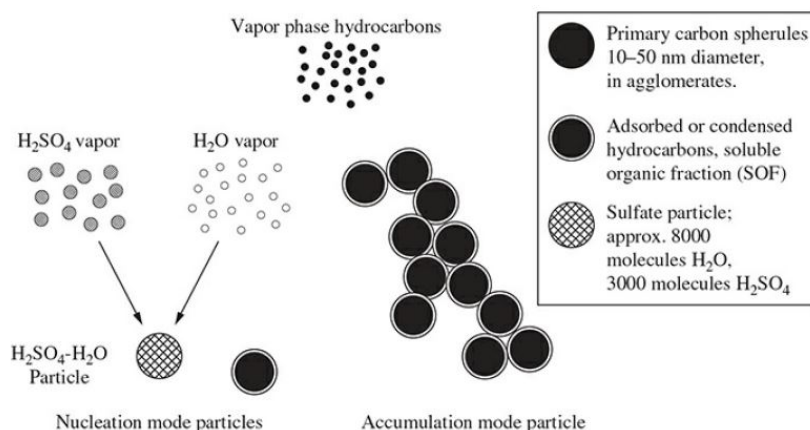


Figure 2.5: Components of diesel particulate matter: nucleation mode and accumulation mode particles [5].

Considering particulates distribution in terms of mass and number, as depicted in figure 2.6, we can notice that nuclei mode particles form the majority of the particle number (almost 90%), but they only retain a few percent of the PM mass, and conversely for accumulation mode particles. This analysis and classification of exhaust particulate emissions as concerns their number and dimension has brought, in recent years, to the introduction of an emission limit not only in terms of mass but also in number, since the smallest particles result to be even the worst from the human health perspective. Figure 2.6 reports a further subdivision in terms of particle aerodynamic diameter (particle size), which is characterized from 4 main regions dividing respectively: PM<sub>10</sub> ( $D_p < 10 \mu\text{m}$ ), fine particles ( $D_p < 2.5 \mu\text{m}$ ), ultrafine particles ( $D_p < 100 \text{ nm}$ ) and nanoparticles ( $D_p < 50 \text{ nm}$ ).

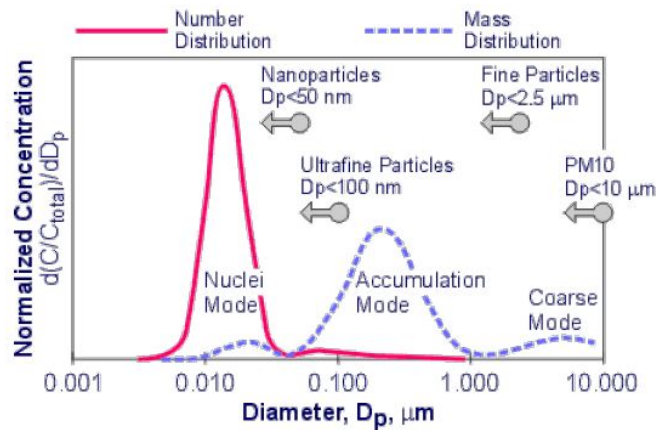


Figure 2.6: Normalized mass and number distribution of PM as a function of the aerodynamic diameter of the particles [17].

The chemical composition of PM can be identified by means of physical methods, such as thermogravimetric analysis, or by means of chemical methods which involve the use of a solvents to partition the different particulates fractions, either way, they produce comparable results and PM is usually divided into three main fractions, as reported in different colors in figure 2.7:

- Solid fraction (SOL), constituted of elemental carbon and metallic ash (nearly 54% of the total mass);
- Soluble organic fraction (SOF), composed from organic material (hydrocarbons) derived from engine lubricating oil and from fuel (about 32%);
- Sulfate particulates ( $SO_4$ ), formed from sulfuric acid and water (about 14%);

Metallic ashes consist of a mixture of different chemical species, which mostly come from lubricant oil additives used for several purposes. Being a considerable portion of the solid particulate fraction and affecting the life-span of diesel particulate filter (DPF), engine oils are expected to be not only low-sulfur but also low-ashes. Soluble organic fraction can be found as liquid only after the cooling in the atmosphere or in the laboratory dilution tunnel below 52 °C, while at diesel exhaust temperatures, most of SOF species exist as vapors especially at high engine loads. Thanks to spectroscopy analysis, SOF were seen to be composed in major part by hydrocarbons coming from lubrication oil and a minority by fuel HCs. As a consequence, oil adoption in diesel engines represents a choice of paramount importance to obtain acceptable particulate emissions.

Finally, the proportions, reported in figure 2.7, are representative of the specific case analyzed and not of general share of diesel exhaust particulates. Indeed, PM composition is affected by the engine operating conditions, therefore we have different distributions corresponding to diverse engine working points. In particular, we can distinguish at low load a higher share of SOF (wet PM) while at high load the solid fraction is dominant (dry PM).

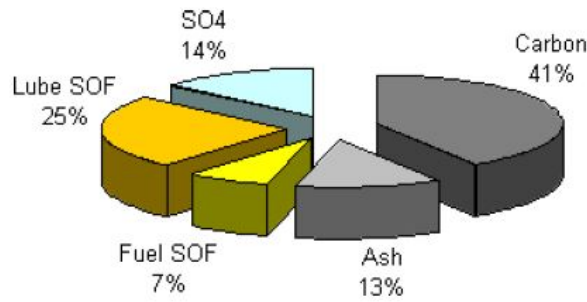


Figure 2.7: Particle composition typical of heavy-duty diesel engines under transient test cycle operating conditions [18].

### Soot formation

As previously suggested, the carbonaceous particles comprising part of the solid component of PM, also referred to as soot, form within the fuel-rich core of each combusting spray, while the SOF of the particulate and nucleation mode particles are later formed during the exhaust process, due to cooling and dilution when the gases leave the tailpipe (absorption and condensation). More in detail, soot formation occurs after the start of combustion in very rich-fuel region ( $\phi \approx 2-4$ ) inside the spray at temperatures of about 1600 K and pressure of 100 bar. In those conditions, fuel pyrolysis processes lead to fragmented fuel molecules which, in turn, react to form polycyclic aromatics. The latter molecules grow within the spray until forming soot particle nuclei (nucleation) which keep growing (surface growth) into soot individual particles that agglomerate each other to constitute accumulation mode particles (agglomeration). In this regard, PAHs are considered one of the principal soot precursor species. Pyrolysis process of fuel molecules which occurs in very fuel-rich mixture involves several mechanisms such as thermal cracking, condensation and polymerization, and dehydrogenation, that culminates in soot nuclei production. Two main reaction paths for soot production can be identified on a temperature and mixture composition basis as shown on the left side of figure 2.8. At relative low temperature ( $< 1700$  K) condensation reactions take place between PAHs with substantial rate of soot production, which are typical of fuel-rich premixed burn condition. At higher temperature and less rich mixture, fragmentation reactions involving both aromatics and aliphatics molecules generate soot nuclei with a slower production rate, close to diffusion flame region of the combustion plume.

About soot particle, lattice-imaging shows that particles are made of carbon atoms which are arranged in plane with hexagonal face-centered arrays, named platelets, which in turn are organized in layers to form crystallites, as depicted in figure 2.8 (right).

The latter are then structured with their planes in such a way to realize concentric lamellae around the particle center.

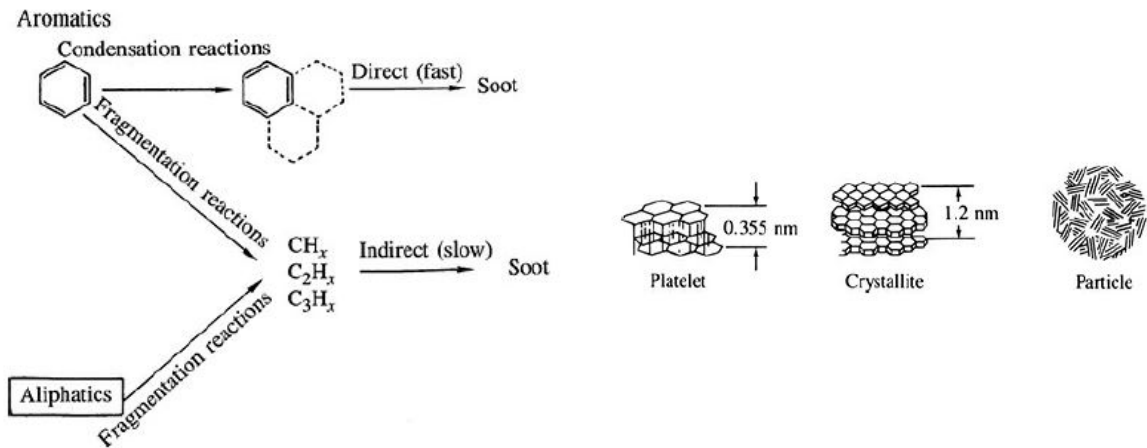


Figure 2.8: *Left:* Soot formation mechanisms paths from aromatic and aliphatic HC compounds. *Right:* Soot particles substructure [5].

Figure 2.9 graphically resumes the overall path which directs to particulate emissions, highlighting the in-cylinder steps for soot (accuulation mode) particle formation. The above process explains the reason for which soot concentration temporally and spatially increase along the spray downstream the premixed burn region, up to the jet head vortex in the region adjacent to the on-going diffusion flame, as seen in section 1.3.2. Finally, the last process in PM formation sequence, which occurs when the exhaust gases exit the cylinder, concerns the absorption and condensation of hydrocarbons and other species due to mixing with air, that gives rise to nuclei mode particles.

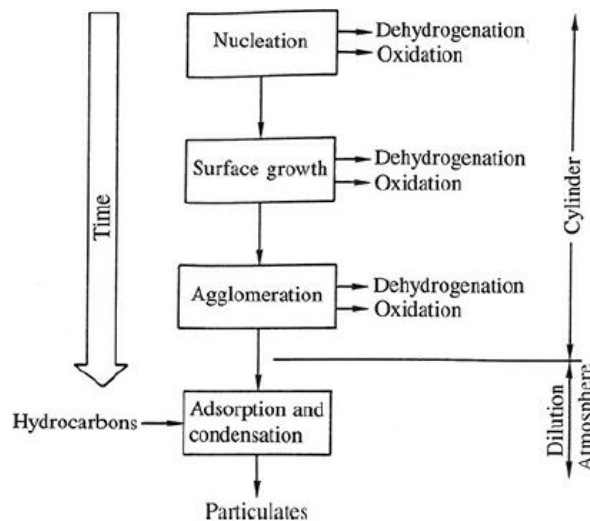


Figure 2.9: Schematic of primary processes for production of diesel particulates [5].

## Soot oxidation

Soot oxidation mechanisms are of primary importance for the understanding of emission level related to the solid fraction of particulate matter. Indeed, soot tailpipe emissions are considered to be the result of a balance between soot formation and oxidation mechanisms. As indicated during the description of the conceptual diesel combustion model, soot oxidation at precursor, nuclei and particle stages within the fuel spray can occur in an almost complete way, before the exhaust process commences. The most significant mechanism leading to soot particle oxidation is due to OH radical attack at diffusion flame level under close-to-stoichiometric conditions. Spray environment nearby and within diffusion flame is characterized by a low concentration of  $O_2$  with respect to OH radicals which are plentiful, therefore soot burning due to O and  $O_2$  is far less significant than that related to radicals attack. Therefore, soot formed within the spray due to the combination of products of a fuel rich combustion (which also provides the local heating for pyrolysis) at a relatively low temperature ( $\approx 1600$  K) enter the diffusion flame from fuel side, then the successive heating to diffusion flame temperature ( $\approx 2700$  K) which causes particles burn out. This process could theoretically lead to complete soot oxidation, however due to the intrinsic complexity and non-homogeneity of the diesel combustion process, local phenomena such as diffusion flame quenching could prevent full soot burning before the exhaust stroke begins. Further details regarding soot burn out process were extrapolated by optical investigation during late combustion phase in [19]. Nevertheless, provided that oxygen disposal and temperature are high enough (at least 650 K) post flame soot oxidation can still take place during the particle travel from the combustion chamber to the exhaust line. As a result of that, tailpipe soot will be dependent on several occurrences and mechanisms, and in that regard, models to predict soot emission level are rather complicated to be conceived.

### 2.1.3 Carbon monoxide

Internal combustion engine carbon monoxide (CO) emission are mainly determined by the value of the fuel/air equivalence ratio ( $\phi$ ) or relative air/fuel ratio ( $\lambda$ ) and by the kinetics of the reactions involved. Figure 2.10 show the variation in CO emissions for eleven different gasolines (i.e. with diverse stoichiometric air to fuel ratio) which fall nearly on the same curve, underlining the dependence of this emission level from the relative air/fuel ratio and not on the fuel composition. Moreover, the fundamental role of chemical kinetics on the definition of CO level at the exhaust, it is reported in figure 2.11, where kinetically controlled calculation were compared with actual CO measurement and curves at TC combustion and exhaust conditions equilibrium value. It can be noticed that experimental measured values fairly agree with the kinetically derived curve, while curves at equilibrium value feature large discrepancy in CO levels, emphasizing once more the importance of reaction kinetics knowledge.

Being CO emissions basically defined by the air/fuel ratio, this pollutant is of primary concern for spark-ignition engines (the highest in terms of volume among the other pollutants) which typically operate at stoichiometric value until part load and at slightly rich values at full load or during engine warm up. Instead, for conventional diesel engine which always operate on the lean side of stoichiometric, CO level are far lower than in SI engines and they are not considered to be of importance with respect the other pollutants. However, for sake of completeness a brief and general description regarding CO production mechanisms as a function of air-to-fuel ratio is hereto discussed.

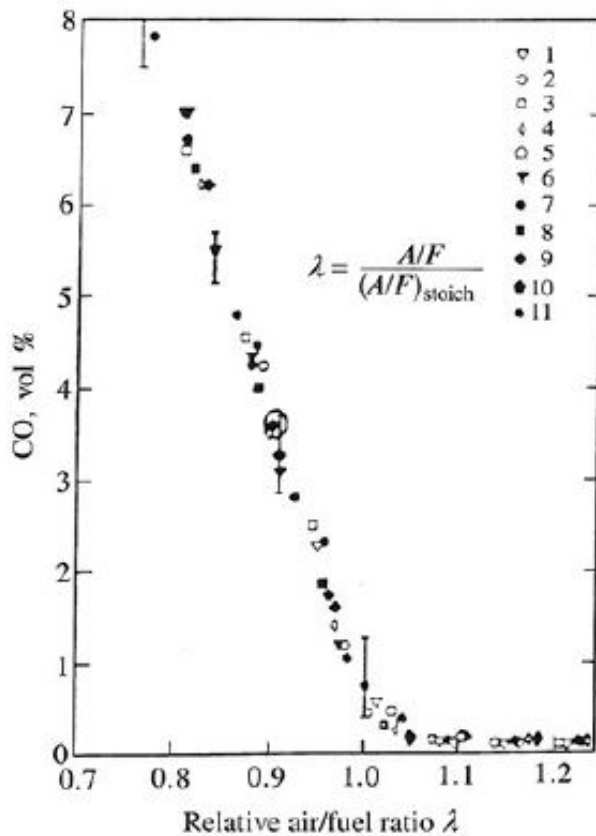


Figure 2.10: SI engine CO emissions for eleven different fuels as a function of relative air/fuel ratio  $\lambda$  [4].

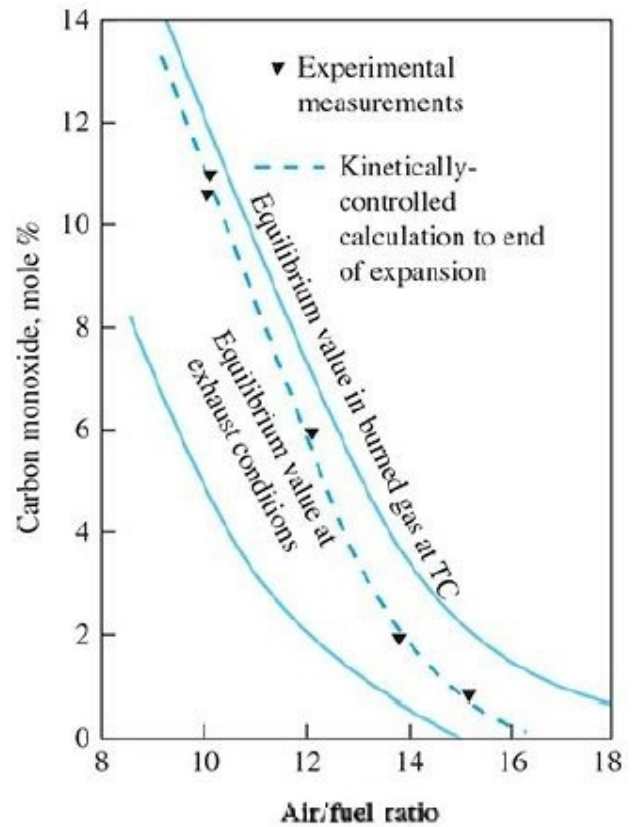


Figure 2.11: Kinetically predicted CO emissions compared to experimental measurements and equilibrium curves at TC combustion and exhaust conditions versus air/fuel ratio [5].

The combustion process is constituted by several reactions which bring fuel hydrocarbons to complete their oxidation process. CO formation is one of the principal reaction in the hydrocarbon combustion mechanism, as summarized below.



where R stands for hydrocarbon radical. Then, the formed CO is oxidized in  $CO_2$ , by a principal oxidation reaction 2.8 which represents the last and the slowest step in the combustion path.



Therefore, in rich mixture all the fuel might reach the intermediate oxidation level of CO, but only part of the formed carbon monoxide will complete the oxidation turning into  $CO_2$ , due to lack of oxygen. However, even for stoichiometric mixtures, where a sufficient amount of oxygen is available for CO oxidation, notable presence of this pollutant can be found at the exhaust. This can be explained considering the fact that at high temperatures during the combustion process ( $\approx 2800$  K) chemical equilibrium can be reached, therefore, the dissociation of  $CO_2$  into CO and OH (reverse reaction) contributes significantly to CO production. Moreover, dissociation consistently participates to CO emissions level even in case of rich operation where maximum peak combustion temperature is achieved. In fact, dissociation reaction rate becomes considerable only over a temperature threshold of about 1850 K, which is well-overcome especially in the slightly rich side. Considering a lean field of operation, CO concentration is far lower thanks to the high excess of oxygen, however, its presence is justified again by a small contribution of dissociation and from the late oxidation of some hydrocarbons. Finally oxidation of CO in the exhaust system cannot occur without a devoted after-treatment system because the gas temperature is too low. Indeed, CO oxidation reactions are effectively prevented by the sudden decrease in temperature which the gases experience during the expansion stroke, which does not allow any significant change in chemical composition of the burned gases.

#### 2.1.4 Unburned hydrocarbons

Hydrocarbon emissions results from the several processes which prevents these organic compounds, constituting the injected fuel, to complete the combustion reaction or even to utterly escape the in-cylinder oxidation reactions. Contrarily, to nitrogen oxides and carbon monoxide, organic emissions are not a well-defined chemical species and they can be constituted of pure HCs, partially reacted and fragmented fuel compounds. The level of unburned hydrocarbons in CI engines is significantly lower than that of SI engines, however, due to their high reactivity and high molecular weight nature, the amount of emissions is not an accurate index of their impact on environmental pollution, as a consequence their reduction is still of primary importance. Once again, the complex and non-homogeneous features of diesel combustion results in several processes which can contribute to hydrocarbon emission in these engines. HC formation mechanisms which are relevant for SI engine such as fuel adsorption and desorption in the oil layer and fuel trapping and leakage due to the crevice volume are not of importance because fuel injection commences just before the start of combustion therefore during the compression stroke only air is present within the cylinder. Taking into account the four stages into which the CI combustion process has been divided and the sequential or

simultaneous occurrence of fuel evaporation, fuel-air-burned gas mixing, premixed rich and diffusive flame burn up, typical of multi-sprays DI diesel engine, the following phenomena have been identified as the main sources of engine-out hydrocarbon emissions.

**Overmixing** During the ignition delay, the fuel injected vaporizes and mixes with the hot air entrained within the spray creating a distribution in fuel/air equivalence ratio, as shown in figure 2.12.a, which goes from a rich mixture region ( $\phi \approx 2-4$ ) in the bulk of the spray to a lean region at the boundary of the developing jet. At the spray periphery, where a higher disposal of air is present, some fuel will overmix producing an overlean mixture beyond the lean combustion limit ( $\phi \approx 0.3$ ) and as a result, this mixture will not autoignite. Although, part of the previous mixture might burn later early enough in the expansion stroke thanks to the mixing with hot burned products, these oxidation reactions are relatively slow so the fuel may not be fully oxidized. Therefore, the presence of this overmixed region generates unburned fuel, partially oxidized products and fuel fragments which might escape the cylinder without being completely burned. The impact on HC emissions of these overlean region is strictly connected to the amount of fuel injected during the ignition delay, the mixing rate with air and the extent of the ignition delay itself. Typically, the longer the ignition delay the more significant is the overleaning mechanism as a source of hydrocarbons emissions.

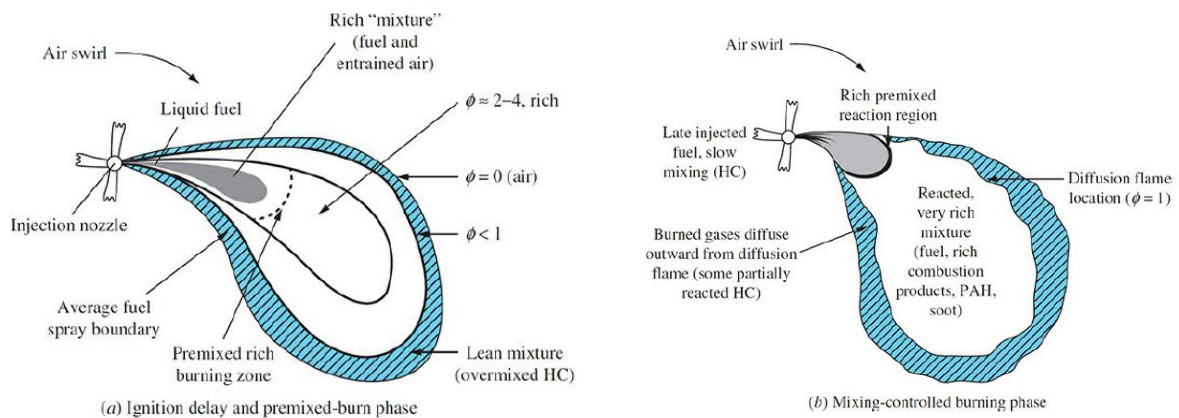


Figure 2.12: Combustion plume development and composition during premixed (a) and mixing-controlled combustion (b) phases in DI diesel engine with swirl [5].

**Undermixing** For fuel injected when the combustion is commenced, slow or under mixing with air has been found to be the major cause of HC emissions, as shown for example in figure 2.12b. Mixture over-riching can be the consequence of fuel which enters the combustion chamber from the injector nozzle at low velocity and of working conditions in which the engine operates with an excess of fuel. Being the injector closure not ideal, i.e., not instantaneous, during this phase the needle is throttling the fuel at nozzle

level reducing the difference of pressure between the sac volume and the combustion chamber environments, which consequently reduce the injection velocity of the fuel and deteriorates the atomization and vaporization processes as well as fuel mixing with air. Moreover, the small volume present in the tip of the injector after the needle seats, the sac volume, is filled with fuel which during combustion and expansion phases is heated and vaporized leading to its ingress in the cylinder at low velocity and/or late in the combustion process again penalizing proper mixing and eventually escaping the primary oxidation process. Therefore, the sac volume represent the parameter which affects the amount of HC emission due to this mechanism. Generally the smaller this volume the lower are the extent of the emissions, however, the presence of such volume in the nozzle tip is meant to uniformly distribute the fuel pressures on the nozzle orifices which, in turn, helps reducing exhaust smoke level, so trade-off solutions for the injector has to be adopted (micro-sac injector). Engine over-fueling is another condition in which local mixture over-riching can occur. Though, for DI diesel engine the full load overall equivalence ratio is limited by the black exhaust smoke (about  $\phi=0.7$ ), under transient condition especially during acceleration phases, an excess of fuel might enter the cylinder and locally create over-rich condition which prevents proper HC oxidation and last until the exhaust stroke. Then, under normal operating condition this mechanism is not relevant, while during vehicle tip-in manoeuvre it can contribute to HC emissions which drastically increase for equivalence ratio of about 0.9.

**Quenching** Another mechanism contributing significantly to engine-out HC emissions regards the combustion flame quenching mainly due to the interaction between combustion plumes (bulk quenching) and wall quenching. The first process involves the interaction among sprays (spray overlap), which develop downward and radially during the combustion phase, and they might come in contact each other generating confined air pockets in which oxygen is quickly consumed, hence leading to partial diffusion flame quenching. The second and more relevant mechanism is related to the wall quenching of the flame. Similarly to spark ignition engines, when the flame reaches the combustion chamber walls, which for CI engine means to reach the piston bowl walls, it encounters an air layer which temperature is approaching that of the wall itself. This temperature is far lower than that to support combustion, therefore mainly due to thermal exchange process the flame quenches. Another interaction with the wall which leads to diffusion flame termination is connected to oxygen starvation, i.e., the rugged profile of the jet periphery due to its turbulent nature results in having different contact points between the combustion plume and the piston wall bowl, this create confined regions in which oxygen is rapidly consumed leading the extinction of the flame. Further details regarding diffusion flame interaction with the wall and the corresponding extinction mechanisms can be found in [20]. The extent to which wall quenching impacts on HC emissions is related to the degree of spray impingement on the combustion chamber walls and so it is strictly related to the characteristics of the injection system.

Finally, the relative importance of the different mechanisms leading to the presence of unburned HCs at the exhaust obviously varies with engine operating conditions. Typically, mixture overleaning results to be a relevant source of hydrocarbons under engine light-load operation, while over-riching is more relevant under overfueling conditions, that is, during transient operation from low to high load working points. Generally, engine-out HC emission in diesel engine are higher during engine idling and low load condition and less significant at near full-load operation.

## 2.2 Diesel combustion noise

Noise generation coming from internal combustion engines is a significant problem with which engine designers have to deal with, especially for diesel engines, in order to comply with the ever stringent vehicle regulations regarding noise pollution. Nowadays, the demand for vehicles with increased specific power, reduced weight and improved fuel consumption is technically requiring engines with higher in-cylinder pressure level and reduced overall weight, characteristics which call for further efforts in diminishing noise emissions coming from ICEs.

The major sources contributing to engine noise can be schematically divided as follows:

- **Combustion noise**, caused by the steep combustion-produced in-cylinder pressure rise which is transmitted to the piston, cylinder head and walls. The impact due to the sudden pressure rise results in vibrations which are conveyed throughout the engine structure, hence causing noise generation;
- **Mechanical noise**, produced by the impacts between the different engine's mechanical parts constituting its main kinematic chains, under normal operating conditions. Then, there are several sources generating this noise contribution among which we have: vibrations caused from the piston slap phenomenon due to the forces acting on the piston which at TC position moves from one side to the other of the liner, noise generated by the impacts of the valves on their seats, noise coming from the fuel-injection system (injectors closure), noise due to the drivetrain (gear and chain drives) and vibration inducted on the crankshaft bearings due to the oscillating nature of forces acting on it;
- **Gasdynamic noise**, generated by the cyclic substitution of the working fluid within the engine's cylinders. Therefore, we can distinguish intake noise, generated by the pressure waves set up by the periodic induction processes into each cylinder, and exhaust noise due to pressure waves created by each cylinder blowdown process in the engine's exhaust system. Once these pressure pulses, of not negligible amplitude, flow across the intake and exhaust systems, they enter the atmosphere producing the associated audible noise. Typically, gasdynamic noise has a higher contribution to the overall engine noise emission than that of mechanical origin;

Internal combustion engines featuring boosting have an additional source of noise which, in case of constant-pressure turbocharging, is related to the turbocharger.

However, their implementation brings some noise reduction enhancement, since the turbocharger upstream plenum dampens the exhaust pressure pulsation which obviously less true for alternative impulse boosting system [21]. As previously said, the contribution of combustion noise component on the other noise sources is particularly significant in compression-ignition engines. The typical diesel combustion noise is strictly related to the combustion features of these engines, because the sudden rise of the in-cylinder pressure, which excites the engine structure generating the distinctive acoustic emission of CI engines, is the result of the almost instantaneous burn of the fuel accumulated during the ignition delay. Therefore, there is an obvious dependence between the intensity of the premixed-burn phase and the level of noise emitted. Techniques to attenuate this phenomenon primary rely on the reduction of the in-cylinder pressure first derivative, by adopting different injection strategy, such as pilot injections or injection rate shaping, which both allow to reduce the mass of fuel burned in the premixed phase. Finally, engine structural design actions, like engine block stiffening, can play as well an important role in combustion noise dampening by reducing vibration and sound radiation.

## Chapter 3

# Exhaust gas recirculation

In this chapter exhaust gas recirculation (EGR) technology will be illustrated due to its relevant importance to the thesis herein discussed. First, its basic definition will be addressed together with its current, new and past applications for diesel engines. Then, EGR working principles are described, pointing out its calculation methods and spending some words on its relevant effects on emissions and performance. Afterwards, EGR system configurations will be discussed with attention to the most diffused layouts. Finally, some details regarding the implementation of cold exhaust gas recirculation and the corresponding device utilized will be presented.

### 3.1 Definition

Exhaust gas recirculation is an emission control technology which involves returning a portion of the engine's exhaust gas to the combustion chamber through the inlet system, as schematically shown in figure 3.1.

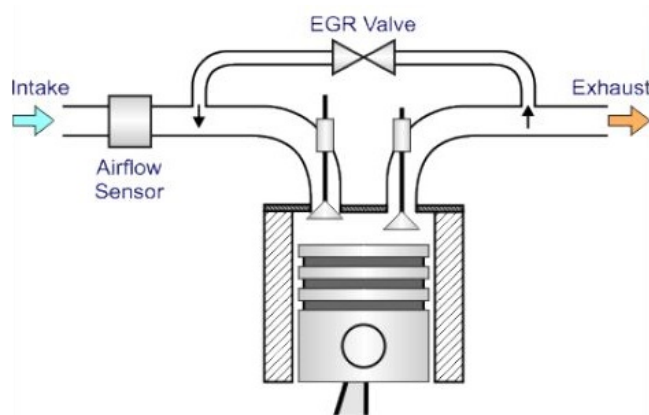


Figure 3.1: Schematic representation of an EGR system for diesel engines [22].

This method was conceived to reduce  $NO_x$  emissions and it is today utilized in most types of modern diesel engines (light duty, heavy duty) and with a reduced extent also for gasoline engines.

Such result is achieved thanks to significant heat extraction from the combustion process which lowers the peak combustion temperature, and to the displacement of some inducted fresh air charge which reduces the inlet charge oxygen concentration, both of which degrades nitrogen oxides formation during the combustion process.

The first commercial employment of EGR as a  $NO_x$  control measure is dated back to the 1970s starting with gasoline engines even if experimental applications have been already previously explored. Gradually, it was introduced to passenger car diesel engines in the early 90's and at the beginning of 2000s even for heavy-duty diesel engines in order to comply with the ever-stringent emission standard regulations [22]. Nowadays, the aforementioned regulations are driving engine researches to develop alternative combustion modes applicable to diesel ICE to reach simultaneous abatement of PM and  $NO_x$ . These combustion approaches are characterized by lower combustion temperature and a higher degree of charge homogeneity with respect the conventional diesel combustion and, as it will be described in detail in chapter 4, to realize such advanced combustion strategies a large degree of dilution is necessary. As a consequence, EGR technologies also becomes an important enabler to achieve low temperature combustion (LTC).

## 3.2 Working principles

As already said, intake charge dilution with exhaust gases results in the simultaneous reduction of the peak combustion temperature and the oxygen mass fraction entering the cylinders and so in nitrogen oxides production degradation. Temperature lowering represents the primary factor in  $NO_x$  emission inhibition and Ladommatos et. al. experimentally identified three different effects concurring to the temperature diminution during compression stroke and combustion process [23, 24, 25, 26].

**Dilution effect** It consists in the reduction of oxygen mass concentration due to the displacement of oxygen in the fresh intake air charge by inert gas. This results in a reduction in the local flame temperature caused by the widening of the combustion flame zone related to the diminution of the oxygen mass fraction [26]. In this broadened flame zone an increased proportion of non-oxygen molecules is present and absorb heat from the combustion process;

**Thermal effect** It involves the increase in the average specific heat capacity of the intake charge due to the large amount of  $CO_2$  and  $H_2O$  contained in the recirculated exhaust gas. Indeed, these chemical species substitute part of fresh air molecules which are characterized by lower specific heat capacity, therefore resulting in a augmented heat absorption ability;

**Chemical effect** It regards the reduction of the average combustion temperature due to endothermic dissociation reactions of carbon dioxide and water;

Figure 3.2 depicts the relative importance of the three effects on  $NO_x$  reduction considering the amount of recirculated gas. It can be noticed that the dilution effect is the dominant factor in reducing the average combustion temperature while a smaller contribution comes from the chemical effect. Thermal effect was found to have an almost negligible influence on burning temperature and so on  $NO_x$  production rate.

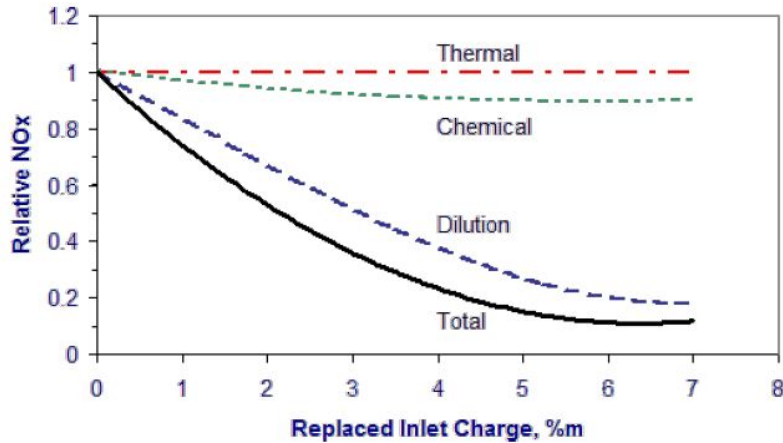


Figure 3.2: Relative  $NO_x$  reduction due to the three different effects of EGR as a function of the replaced inlet charge mass percentage [7];

An additional effect which could be included in the thermal effect of EGR is the so called thermal throttling. This consists in the increase in the inlet charge temperature as the EGR level is increased, since the exhaust gas temperature is higher than that of fresh air. Consequently, a decrease in the inlet charge density and in the in-cylinder trapped mass occurs. This behavior has a detrimental effect on nitrogen oxides reduction, since almost the same heat release due to combustion has to be shared with a smaller in-cylinder charge which has also entered the cylinder at a higher temperature. This determine an increase in the maximum temperature of the burned gases and sometimes this negative effect can prevail over the beneficial thermal effect previously discussed. As it will be explained, thermal throttling mitigation is one of the reasons for which cooled EGR implementation was introduced.

### 3.3 Effects on emissions and performance

Reduction of nitrogen oxides through EGR technology does not come free from some penalties regarding emissions and performance. Indeed, engines employing EGR strategy for  $NO_x$  abatement have to typically face increase in fuel consumption, PM, HC and CO emissions, worsened engine wear and reductions in engine durability. Considering conventional diesel engines, two main competing approaches are used to abate oxides of nitrogen which are EGR and injection timing retard. As depicted in figure 3.3, both in-cylinder control strategies presents pronounced drawbacks in terms of brake specific fuel consumption and particulate emissions.

Although the results reported are not only dependent from the engine operating point but also engine dependent, in a qualitative way it can be affirmed that EGR allows to achieve comparable reduction in  $NO_x$  emissions with less increase in bsfc with respect to injection timing retard. Conversely, injection timing retard permits nitrogen oxides diminution with less penalties in terms of PM emission in comparison to EGR.



Figure 3.3: Comparison between injection timing retard and EGR as strategies to achieve  $NO_x$  reduction and corresponding brake specific fuel consumption and PM emission penalties [7];

Figure 3.4 offers a deeper insight on how particulate matter emissions changes not only in terms of mass but also in terms of composition. It can be noticed that as EGR level is increased from level A to level D the total PM emission augmented, moreover the soluble organic fraction remains constant while the solid carbonaceous fraction increased from A to D. In addition to that, other research studies such as [31], demonstrated that increasing level of EGR causes a corresponding increase in particle number emissions as well as the emission of particles with larger size. It was hypothesized that soot particles reintroduced into the engine through EGR acts as nuclei for new particles and agglomerates to form larger particles.

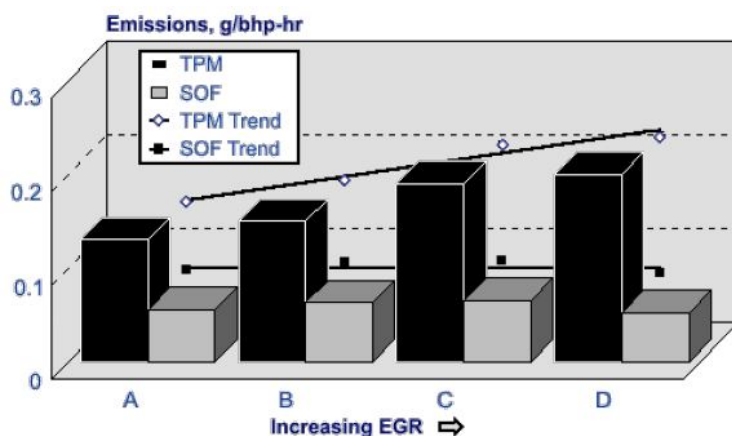


Figure 3.4: Effect of exhaust recirculation system on particulate matter emissions [29];

Apart from the above cited effect of EGR on soot emissions, generally engine-out smoke level is always the results of a balance between soot formation reactions and soot oxidation reactions. The introduction of EGR causes the reduction of inlet charge oxygen concentration which has been seen to deteriorate soot oxidation reactions rather than soot formation ones, which remains unaltered[27, 8]. Finally, depending on the operating load and the amount of recirculated gas, the impact of EGR on carbon monoxide and unburned hydrocarbons presents different patterns. Typically, when an increase amount of EGR is employed, lower load conditions features penalties in terms of CO and HC emissions which are less than those at higher load due to the large amount of oxygen contained in the exhaust. Moreover, EGR could worsen mechanisms such as over-mixing and bulk quenching which together with contemporaneous combustion phasing retard lead to increased emissions levels when a larger quantity of EGR is utilized.

### 3.4 Calculation methods

In order to quantify the amount of recirculated exhaust gas two commonly EGR rate ( $X_{EGR}$ ) definitions can be adopted depending on the experimental equipment at disposal. Indeed, EGR level can be computed by employing its basic mass-based definition or alternatively considering a gas-concentration calculation which is related to the strict connection between  $CO_2$  or  $O_2$  variation with EGR quantity as shown in figure 3.5.

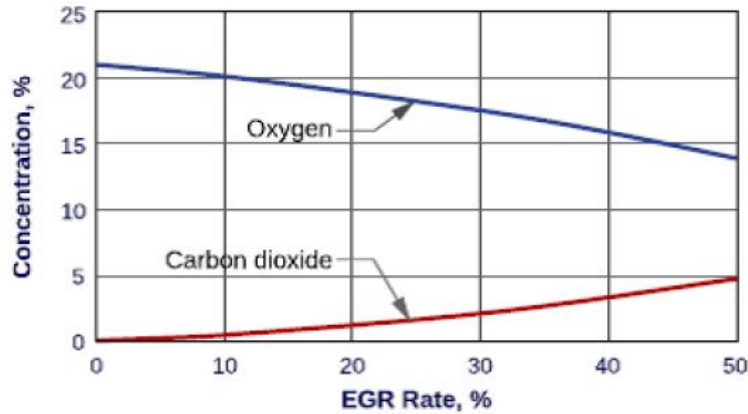


Figure 3.5: Inlet charge oxygen and carbon dioxide concentration as a function of EGR rate [22];

**Mass-based EGR** The EGR mass fraction can be defined as the ratio between the recirculated exhaust gas mass flow rate and the total mass flow rate which is inducted in the cylinder:

$$X_{EGR} = \frac{\dot{m}_{EGR}}{\dot{m}_{air} + \dot{m}_f + \dot{m}_{EGR}} \quad (3.1)$$

where  $\dot{m}_{EGR}$ ,  $\dot{m}_f$  and  $\dot{m}_{air}$  are the EGR, fuel and fresh air mass flow rates, respectively.

Since fuel mass flow rate is typically an order of magnitude lower than air mass flow, a simplified definition is more often utilized:

$$X_{EGR} = \frac{\dot{m}_{EGR}}{\dot{m}_{air} + \dot{m}_{EGR}} \quad (3.2)$$

EGR rate definitions 3.1 and 3.2 are practically difficult to be employed because of the complications in measuring the EGR mass flow rate due to the tough exhaust environment conditions. Therefore, a practical mass-based computation of the EGR level is performed by exploiting the mass air flow sensor (MAF) and the following equation:

$$X_{EGR} = 1 - \frac{\dot{m}_{air(wEGR)}}{\dot{m}_{air(w/oEGR)}} \quad (3.3)$$

where  $\dot{m}_{air(wEGR)}$  and  $\dot{m}_{air(w/oEGR)}$  are the measured fresh air mass flow rate with EGR and the air mass flow rate without EGR application, respectively.

**Gas concentration-based EGR** Definitions based on gas concentration measurements are commonly employed during test bench experimental investigation. These requires the knowledge of the volume concentration of species at the engine exhaust and the estimation of the combustion air composition at the engine intake. Typically, EGR mass fraction can be evaluated by  $CO_2$  volume concentration measurements in the intake and exhaust manifold according to the following formula:

$$X_{EGR} = \frac{[CO_2]_{int} - [CO_2]_{amb}}{[CO_2]_{exh} - [CO_2]_{amb}} \quad (3.4)$$

where  $[CO_2]_{int}$ ,  $[CO_2]_{exh}$  and  $[CO_2]_{amb}$  are intake, exhaust and external environment carbon dioxide volume concentration, respectively.

An alternative definition to calculate the recirculated EGR level, conceptually identical to the previous one, is based on the measurement of oxygen volume concentration:

$$X_{EGR} = \frac{[O_2]_{int} - [O_2]_{amb}}{[O_2]_{exh} - [O_2]_{amb}} \quad (3.5)$$

where  $[O_2]_{int}$ ,  $[O_2]_{exh}$  and  $[O_2]_{amb}$  are intake, exhaust and external environment oxygen volume concentration, respectively.

### 3.5 EGR configurations

Exhaust gas recirculation strategy can be implemented in diesel engine through different configurations. A first distinction can be done by considering the way in which the exhaust gas are recirculated, differentiating the use of external EGR and internal EGR applications.

In the latter typology, no external circuit is necessary to drive the exhaust gases back into the cylinders, but recirculation is realized by acting on intake or exhaust valve control. Indeed, internal EGR is performed by means of additional opening events such as exhaust valve post-opening during the intake phase or intake valve pre-opening during the exhaust phase. This internal EGR system requires the adoption of a modified valve actuation technologies, including:

- Modified cams with permanent double openings;
- Dual lift systems which allows to avoid the additional openings when they are not required;
- Variable valve actuation system (VVA), which permits to freely control the activation/deactivation of the additional openings as well as to modulate the valve lifts;

As far as external EGR strategies are concerned, they require the realization of a devoted circuit which collects the exhaust gas and guide them back into the intake manifold. Different layouts have been developed over the years and the most commonly employed in turbocharged heavy-duty diesel engine are herein reported. The configuration depicted in figure 3.6 is the so called high-pressure loop (HPL) or short route EGR. In this systems, exhausts are intercepted in a point upstream of the turbocharger in the exhaust manifold and they are routed through an EGR cooler, an EGR control valve and then inducted into the intake manifold downstream of the intercooler. The pressure differential between the exhaust and intake environments together with the EGR valve controls the EGR flow toward the engine cylinders. When high EGR rate are necessary the natural pressure differential could be not high enough, therefore, a couple of solution to facilitate the EGR flow towards the inlet duct were developed. These are intake or exhaust valve throttling (more common in light and medium duty diesel engines) and the use of a venturi (typically used for heavy-duty), as shown in figure 3.6. The latter solution generally provides less fuel economy penalties with respect to the first two, and its proper design could improve EGR-fresh air mixing reducing the EGR distribution unbalance in the cylinders.

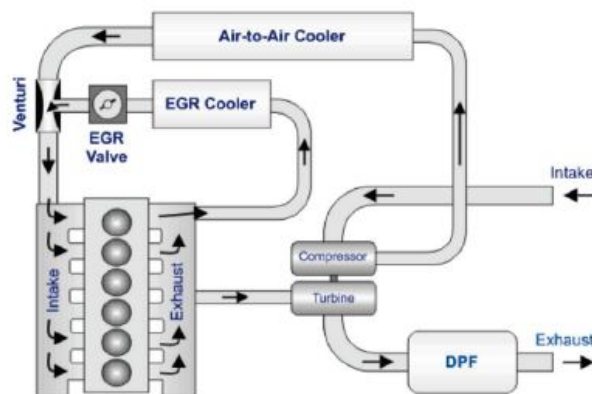


Figure 3.6: Schematic representation of a high pressure loop (HPL) or short route EGR system [22].

Common shortcomings associated with HPL EGR system are related to EGR cooling capability, turbocharger efficiency and penalties in terms of fuel consumption and PM emissions with respect other configuration. However, it offers very fast response during engine transient operation and its plumbing is straightforward and well-adaptable to today engine-vehicle layouts.

Another scheme for external EGR adoption in heavy-duty diesel engine is the low-pressure loop (LPL) or long route EGR system, shown in figure 3.7. In this case, the exhaust gases are not directly sourced from a pre-turbine location, instead, they are filtered through a diesel particulate filter (DPF), and then recirculated from a point downstream the latter. Exhaust gas pressure downstream the turbine (or DPF) is at lower level than that of the intake manifold where air is boosted, therefore, to promote the flow, EGR is introduced back in the engine just upstream the turbo-group compressor after being cooled. In this way, the natural pressure differential between these two environments is usually adequate to guarantee the required EGR flow rate, which is controlled by the EGR valve and if necessary it is increased through intake throttling in similar fashion to HPL layout.

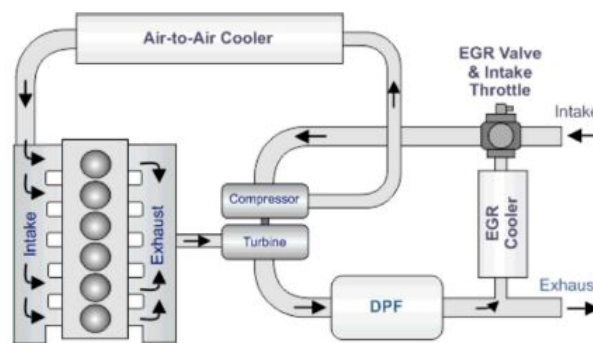


Figure 3.7: Schematic representation of a low pressure loop (LPL) or long route EGR system [22].

Advantages of the long route EGR system include:

- Lower fuel consumption than HPL configuration as a result of better turbocharger efficiency, since in HPL implementations exhaust gas are taken from point upstream the turbocharger resulting in a loss of exhaust kinetic energy through the turbine wheel;
- With the presence of the DPF, the LPL EGR provides filtered exhaust to the engine inlet manifold through the turbocharger compressor. As a result, engine durability can be better preserved;
- Exhaust gas taken from downstream the turbocharger turbine is cooler than that furnished from upstream the turbo-group, as in the HPL case. As a consequence, long route EGR provides a higher heat absorbing capacity for similar flow rates to those of short route EGR. This characteristic gives the opportunity to reduce the EGR cooling requirements (size of the EGR cooler) as well as reducing the cooling load rejected in the engine water jacket to be handled by the radiator;

- The introduction of EGR upstream the turbocharger compressor results in better EGR and fresh air mixing which in turns reduces the cylinder-to-cylinder EGR distribution imbalance;

Despite its advantages, the LPL EGR system presents a number of reasons for which it has not been favored over the HPL EGR system application:

- Although the long route EGR is sourced with exhaust gas taken downstream the diesel particulate filter, its content of carbonaceous material (soot particles) is far from being null, since the trapping efficiency of the filter is less than 100%. With the presence of carbonaceous material in the recirculated exhaust stream, its impact on the compressor wheel during high speed operation may potentially erode the wheel itself, that would require special machining and surface treatment;
- In cases where air-to-air intercoolers are used, unfiltered matter flowing through the narrow cooler passages would likely be trapped and it would accumulate over time. Consequently, air flow to the engine would be compromised leading to performance, emissions and fuel economy degradation;
- Long route EGR is characterized by a slower response during engine transient operation than that of HPL EGR, because of the higher volume of residual gas between the EGR valve and the combustion chamber to be displaced during rapid acceleration manoeuvres;
- LPL EGR configuration calls for cumbersome and complicate plumbing arrangements;

In order to overcome the shortcomings of both LPL and HPL EGR system, or better to combine together their points of strength, the integration of the two system has been explored by engine researches. Typical utilization strategies establish that during engine warm up phases and when high transient response are required short route EGR is employed, conversely in all the other working conditions.

### **3.6 EGR cooling and EGR coolers**

The utilization of cooled EGR was driven by the benefits brought in terms of trade-offs between  $NO_x$  and fuel consumption and particulate matter. As a matter of fact, the lower the temperature of the recirculated gas the higher the heat absorption capacity during the combustion process and so the lower the rate of nitrogen oxides formation. Moreover, lower temperature EGR means that a reduced volume of inlet fresh air is displaced, resulting in improved volumetric efficiency and less oxygen diminution which helps maintain combustion efficiency. As a consequence of that, it can be desirable to adopt cooled EGR approach to diesel engines.

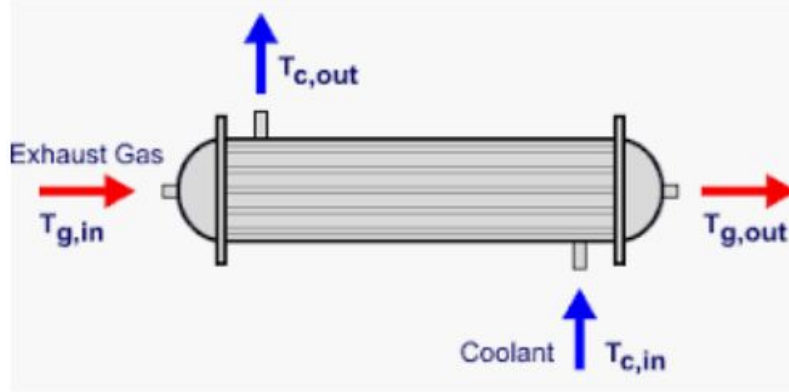


Figure 3.8: Schematic representation of an EGR heat exchanger [28].

Figure 3.8 shows a schematic representation of an EGR cooler through which exhaust gas flow through tubes of a shell-and-tube heat exchanger, meanwhile they cool down thanks to the heat transfer with the cooling water flowing outside these tubes. Materials selected for tubes have to feature high heat conductivity, strength and resistance to corrosion which are typically found in stainless steel with chromium, nickel and molybdenum. EGR coolers are generally characterized by tubes with one, two or three-pass cooling flow paths, whose number is determined by the trade-off between cooling capacity and pressure drop loss. The higher the number of cooling flow paths the larger the temperature reduction achievable, but the higher the pressure drop across the heat exchanger which is a critical design factor to be accounted for EGR flow management. Another element reducing the cooler effectiveness and pressure loss is the so called EGR fouling problematic resulting from the condensation mechanism of hydrocarbon and PM on the wall of the cooler. Apart from the discussed improvement given by the exploitation of cooled EGR, there are engine working conditions where EGR cooling could not be expedient in terms of fuel economy improvement and HC and CO diminution. For instance, hot EGR could be beneficial during cold temperatures and idle/no-load operations for which the recirculated gas can be by-passed from the cooler by employing a devoted by-pass valve. Similar strategy are also usually utilized during engine warm-up period to shrink the time to light-off for the after-treatment system devices.

## Chapter 4

# Advanced diesel combustion modes

In this chapter, advanced combustion modes will be addressed focusing on practical diesel application strategies. The fundamentals concerning these relatively new combustion approaches will be presented together with the main advantages and limitations. Then, a recently developed conceptual combustion model [33], in a similar fashion to Dec's conventional model, will be reported to provide the general traits of the in-cylinder combustion processes involved in advanced diesel compression-ignition engines.

### 4.1 Generalities

Advanced compression-ignition combustion is a general term regarding alternative forms of CI combustion which involves conventional diesel fuels as well as gasolines, or even other fuel typologies. Conventional CI diesel engines are the most fuel-efficient engines thanks largely to their reduced throttling losses and their rather high compression ratio, however, they feature a relatively high pollutant emissions, especially nitrogen oxides and particulate matter. Earlier emissions targets were initially met without the need of exhaust-gas aftertreatment systems, but by means of in-cylinder strategies utilizing both engine calibration and design parameters, such as higher fuel injection pressure, higher boost, exhaust-gas recirculation employment and improved combustion chamber design. Thereafter, a combination of in-cylinder strategies and aftertreatment systems were necessary to be in compliance with the emissions regulations, with the obvious added cost of the latter technologies. As a consequence, the need for further reducing engine-out noxious emissions, driven by the ever stringent pollutant emissions limits, and the request for high efficiency, to reduce fuel consumption, led engine-combustion researchers and development engineers to investigate new combustion approaches reasonably capable of offering contemporaneously both attributes. Different methods were begin investigated, all of which rely on the principle of dilute premixed or partially premixed combustion to reduce emissions. Charge dilution can be realized either being lean with fuel/air equivalence ratio, hence using a large excess of air, or by using high levels of EGR for different values of  $\phi$ . The effect of dilution is that of lowering the combustion temperature, while the enhanced mixing aims to uniform the fuel/air equivalence ratio across

the combustion chamber, therefore, trying to obtain an almost homogeneous lean mixture before the compression ignited combustion occurs. This combustion approach is exemplified by a process which is commonly known as *homogeneous charge compression ignition* (HCCI), in which a diluted and well-premixed charge is compression ignited. The lower combustion temperatures together with the high degree of mixture premixing result in low emissions of  $NO_x$  and inhibition of particulate matter formation, with thermal efficiencies comparable with those of conventional diesel engines. Practical application of classic HCCI with diesel fuel is hindered due to the fuel's low volatility, which complicates the mixture formation process, and its ease to autoignite, which does not permit an easy control on the start of combustion. As a result of that, alternative HCCI-like combustion involving the use of conventional diesel fuel are pursued by engine manufacturers and they are commonly referred to as *diesel low temperature combustion* (LTC). Actually, HCCI can also be considered as a low temperature combustion approach, however the main difference with LTC modes is related to the degree of premixing the charge undergoes. Indeed, several diesel LTC strategies with various names and acronyms have been investigated in literature, all with the aim to obtain a sufficient partial premixing of the diluted charge so that combustion temperature and equivalence ratio combinations are such that to avoid  $NO_x$  and soot formation, as shown in figure 4.1. Therefore, even if low temperature combustion strategies do not feature a complete premixing, they basically adopt the same principle of HCCI to reduce PM and nitrogen oxides, i.e., dilution and enhanced mixing with respect conventional CI combustion.

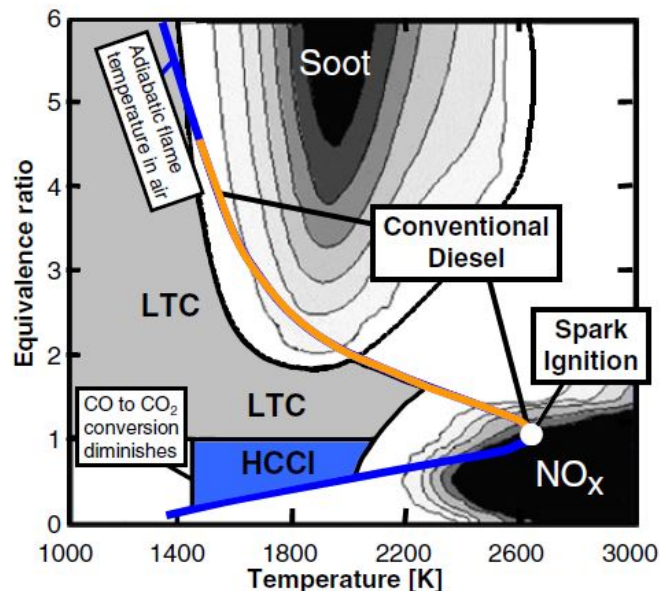


Figure 4.1: Kamimoto-Bae diagram or  $\phi$ -temperature diagram showing ranges of mixture composition and temperature for  $NO_x$  and soot formation as well as conventional combustion path and regions for HCCI and LTC combustion modes [32].

Figure 4.1 represents the  $\phi$ -temperature diagram, or even called Kamimoto-Bae diagram, which depicts the combinations of equivalence ratio and local flame temperature leading to

formation of soot and nitrogen oxides (darkened contours highlight increasing concentration) and distinguish the regions of application of LTC and HCCI combustions. The blue-orange line can be thought to be representative of the chemical and thermal path a diesel fuel particle burning under conventional combustion conditions, which, as already discusses, bring to the production of non negligible amount of  $NO_x$  and soot. As it will be addressed, major drawbacks concerning those advanced combustion modes consist of the increased amount of carbon monoxide and unburned HC, mainly due to the high charge dilution which reduces the cylinder oxygen content, and the related worsening of combustion efficiency. Furthermore, combustion noise associated to the rapid in-cylinder pressure rise has also to be managed because of the longer ignition delay, typical of advanced combustion modes, which are needed to achieve a sufficient premixing.

## 4.2 HCCI combustion

Homogeneous charge compression ignition combustion represents an ideal combustion process for ICE, because it would allow to achieve near-zero level of nitrogen oxides and particulate matter as well as comparable thermal efficiency to conventional diesel engines. Conceptually, these goals can be reached by realizing a diluted homogeneous mixture which autoignites due to compression-heat at temperature lower than those typical of conventional ICE. If ideal HCCI conditions were created, the spontaneous autoignition event occurs simultaneously in the whole cylinder, as shown in figure 4.2, without taking place at a specific location of the spray as in conventional diesel and with the absence of a high temperature propagating flame as in spark ignition engines. In real HCCI application, the mixture would not be perfectly homogeneous either in composition or temperature, hence, combustion happens sequentially beginning in the hottest zone of the combustion chamber, and following in the next ones.

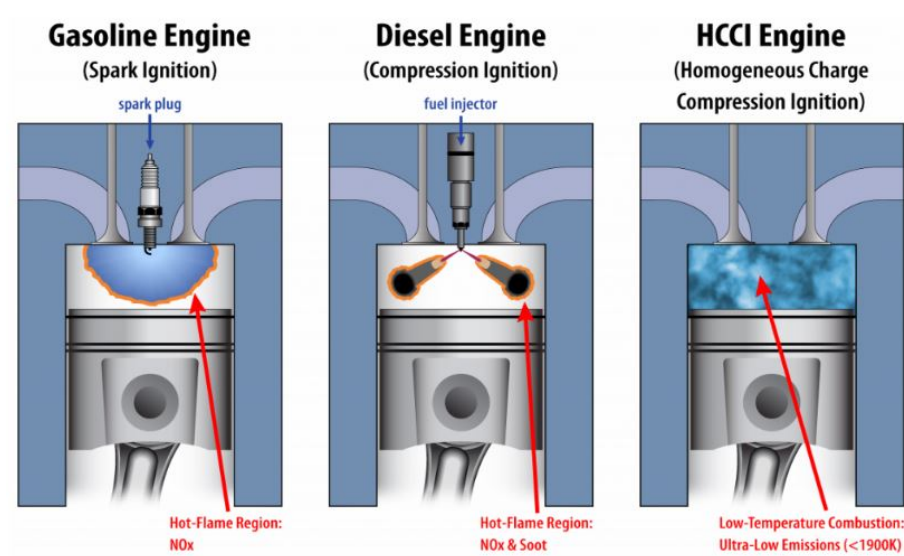


Figure 4.2: Schematics representing combustion process attributes in conventional gasoline and diesel fueled engines, and homogeneous charge compression ignition engine [31].

In practical HCCI, the high degree of premixing between the vaporized fuel and air, needed to obtain a lean homogeneous charge prior to compression, can be realized by allowing long in-cylinder mixing times or even external mixing strategies. In particular fuel is delivered by employing:

- **Port-fuel injection**, fuel is injected in the intake port prior or during the induction process;
- **Direct injection**, fuel is directly injected into the combustion chamber during the intake stroke or very early in the compression stroke;

Direct injection combustion systems permit to realize partially stratified HCCI with the aim to intentionally produce a more heterogeneous lean mixture which allows to mitigate some of the major limits of this combustion typology. As a matter of fact, HCCI combustion is promising in terms of in-cylinder  $NO_x$  and PM emissions reduction, however, the intrinsic characteristics of this combustion results in some main technical hurdles [32] to deal with, which limit HCCI operating range and hinder its adoption to transportation engines. The major working limitations affecting homogeneous charge compression ignition combustion can be summarized as follows:

- **Low load combustion efficiency, CO and unburned HC emissions**, HCCI power output depends on the fueling rate, and theoretically without the aid of any throttling. Therefore, as the load reduce the mixture becomes leaner and leaner causing combustion efficiency reduction and a significant amount of carbon monoxide and unburned hydrocarbons to be emitted. The reason behind these occurrences are connected to the fact that at low load such high degree of mixture dilution results in combustion temperature reduction ( $\approx 1500$  K), preventing bulk gas reactions, such as  $CO$ -to- $CO_2$ , to go to completion before the expansion stroke begins. Even if emissions are not of second importance, they can be managed with basic oxidation catalyst, while the combustion efficiency diminution is of major concern. The obvious dependence of these quantities from the equivalence ratio could suggest the introduction of throttling for idle and low load conditions which, in turn, leads to pumping losses which penalize the cycle efficiency. One suitable solution which brings higher combustion efficiency and reduced CO and unburned HC is the adoption of charge stratification by injecting the fuel sufficiently late after the end of the intake stroke. The latter strategy allows to create a mixture which is locally richer and so which burns hotter and more completely ensuring lower CO and HC emissions and so higher combustion efficiency.
- **High load limit**, HCCI upper load operation is limited by the excessive increase of the pressure rise during combustion, which results in engine knock phenomenon. As fueling progressively increases from low to moderately high loads, pressure-rise rate features a consequent rise, eventually reaching values of  $\phi$  for which it causes the engine structure to resonate generating the typical noise and pressure trace ripple associated

with a knocking engine. As a consequence, the value of pressure-rise rate has to be kept under control in order to guarantee acceptable level of noise emission and prevent engine damages. The maximum value of the in-cylinder pressure first derivative (max pressure-rise rate) strictly related to the engine type and operating conditions, and above all from the value of equivalence air-fuel ratio. Consequently, HCCI engine allowable  $\phi$ , and so its upper working load, is limited by the maximum admissible value of in-cylinder pressure rise which prevents the occurrence of knock. Actions as mixture thermal stratification and combustion-phasing retard are the main tools to slow down the in-cylinder pressure rise so as to render the engine more tolerant to higher working  $\phi$  and improve its operating load range.

- **Fuel effects**, Gasoline and diesel conventional fuels are characterized by opposite features which would be advantageous to mix to obtain the best possible fuels for HCCI and HCCI-like combustion modes. On one hand, gasoline fuels are relative volatile and this is beneficial for mixture formation, however, they require relatively high temperature to be compression ignited due to their typical low molecular weight, compact and rigid hydrocarbon blend composition. On other hand, diesel fuels are characterized by a relatively high boiling temperature which complicates the mixture formation process requiring intake heating, moreover they exhibit a relatively easy tendency to autoignite making difficult to control the start of combustion in case of premixed mixture. As a result, merging the above attributes, fuels suitable for HCCI combustion which exhibit intermediate characteristics, i.e., which are sufficiently volatile for correct mixture formation and adequately prone to be compression ignited, can be beneficially employed. Nevertheless, researchers are focusing their attention on developing combustion strategy and design solution which enables to use standard fuel due to their availability for transportation engines.
- **Combustion phasing control**, HCCI ignition timing is kinetically controlled, namely, chemical kinetics plays a major role on the temporal location of the ignition event. As a result, start of combustion is decoupled from injection timing and consequently its occurrence cannot be controlled as done for conventional diesel engines, but it should be regulated by managing mixture temperature and composition. A substantial control on combustion phasing is of primary importance, since too advanced combustion leads to efficiency penalties, high noise and increase knocking chances while too late phasing increase the probability of having misfiring cycles which cause high HC emissions and reduced engine performance. As said, combustion phasing control can be conceptually reached by either controlling mixture reactivity (or equally composition) or the temperature evolution along the engine cycle. Some practical approaches concern of conditioning intake charge temperature, changing intake charge composition by employing different exhaust gas recirculation rates or by controlling its degree of homogeneity, modifying gas temperature during the compression stroke with variable compression ratio or variable valve timing technologies or even water injection. Even

so, these methods are often not enough to guarantee a sufficient cycle-to-cycle control.

Research efforts are aimed to overcome the previous technical limitations, so as to provide an extended working range for HCCI mode, not only for full HCCI engine applications but also for ICE in which hybrid combustion strategies are adopted, i.e., the engine operates in HCCI combustion mode at low loads while it switches to conventional diesel combustion (or SI) operation at high loads.

### 4.3 Diesel LTC

Research groups and development engineers have been trying to apply HCCI combustion to diesel engine due to the potential low emission and high efficiency characteristics of this advanced combustion mode. However, as already mentioned, diesel fuel attributes such as low volatility and high cetane number render rather complicate the mixture formation process and the combustion phasing control. Other fuel could be advantageously used but the promising implementation of hybrid combustion strategies still make diesel fuel desirable. First attempt to realize a proper HCCI diesel combustion, required intake charge heating, especially for PFI (port-fuel injection) in order to minimize liquid fuel accumulation and reduce in-cylinder inhomogeneities which are responsible for worsened soot,  $NO_x$  and HC emissions. Due to latter heating and diesel ease to autoignite the engine geometrical compression ratio was reduced to prevent knock, moreover poor combustion efficiency was achieved due to high levels of HC emissions. As a consequence of the reduced CR and incomplete combustion, fuel consumption resulted to be substantially higher than conventional diesel engine, even if  $NO_x$  and soot emission were noticeably reduced.

Difficulties found in advantageously implementing homogeneous charge compression-ignition combustion on diesel engines, led to the development of HCCI-like diesel combustion or diesel low temperature combustion were pursued, with the main distinctions regarding the degree of mixture homogeneity formed before ignition and the fact that start of combustion is more closely coupled to fuel injection event than HCCI case, even though chemical kinetics still play an important role. Several diesel LTC combustion strategies can be found in literature, herein two broad subcategories, comprising their common features, will be discussed.

#### 4.3.1 LTC strategies

Diesel LTC combustion are advanced combustion modes which exploit the same principle of HCCI, namely, the realization of a premixed diluted mixture so as to obtain a low temperature combustion and a higher charge homogeneity in order to avoid PM and nitrogen oxides formation during the fuel oxidation process. These advanced diesel combustion approaches are even termed as *partially premixed compression ignition* modes since they adopt direct injection with shorter mixing time than HCCI obtaining a more heterogeneous charge which can be not only fuel-lean but also fuel rich (smokeless rich combustion approach). For LTC strategies the ignition dwell, namely, the time between the end of injection and the ignition

event, is usually positive in contrast with conventional diesel conditions for which this dwell time is negative. Therefore, diesel LTC are characterized by combustion for which the ignition delay is longer than the injection duration (positive ignition dwell). The request for a positive ignition dwell is motivated by need to obtain a sufficient premixing before autoignition. Indeed, for conventional diesel only part of the fuel is premixed before the ignition, while for diesel LTC being the injection event ended before the initiation of combustion, there is enough time to obtain a high degree of premixing which also involves the portion of fuel at the very end of injection. Such combustion features can be achieved by using moderate to high EGR rates, which reduces the mixture reactivity and so delay ignition. Furthermore, injection duration is primary factor to guarantee a positive ignition dwell, fact which is translated in the necessity to have short injection duration, therefore limiting the LTC approaches to low load operation. Diesel LTC strategies can be divided into two categories on the base of fuel-injection and combustion timing, which are also referred to as *early direct-injection LTC* and *late direct-injection LTC*. Injection timing is either earlier (early LTC), in the middle of the late part of compression stroke, or later (late LTC), near TDC or at the beginning of the expansion stroke, than conventional diesel engine. Compared to conventional timing, in both case the fuel is injected in a lower temperature and density in-cylinder environment, either because of the reduced compression or as a results of the cooling due to expansion. These thermodynamic conditions at the initiation of injection together with ignition-delaying and temperature-lowering effects of EGR, guarantee enough time to accomplish a sufficient pre-combustion mixing and having reduced combustion temperature, approaching HCCI combustion characteristics.

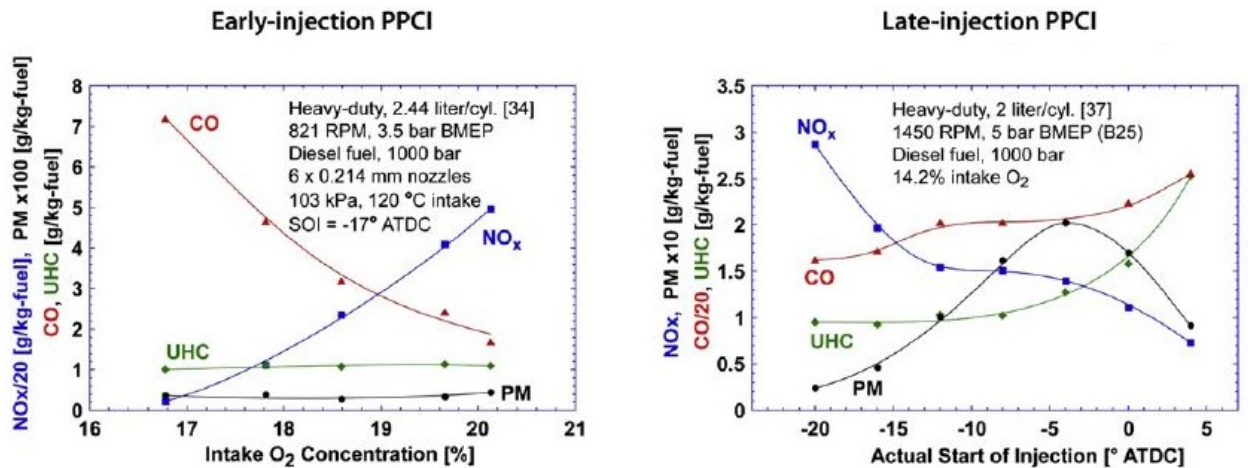


Figure 4.3: Emissions patterns for both low load early-injection and late-injection LTC operation in a heavy-duty engine application as a function of intake oxygen concentration and start of injection [33].

Despite the promising  $NO_x$  and soot engine-out emissions given by the adoption of these low temperature combustion approaches, other emissions such as CO and unburned HCs are difficult to be kept under control. Moreover, the typical LTC fuel burning process is

associated to high pressure-rate rise, therefore combustion noise can be another quantity which determines constraints in terms of injection timing and dilution, leading to further penalties in terms of CO and unburned HC emissions. Figure 4.3 depicts typical emissions patterns concerning a heavy-duty diesel engine operated at relatively low load with early LTC (left) and late LTC. The left diagram describes how emissions varies as dilution, and so oxygen concentration, is changed for a fixed early injection timing, while the right plot highlights the effect on emission of the injection timing for a fixed oxygen concentration in case of late LTC. In either cases, working conditions corresponding to high level of carbon monoxides and unburned hydrocarbons emissions, are associated to reduced combustion efficiency, which, in addition to improper heat release phasing, results in higher fuel consumption than the conventional diesel case. Therefore, proper engine design and adequate parameters calibration represent a major challenge to obtain the largest benefits from LTC applications.

### **Early direct injection LTC (PCCI)**

As said above, early direct injection LTC is a way to realize a near-HCCI combustion which is also referred to as *Premixed-Charge Compression Ignition* (PCCI). With this approach, direct-injection of fuel typically occurs after halfway the compression stroke, where higher in-cylinder gas temperature and density enhance vaporization and mixing processes with respect to the conventional close to TDC ( $\approx 10^\circ$ bTDC) injection. The larger degree of premixing obtained with early-DI system and the already cited diesel fuel characteristics, require the use of a high level of cooled EGR in order to control the mixture reactivity, thereby slowing autoignition process in order to avoid early ignition and knocking. Other actions to improve the control on the initiation of combustion are directed to the adoption of engines with reduced compression ratio, or/and valve actuation technologies which permit to adapt the intake valve closure so as to control the effective compression ratio. However, these solutions are often not capable of offering a robust combustion-phasing control with changes in engine speed and load, because in early injection techniques the autoignition timing is highly depending on the mixture characteristic (pressure, temperature and dilution) and less coupled with injection timing. As for all LTC strategies, PCCI is attractive for the extremely low  $NO_x$  and particulate matter emissions, however, CO and unburned HCs level are usually higher than conventional diesel combustion. One solution to reduce hydrocarbon emissions is connected to the use of different diesel injector typologies which can attenuate wall wetting caused by injection taking place relative lower temperature and density in-cylinder environment which results in spray over-penetration. Conventional diesel injectors spray attributes does not match the need of a softer and more disperse jet to reduce fuel-liner impacts and so HC emissions. Nevertheless, the use of traditional DI diesel injector would allow to realize hybrid combustion strategies for low and high load working points. As a result of that, more-conventional injector with narrowed spray-cone angle could be an intermediate solution to simultaneously decrease spray impingement on the cylinder liner and being able to run the engine with classical diesel combustion at high load. Early-injection LTC load range

limitations involves the risk of misfire at low loads for too EGR diluted mixture, and the excessive burning rate causing high noise and even engine knock at moderate-high loads.

### **Late direct injection LTC (HPLI)**

Another approach explored to achieve an HCCI-like combustion involves late fuel injection in proximity or even slightly after TDC, which is even called in literature as *Highly-Premixed Late Injection* (HPLI) or late PCCI. Being the injection event close to TDC or even in the early part of the expansion stroke, high pressure are typically required to provide a sufficient rapid mixing. Moreover, dilution with EGR as well as injection timing are the main tools exploited to both extend the ignition delay to increase the premixing time and to realize a low temperature combustion process, so as to achieve the typical emissions benefits. The effect of retarding the injection timing is that of letting the fuel enter the combustion chamber and mix with air-EGR charge during the early part of expansion stroke, therefore at a lower temperature, which lengthens the jet-mixing process (delay autoignition). In this LTC strategy, combustion timing is more closely related to injection timing, therefore, even if chemical kinetics is still a relevant element in controlling the combustion-phasing, a somewhat easier heat release positioning can be realized for HPLI by acting on start of injection. On the contrary, the degree of mixture homogenization reached is lower, then combustion instability is further worsened and closed-loop combustion control should be adopted in similar fashion to PCCI. Comparing this second approach to early LTC, it allows to achieve slightly higher load working points thanks to its retarded injection which permits a lower pressure-rate rise and so combustion noise. Nevertheless, in this case fuel consumption is not only penalized by the increase in CO and hydrocarbons emissions but also by a shifted combustion center of mass after TDC, which results in having a large portion of the fuel burning process during the expansion stroke.

Finally, proper diesel LTC implementation requires the support of technologies capable of providing an improved combustion and charge control, as well as enhanced fuel injection systems. The development of such hardware is of pivotal importance to realize practical engine applications which take the highest advantages of LTC modes, especially when mixed combustion strategies want to be accomplished.

### **4.3.2 LTC conceptual model**

In order to fully exploit the potentiality of those low temperature combustion strategies, a deep understanding of the in-cylinder physical and chemical processes responsible for engine performance and pollutant emissions is necessary. Indeed, optical diagnostic investigations on conventional diesel combustion engines led to significant knowledge of the spray formation, vaporization, mixing and ignition as well as pollutant formation and destruction. Therefore, in similar fashion to Dec's conventional diesel combustion model, a general phenomenological description of advanced combustion approaches was proposed [33]. The combustion

conceptual model conceived by Pickett and co-workers is not representative of all the LTC strategies, indeed, it is meant to characterize a subset of low-load, single-injection (early or late), partially premixed, exhaust-gas diluted compression ignition conditions. This model will feature diesel fuel-type injections with longer liquid-fuel penetration, prolonged ignition delay to guarantee an enhanced mixing between air and fuel and a more visible and extended two-stage ignition chemistry than conventional diesel case.

### **Two-stage ignition**

Ignition and heat release patterns for low temperature combustion modes as well as HCCI combustion are rather diverse from those of conventional diesel, as shown in figure 4.4 for early LTC case. This differences are caused by the greater mixture dilution, improved premixing and in-cylinder gases temperature and pressure when fuel enters the combustion chambers. Diesel fuel's autoignition chemistry is characterized by two stages, namely, a low temperature oxidation reactions which occurs at about 800 K where initial fuel breakdown leads to formation of free radicals, aldehydes and hydrogen peroxides, and a high temperature stage at about 950 K, reached thanks to the heat released in the previous stage and the compression heat, where the main energy release takes place. Depending on the relative reaction rate achieved during these low and high temperature oxidation steps, a two-stage ignition mechanism can be established, in particular when the low temperature oxidation path is slower than the other one. This autoignition pattern is strictly connected to the fuel's composition and the molecular structure of the individual hydrocarbons involved as well as mixture temperature. As a result, all diesel combustion approaches regardless of the persistence or not of a jet structure, either HCCI and LTC or conventional, feature this two-stage ignition chemistry, which is more distinct in the heat-release rate analysis for advanced combustion modes due to the slower first stage oxidation rate, while this transition is usually less evident for diesel conventional combustion where the two processes tend to merge in one continuous autoignition mechanism.

Figure 4.4 depicts the typical heat release and in-cylinder pressure trace trends, and needle lift for conventional and early-injection LTC. As discussed in chapter ??, classical diesel combustion is commonly divided in four phases considering the the apparent heat release shape: ignition delay, premixed burn, mixing-controlled burn and late combustion period. Injection event occurs near TDC in a relatively high temperature and dense environment where fuel mixes and eventually vaporizes with ambient gases which is manifested in the AHRR (apparent heat release rate) as a negative dip.

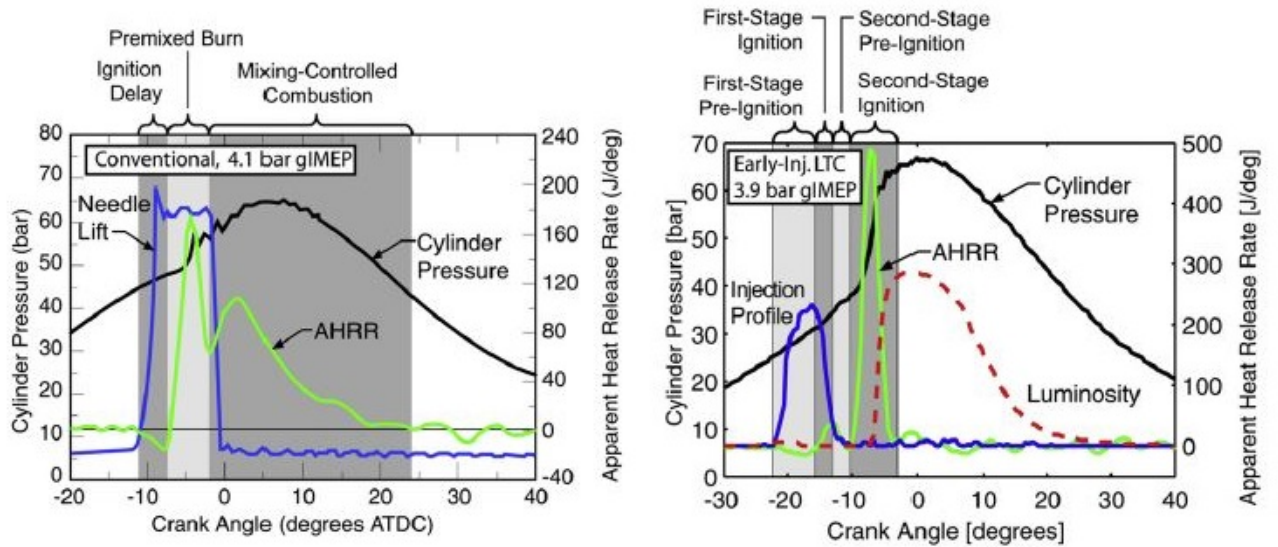


Figure 4.4: Apparent heat release rate, in-cylinder pressure and needle-lift or injection profile for low-load conventional diesel combustion and low-load early direct-injection low temperature combustion [33].

As the ignition reactions proceed in the hot mixture and become more exothermic, exceeding the vaporization rate, the AHRR turns positive marking the thermal start of combustion and the end of the ignition delay. The heat release during this first burning phase (premixed burn) is mainly controlled by the chemical kinetics, i.e., by the mixture formed during the ignition delay, and by the mass of fuel accumulated throughout the delay period. After the premixed burn AHRR peak, the latter decrease to lower values as the appearance of the diffusion flame marks the beginning of the mixing controlled combustion phase. During this burning period combustion occurs in a standing premixed flame within the jet, fed by rich air/fuel mixture and in the diffusion flame at the jet interface between fuel-rich combustion products and surrounding ambient gases. Rate of combustion is now controlled not by chemical kinetics but by mixing, namely, by the rate at which rich mixture is provided at the standing flame and fuel and air is delivered to the diffusion flame. As the injection ends, combustion occurs only at diffusion level. For typical LTC conditions, the AHRR holds additional traits connected to the chemical kinetics of diesel-fuel ignition, usually not visible in traditional diesel combustion. Considering early-injection case, the AHRR behavior is at first similar to that of conventional diesel combustion, however injection is almost ended before the first stage of positive heat release takes place, and the latter results to be not significant and short-lived compared to the traditional diesel case. Indeed, a subsequent heat release fall occurs, corresponding to the so called negative temperature coefficient chemistry which lasts up to the second stage high temperature autoignition. Thereafter, the HRR steeply rise resulting in a peak far greater than conventional combustion, leading to greater combustion noise level. Then, the heat released decrease almost to zero, with a minor mixing controlled combustion portion. Late-injection LTC is characterized a similar AHRR pattern, with a

somewhat lower peak and a larger mixing-controlled combustion portion. Regardless of the LTC strategy, the AHRR portion for low temperature combustion can be approximately divide into four parts preceding the small mixing controlled portion, that are: first-stage pre-ignition, first-stage ignition, second-stage pre-ignition, second-stage ignition. All of them are strictly related to separated chemical kinetics occurrences.

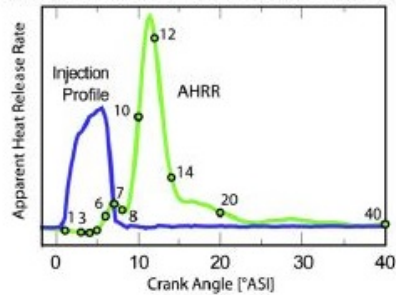
### Conceptual model

The conceptual combustion model conceived by Pickett and co-authors herein reported represents an extension of Dec's model for low-load, EGR diluted, partially premixed, single injection low-temperature diesel combustion for which ignition occurs at or after the end of injection. Figure 4.5 shows a schematics for a heavy-duty case which applies to both early and late injection LTC strategies, even though some spatial and temporal quantitative characteristics are obviously diverse depending on the operating conditions and fuel injection timing. In similar manner to the conceptual conventional diesel combustion model, the temporal and spatial evolution of the fuel-jet entering the combustion chamber is provided, with no distinction between soot and its precursors and additional information about the first stage of ignition pattern.

Shortly after start of fuel injection ( $\approx 3^\circ$  ASI), diesel LTC jet evolution is analogous to that seen in conventional conditions, i.e., liquid and vapor fuel penetrate together up to when liquid penetration is stopped by vaporization process and only the vapor phase keeps advancing in the combustion chamber. For early LTC the cooler and less dense environment, in which fuel is injected, determines longer liquid length and faster penetration than conventional conditions. Instead, for late LTC, being in-cylinder gases temperature and density similar to those of conventional case, liquid length and penetration velocity are of the same order of magnitude, as well. As the injection rate peaks, the successive deceleration of liquid fuel exiting the injector increases the local ambient gases entrainment next to the nozzle. As the injection ramps down and eventually ends, an increased entrainment region is formed in the wake of a propagating wave ( $5.0^\circ$  ASI) downstream the fuel jet. When the head of the entrainment wave passes the liquid length ( $7.0^\circ$  ASI) the enhanced mixing helps to vaporize the downstream liquid portions of the spray and typically fuel is fully vaporized within  $\approx 1^\circ$  after the end of injection ( $\approx 8.0^\circ$  ASI) in LTC conditions.

As the jet continue to penetrate the cylinder, first chemiluminescence emission are noticeable at about  $6^\circ$  ASI (indicated by the double-ended arrows), highlighting a divergent behaviour between conventional and LTC ignition processes.

Heavy-Duty Low-Load, EGR-Diluted, Partially Premixed Low-Temperature Combustion



- Liquid Fuel
- Pre-ignition Vapor Fuel
- Head of Entrainment
- Wave
- First-Stage Ignition ( $H_2CO, H_2O_2, CO, UHC$ )
- First-Stage Chemiluminescence Emission Region
- Intermediate Ignition ( $CO, UHC$ )
- Second-Stage Ignition of Intermediate Stoichiometry or Diffusion Flame ( $OH$ )
- Second-Stage Ignition of Fuel Rich Mixtures
- Soot or Soot Precursors (PAH)

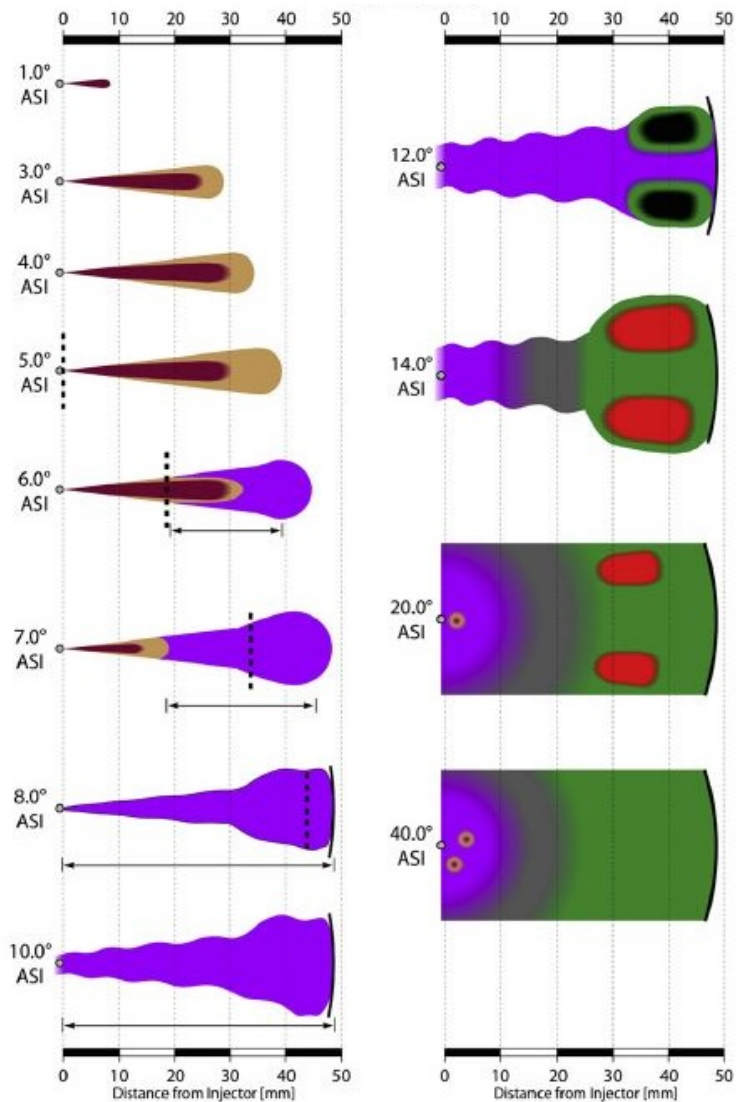


Figure 4.5: Schematics describing low temperature combustion conceptual model for low-load, single injection, EGR diluted, partially premixed, heavy-duty direct injection diesel engine [33].

As a matter of fact, in conventional diesel jet the premixed burn start some 2° after the first chemiluminescence appears (few degree after start of injection), and no distinction among first and second ignition stage can be described by the AHRR trace. For LTC conditions, the chemiluminescence appearance is not only delayed but it also persists much longer than classical diesel combustion, then producing a visible first ignition stage event near 7° ASI. After the end of injection the jet structure tends to widen from the early conical shape and eventually, very late in the cycle, this original shape is no more distinguishable due to jet-to-jet mixing (or jets blending) and interaction with piston bowl-wall. A near to stoichiometric second stage of ignition begins when fuel injection is ended (near 12° ASI), therefore no steady diffusion flame is established as in conventional case and OH radicals distribution

is spread across the downstream cross section in a mixture of intermediate stoichiometry and not confined at the jet periphery. As the combustion process proceeds some fuel-rich pockets containing soot precursors and/or soot appear for LTC far downstream the jets, typically near the head vortex or in region where jets interaction or impingement on the piston bowl-wall take place. These rich pockets, after an initial growth in size, are oxidized as the combustion progresses ( $\approx 40^\circ$  ASI), since they are surrounded by OH radicals. Finally, for some LTC conditions part of the mixture could not have enough time to reach the second stage of ignition before expansion cooling, therefore, part of the mixture do not complete the oxidation process leading to unburned hydrocarbons and carbon monoxide emissions.

# Chapter 5

## Experimental set-up

This chapter will address the experimental setup utilized to perform the herein described research activity. First, the tested engine will be illustrated focusing on its design modifications for PCCI adaptation as well as its installation layout at the bench. Then, engine instrumentation necessary to collect temperature and pressure data will be described. Afterwards, the dynamic test bench layout specification of ICEAL (Internal Combustion Engine Advanced Laboratory) at Politecnico di Torino will be presented, by depicting the software employed for bench control and data acquisition, and by describing the corresponding hardware exploited for engine experimentation, management and data collection.

### 5.1 F1C PCCI engine

The tested engine has been derived from conventional FPT F1C engine, homologated Euro VI regulation, which was especially designed to run in PCCI combustion mode. Details concerning the engine hardware modifications and the utilized engine sensors are shown in the following sections.

#### 5.1.1 Engine layout

F1C conventional diesel engine is a four-stroke, four-cylinder, direct injection, 3.0 L displacement engine manufactured by FPT Industrial, shown in figure 5.1. This engine is endowed with a single-stage variable geometry turbocharger (VGT), high-pressure common-rail injection system and short-route cooled EGR system. The latter engine layout was modified in order to better suit PCCI combustion working mode, i.e., adapt the combustion chamber design and EGR system to operating conditions typical of such low temperature mode. By means of 3D CFD combustion model, the engine piston bowl shape, compression ratio and injection geometry were redesigned in order to mitigate common early LTC shortcomings such as fuel impingement on the liners and piston top, as well as the limited load working range.

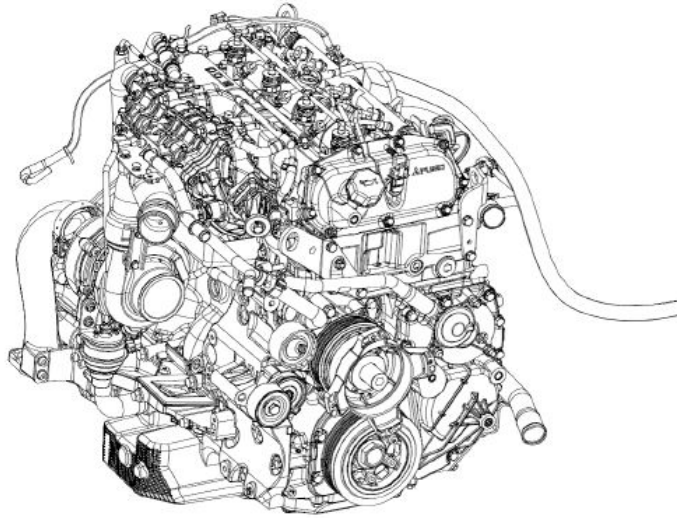


Figure 5.1: Perspective view of F1C conventional diesel engine design [34];

Detailed engine hardware modifications regarding combustion chamber design, turbocharger and after-treatment system (ATS) are below reported, while EGR system adaptation will be discussed in a successive dedicated section:

- **Compression ratio reduction**, compression ratio was reduced from 17.5:1 to 14.6:1, with the purpose of lowering in-cylinder pressure and temperature when injection event takes place, resulting in larger ignition delay to obtain enhanced fuel-air mixing and lower peak in-cylinder temperature which is the main parameter for engine-out  $NO_x$  abatement;
- **Piston bowl design**, diverse piston bowl design was adopted to provide improved fuel spray-air mixing for advanced injection timings;
- **Injectors**, different injectors featuring reduced spray cone angles (from  $139.8^\circ$  to  $130^\circ$ ) and static flow rate (from  $990\text{cm}^3$  to  $750\text{cm}^3$  in 30s at 100 bar fuel pressure) were installed. This was done in order to attenuate the risk of cylinder wall impingement due to increased penetration and advanced injection timings occurring when early PCCI combustion is run;
- **Turbo-group**, a downsized turbocharger was precisely designed and installed to guarantee higher boost levels at lower engine loads;
- **ATS**, the after-treatment system implemented for the F1C PCCI engine consists of a diesel oxidation catalyst in order to abate the high level of unburned hydrocarbon and carbon monoxide typical of low temperature diesel combustion operation;

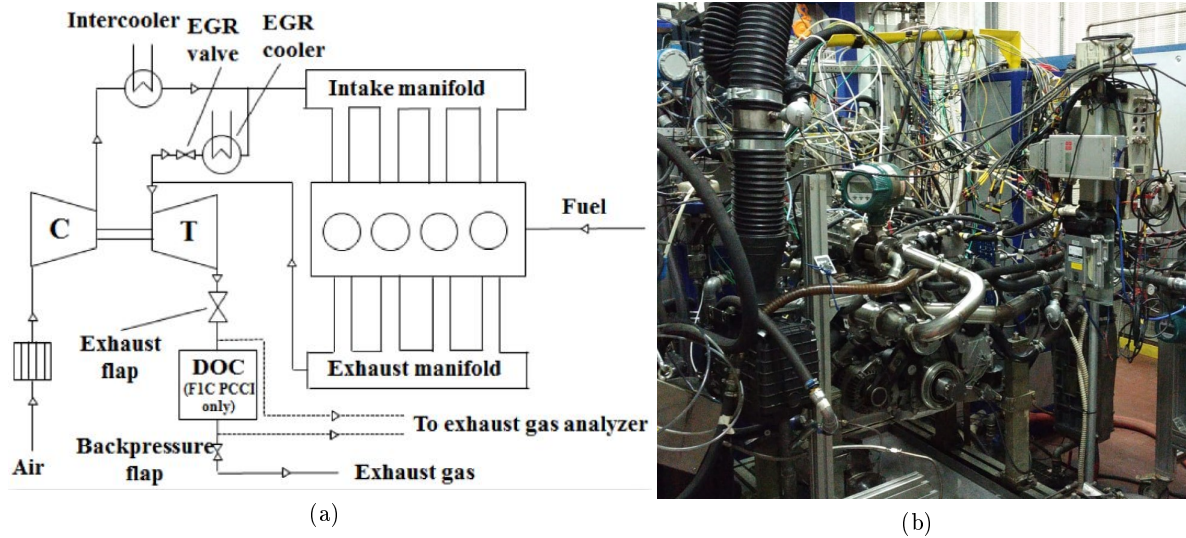


Figure 5.2: (a): Schematic representing the engine installations at the test bench [39], (b): Picture of test bench installation of FIC PCCI engine;

Figure 5.2 (a) depicts a schematic representation of the engine installation at the test bench, putting in evidence the air, fuel and exhaust flow paths together with the positioning of intercooler, turbo-group and diesel oxidation catalyst (DOC). Moreover, the location of the exhaust analyzer trains employed for emission level measurement is displayed, considering as engine-out emissions those gathered upstream the DOC and tail-pipe emissions those downstream the catalyst. Finally, figure 5.2 (b) reports a picture of the test bench room showing the realized FIC PCCI engine test bench installation.

### EGR layout and EGR cooler

Considering the high level of EGR employed to realize PCCI combustion, the conventional short-route cooled EGR system was also modified to better match requirements about EGR flow management. As shown in test bench engine installation layout in figure 5.2 (a), the recirculated exhaust gas stream is driven back to the intake manifold from the exhaust manifold and so upstream the turbine. The EGR rate is then determined by the pressure difference between intake and exhaust environments and it is adjusted by means of EGR valve actuation which affects the cross-section flow area. When the pressure differential is not enough to guarantee a sufficient flow rate, an exhaust flap placed downstream the turbine is activated to increase the exhaust manifold pressure. Furthermore, this flap is also utilized in vehicle application to shorten the warm-up period of the ATS by increasing the exhaust gas temperature during cold start operations as well as to modify engine braking when the engine is motored by the vehicle (e.g. down-hill driving). Diesel engine ATS system for vehicle application is usually composed by a DOC, a diesel particulate filter (DPF) and an SCR system, in order to comply with emissions standards.

In this test bench application no such ATS configuration was installed except for a DOC, and a back-pressure throttle valve was installed in the exhaust line so as to reproduce the pressure level present in vehicle application. As already pointed out, heavy EGR levels are employed for PCCI combustion achievement, leading to EGR system modification with respect to the conventional layout:

- The original EGR cooler was substituted by a larger one, from a production 11-liter displacement engine, to permit a greater cooling power ( from a nominal maximum thermal power of 6 kW to 32kW),as displayed in figure 5.3 (a), to deal with the high EGR mass flow rates experienced with PCCI combustion. Moreover, the EGR cooling circuit was completely separated from the engine cooling loop typical of vehicle installation, in order to furnish precise control of the exhaust gas temperature at the cooler outlet. This was possible thanks to the disposal of a secondary cooling system installed in the test bench room;
- The EGR poppet valve commonly employed in conventional diesel engine was here replaced by a throttle valve, which was meant to increase the maximum cross-section area and consequently the level of EGR recirculated in the intake manifold;

Figure 5.3 (b) depicts a picture of the tested engine working in EGR cooled configuration, instead, when uncooled EGR testing needs to be performed, the cooler is dismantled and substituted by an ad-hoc built steel pipe, connecting the cooler inlet and outlet exhaust junctions. This provides direct exhaust gas recirculation without any cooling effect and no pressure drop due to the absence of the EGR heat exchanger.

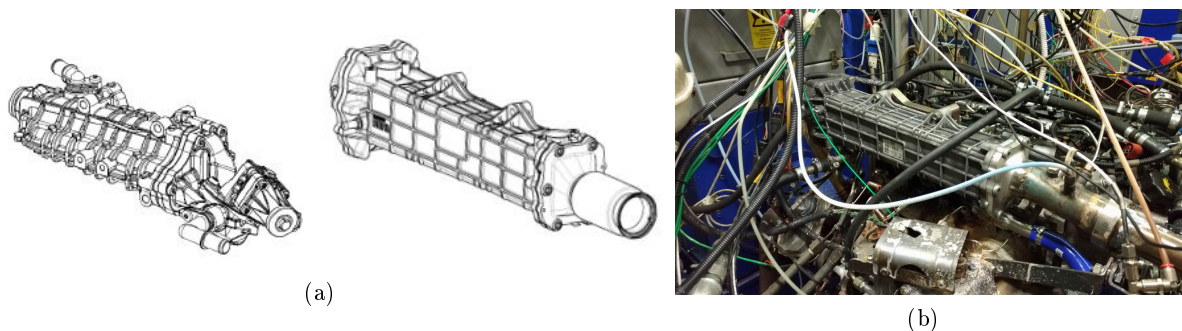


Figure 5.3: (a): F1C EURO VI engine EGR cooler (left side) and F1C PCCI engine EGR cooler (right side), (b): Picture of F1C PCCI engine EGR cooler installation;

### 5.1.2 Engine instrumentation

Prior the testing campaign and test bench installation, the engine was properly instrumented with the aim to collect additional temperature and pressure measurements to the already present default quantities measured and estimated by the ECU (Electronic Control Unit).

These sensors were placed in point of interest which results to be significant to investigate the engine behavior under pre-determined working conditions. Figure 5.4 reports a simplified schematics concerning the positioning of pressure and temperature sensors along the different flow paths such as intake and exhaust manifold, EGR circuit and upstream/downstream of the turbocompressor. Details about the exploited sensor typologies and their relevant characteristics will be described in the following two sections. Other additional engine transducers such as turbocharger speed sensor, engine speed sensor (encoder), lambda sensors and so on, are not herein matter of discussion.

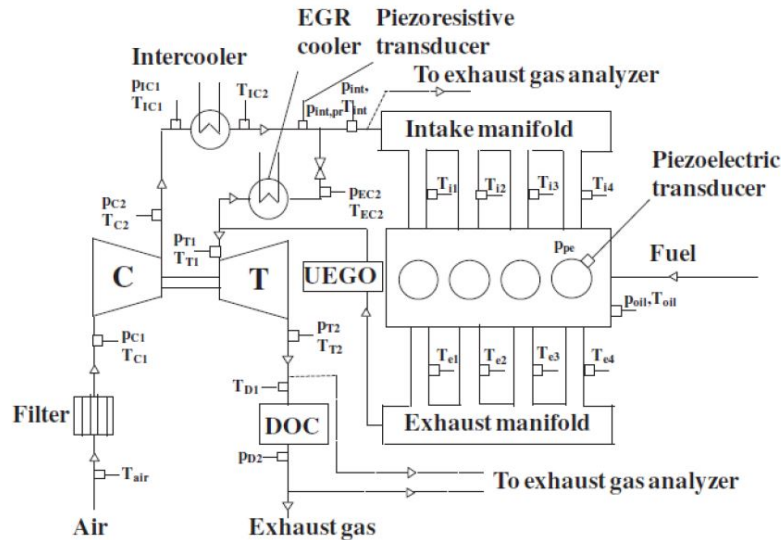


Figure 5.4: Schematic of engine instrumentation concerning temperature and pressure sensors;

## Temperature sensors

Temperature sensors employed to measure and monitor the engine working conditions during the testing activity were basically of two types: Thermistors and thermocouples.

**Thermistors** These temperature sensors are also known as NTC (Negative Temperature Coefficient), and they are made by metallic filament, usually nickel or platinum, whose resistivity is inversely proportional to temperature variation. The change in the material electric resistance property due to temperature is translated to a voltage drop thanks to the connection of the sensor to a Wheatstone bridge. Therefore, thermistors requires continuous current signal in order to visualize a voltage variation. These sensors feature better linearity, precision and stability than thermocouples, however, their sensitivity to temperature variation is far smaller than the other temperature sensors, due to the reduced resistance variation with temperature. Themistors of Pt100 type were installed in this activity along the intake line to measure ambient intake temperature, charge temperature upstream/downstream the compressor and intake manifold temperature, to monitor engine cooling system temperature (engine inlet/outlet coolant temperature)

and EGR cooling system temperature, and to evaluate engine oil temperature. In similar fashion to thermocouples their installation require a properly designed housing which allows them to be correctly inserted in the fluid stream.

**Thermocouples** These temperature sensors are constituted by two electric conductors solder to each other in two distinctive location, conventionally called cold and hot junctions. When a temperature gradient arise between the two connecting points a difference in electric potential occurs between the two ends, due to the so called Seebeck effect. The temperature difference between the junctions is proportional to the value of electric potential, however, in order to measure an absolute value of temperature it is necessary to know the temperature of one junction (usually the cold junction of reference junction). Thermocouples are simple and tough temperature sensors, however, their application is sometimes limited by their reduced linearity and sensitivity to noise which preclude their accuracy level. There are plenty of thermocouple typologies depending on their material (the most widespread nickel or copper) and their measuring range, but, in this experimental layout K and T type, produced by Kistler company, have been employed for instance in the exhaust line where high temperature range and aggressive environment demand their utilization.

### **Pressure sensors**

Pressure sensors utilized to collect pressure data in different engine locations can be divided in two classes: low frequency and high frequency pressure sensors. Another distinction can be made on a sensor typologies basis, i.e., by distinguishing piezo-resistive and piezoelectric pressure sensors. Considering the engine instrumentation, several low frequency piezo-resistive pressure transducers are positioned in different flow path points, while high frequency piezoelectric and piezo-resistive pressure sensor were placed in the four combustion chambers, intake manifold and exhaust manifold due to the measurements requirements in terms of sampling frequency.

**Combustion chamber pressure sensors** Engine combustion chambers were equipped with high-frequency piezoelectric pressure transducer Kistler 6058A in order to collect in-cylinder pressure trace of each cylinder on a crank angle basis. These pressure signals are referenced to the one coming from the transducer in intake manifold pressure (Kistler 4007C). The transducers were all placed in glow-plug adapters, meaning that glow plus were removed from the engine so as to acquire combustion chamber pressure traces with the need of additional holes in the cylinder head. This class of sensors is characterized by good stability at high temperature, high sensitivity and reduced thermal shock errors and long service life. Table 5.1 summarizes technical specification of this transducers.

Table 5.1: Kistler 6058A pressure sensor technical data

<b>Measurement range</b> [bar]	0÷250
<b>Overload</b> [bar]	300
<b>Shock resistance</b> [g]	2000
<b>Temperature working range</b> [°C]	-20÷350; -50÷400
<b>Tightening torque</b> [Nm]	1.2

**Intake manifold pressure sensors** The transducer utilized for intake manifold pressure measurement is the Kistler 4007C, which is a high frequency piezo-resistive sensor which exploit a strain Wheatstone bridge to provide an electric voltage signal proportional to the pressure applied on the sensor itself. Its reduced size and high dynamic response allows an easy installation, where limited space is available, and precise and reliable pressure measurements, moreover, it is capable of working at continuous high temperature up to 200 °C. Mounting can be simply performed on a dedicated threaded hole with the precaution of respecting the sensor tightening torque value. Details about technical specification of this pressure transducer are shown in table 5.2.

Table 5.2: Kistler 4007C pressure sensor technical data

<b>Measurement range</b> [bar]	0÷250
<b>Overload</b> [bar]	15; 30; 40; 100; 200; 400
<b>Reference temperature</b> [°C]	25
<b>Temperature working range</b> [°C]	-40÷200
<b>Tightening torque</b> [Nm]	1.5÷2.5

**Exhaust manifold pressure sensors** Exhaust gas pressure measurement is performed by means of the piezo-resistive water-cooled absolute pressure transducer Kistler 4049BDS. This sensor is equipped with an autonomous cooling system which permits continuous measurement in high temperature environment such as the exhaust manifold. Similarly to the previous sensor, it can be installed on a threaded hole realized on the wanted measuring point by being complaint with its specified tightening torque. Technical data about the sensor are reported in table 5.3.

Table 5.3: Kistler 4049BDS pressure sensor technical data

<b>Measurement range</b> [bar]	0÷5; 0÷10
<b>Overload</b> [bar]	15;25
<b>Temperature reference</b> [°C]	60
<b>Temperature working range</b> [°C]	0÷120
<b>Tightening torque</b> [Nm]	20

## 5.2 Test bench

The experimental analysis on the above-described engine was performed in the ICE advanced laboratory of Politecnico di Torino, in which an engine test bench equipment is present. The test bench equipment is entirely provided by AVL Austrian firm either regarding the bench management software such as AVL PUMA Open 1.3.2 and IndiCom automation systems and measurement devices hardware, for instance, AVL AMAi60 emission analyzer, AVL KMA 4000 fuel flow rate system and AVL smokemeter and opacimeter as well as the AVL APA 100 dynamometer. The test bench is arranged with two wall-divided rooms with visual access allowed by three safety glass and communicating door for engine and instrumentation inspection. The first one, the control room allows the operators to interact with software so as the run experiments and monitor the engine and test bench operation, while the second one, the dyno room, host the tested engine and all the bench measuring hardware but the emission analyzer.

### 5.2.1 Monitoring and acquisition systems

For the purpose of acquire and monitoring the correct engine functioning and the variable of interest, the engine test bench is endowed with software capable to interact with the engine ECU, the engine sensors and all the bench measurement devices. The whole control and management of the dynamic bench is performed by means of PUMA Open 1.3.2 automation system, which is able to handle all the major systems involved needed for engine testing and dyno room governance. The functions performed by this automation system can be summarized as follows:

- It allows to visualize and acquire all the ECU parameters;
- It permits to directly control and monitoring of the test bench cooling systems. Engine and intake charge cooling are performed by means of liquid-to-liquid and air-to-liquid heat exchangers, respectively, which utilizes tap water coming from the water pipeline. EGR cooling is performed in similar fashion, but a separate cooling circuit is utilized;
- Test bench room conditioning is a fundamental requirement in order to guarantee tests repeatability. As a consequence, the cell is equipped with an air conditioning system which maintains constant level of temperature and humidity ( 25 °C and 50% relative humidity, respectively), which can be overseen and managed by means of PUMA;
- The acquired analogical signals coming from the sensors installed on the engine are sent to the so called FireWire Front End Module ( $F\_FEM$ ) structure which performs signals digitalization and feed the software with real-time value of the quantities of interest;

An additional software for direct engine variables monitoring is called IndiCom. This allows to visualize and acquire all the high frequency signal coming from the pressure transducer installed in the combustion chamber, therefore showing the associated four in-cylinder

pressure traces. By exploiting specific algorithms and combustion models, this software is capable of displaying the trends of mass fraction burned and/or apparent heat release rate as a function of the crank angle. Moreover, with the utilization of an amperometric clamp, the software allows the visualization of the electric signal coming from the injection command. Finally, direct communication between the operator and the engine ECU can be achieved thanks to the software INCA provided from ETAS company. In this case, FPT Industrial provided the engine with a control unit with some unlocked variables, in order to evaluate the effect of several calibration parameters on combustion features and emissions. Control actions on the engine calibration parameters is performed by exploiting ETAS rapid prototyping modules and ETK connection with the ECU. Once the hardware has been initialized, calibration maps can be readily visualized from INCA experiment window where the operator can set the desired parameter values among the allowed limits and the unlocked variables. Additionally, the software is able to acquire and store the experiment quantities and subsequently post-processing them with MDA (Measure Data Analyzer) INCA tool.

### 5.2.2 The dynamometer

The ICEAL bench is supplied with a cradle-mounted AVL APA 100 AC dynamometer, shown in figure 5.5, which represents the core of the test bench. This is a reversible machine which can operate in all its four quadrants and so it can behave either as a brake or as an engine with respect to the propulsion system tested, in the same spin speed direction. In braking condition, the dyno can provide resistant torque in both static and dynamic conditions, this allows not only to simulate steady-state working conditions, as done in this thesis work, but also to perform dynamic engine testing. By steady-state testing is intended engine operation at a fixed engine working point, defined in terms of spin speed and torque (rpm x Nm), with preset calibration parameters values and stable operating conditions (e.g. almost stationary pressures and temperatures).



Figure 5.5: AVL transient dynamometer installed in ICEAL;

Instead, considering non-stationary engine testing the dynamometer can simulated transient manouvres or cycle such as those representing vehicle real driving conditions (reproducing upshift/downshift) or vehicle/engine transient homologation cycles (WLTP for light-duty or WHTC for heavy-duty applications). Dynamic testing can be implemented by defining a given manouvre in terms of vehicle parameters such as vehicle speed and gearshift pattern, or in terms of engine parameters, i.e., engine spin speed and torque.

This dynamometer features a double-shaft configuration which permits to have two engine contemporaneously installed in the test cabin while obviously testing them one at a time. The connection between the dyno and the tested engine is realized thanks to a removable joint attached to the engine flywheel by means of an hole flange and to the dyno shaft. As a result, this dynamometer layout is a time-saving solution because only the connecting joint has to be removed from one side to the other in order to test another engine. Technical data regarding the machine employed in this test bench are reported in table 5.4.

Table 5.4: AVL APA 100 dynamometer technical data

<b>Maximum power</b> [kW]	200
<b>Maximum torque</b> [Nm]	525
<b>Maximum rotation speed</b> [rpm]	12000
<b>Inertia moment</b> [ $kgm^2$ ]	0.32

### 5.2.3 The cooling system

The test bench is equipped with a engine cooling system which has the aim to manage the engine coolant temperature as well as the temperature of the intake charge and of the recirculated exhaust gas. Differently from the air-to-liquid radiator present in vehicle layout, a liquid-to-liquid conditioning system is adopted, by exploiting as a coolant medium pipeline water. The system is composed by a heat exchanger, a heater and a circulation pump. The engine coolant is first driven through the heater meant to rise the coolant temperature lower than the set value, then it goes within the heat exchanger and back to the engine. Intercooler heat exchanger and engine coolant heat exchanger are both provided with a devoted valve which allows to control their cooling capacity by regulating the cold water flow through the circuit. Valves opening and closure to maintain target temperatures is performed by means of PID (Proportional Integrative Derivative) controller implemented on PUMA Open 1.3.2. Finally, a separated cooling circuit, with independent pump, heat exchanger and PID control, is utilized to guarantee proper EGR cooling when heavy level of exhaust gas are recirculated under cooled EGR PCCI operation.



Figure 5.6: Engine cooling system

#### 5.2.4 Fuel consumption measuring system

Continuous measurement of engine fuel consumption is performed by the AVL KMA 4000 fuel flow rate system, displayed in figure 5.7. This device is endowed with a feeding pump which aspirates the fuel from an external tank ensuring uninterrupted fuel circulation, a heat exchanger meant to provide fuel conditioning within a restricted temperature range, a fuel filter, a density sensor and a volume flow meter.



Figure 5.7: AVL KMA 4000 fuel consumption measuring system;

Downstream the latter device, a fuel pressure relief valve and a secondary pump are present so as to guarantee constant value of pressure and fuel feeding to the engine, respectively. The fuel recirculated coming from the injection line is reintroduced in the KMA circuit upstream of the secondary pump, after it has gone through a bubble separator. Data collected from fuel density sensor and volume flow meter are utilized to acquire fuel consumption measurements in terms of mass flow rate, within a measurable range  $0.28 \div 110$  kg/h with an average accuracy of 1%.

### 5.2.5 Emissions analyzer

Engine emissions measurements are performed utilizing the AVL AMAi60 emission analyzer apparatus, displayed in figure 5.8, which is provided with three acquisition lines [35]. Two of the three analyzer trains are equipped with devices for the analysis of unburned hydrocarbon, methane, nitrogen oxides, carbon monoxide, carbon dioxide and oxygen levels, and they are positioned along the exhaust line so as to measure engine-out (before DOC) and tail-pipe (after DOC) emissions, respectively. The third line includes a detector which is used to evaluate  $CO_2$  concentration in the intake manifold in order to compute the EGR quantity. As far as emissions measurement is concerned, no exhaust gas dilution is herein performed differently from what prescribed during homologation cycles, therefore, those evaluated are raw emissions.



Figure 5.8: AVL AMA i60 emissions analyzer;

The measuring devices of which the emissions analyzer is provided to quantify pollutants and other chemical species concentrations are hereafter described:

**HFID (Heated Flame Ionization Detector)** This device is able to measure the unburned hydrocarbon concentration. An hydrogen-helium burner generates a carbon-free flame through which carbon atoms can be ionized. Electrons can move across the ionized

gas sample, therefore generating a current flow and potential difference between two electrodes. The current level is proportional to the number of carbon atoms present in the analyzed sample, and concentration of unburned HC is determined by comparing the measured value of current to a known value defined with a reference gas with determined hydrocarbon level.

**HCLD (Heated Chemiluminescence Detector)** The measurement device is utilized to measure the concentration of  $NO_x$  taking advantage of the chemiluminescence produced by the chemical reaction between nitric oxide and ozone:



Ozone is obtained within the instrument by producing a high-voltage discharge which transform molecular oxygen in  $O_2$ , then, its reaction with nitrogen oxide results in the production of excited nitrogen dioxide molecules  $NO_2^*$  (5.1). Afterwards, this molecule naturally undergoes a transition to its normal state (5.2) which is accompanied by emissions of red light (  $h$  is the radiation energy) in the approximate wavelength range of 600 nm to 3200nm, with a peak at about 1200 nm. This chemiluminescence radiation is proportional to the concentration of NO and it is measured by a photo detector which produces a corresponding electrical signal. The determination of total  $NO_x$  can be obtained with the same device, by providing the instrument with a catalytic converter (stainless steel or molybdenum furnace) able to decompose  $NO_2$  to NO and oxygen at high temperature prior the reactor chamber, as shown in figure 5.9 . Then, nitrogen dioxide concentration can be calculated as a difference between the total  $NO_x$  and NO results.

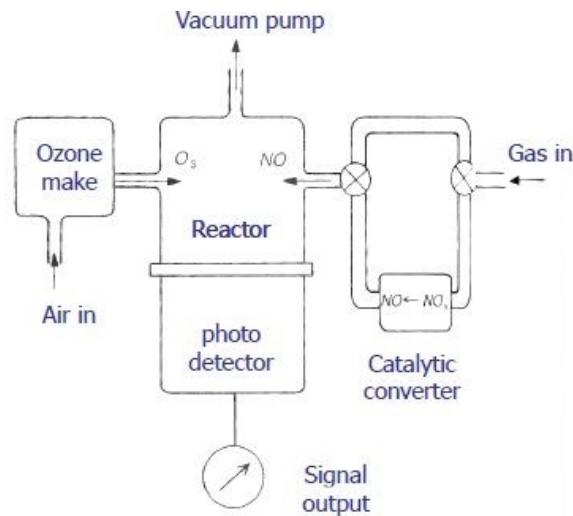


Figure 5.9: Chemiluminescence detector schematic for  $NO_x$  measurements [7];

Instrument configuration equipped with a heater is employed in case of measurement on wet gas, in order to maintain the temperature in a fixed operating range, because of the high conversion sensibility of  $\text{NO}$  into  $\text{NO}_2^*$  to the latter parameter.

**NDIR (Non Dispersive Infrared Analyzer)** Infrared analyzers take advantage of the property of certain gases of selectively absorb infra-red radiation over a narrow range of wave lengths. These devices are utilized to determine the concentration of carbon monoxide, carbon dioxide and other molecular species constituted by at least two different elements, such water, nitrous oxide ( $\text{N}_2\text{O}$ ), and HCs focusing only on a singular specie at a time due to their different characteristic absorption wavelength. When infrared radiation is absorbed by a chemical specie, the latter is converted into vibration/rotation energy of the molecules, which can be measured in the form of heat. Considering figure 5.10, the device is provided with an infrared emitter constituted by a two identical sources which generate twin infrared beams modulated by a rotating chopper. One beam passes through an absorption cell (A) which contains the exhaust gas analyzed, whereas, the other crosses a reference cell (B) filled with an inert gas. The detection receivers are made by the volumes (C) and (D) which are filled with the gas whose concentration has to be determined in the analyzed gas mixture (e.g.  $\text{CO}$  or  $\text{CO}_2$ ). The two chambers are separated by a differential sensor (M) consisting of a diaphragm that moves between the armatures of a capacitor T. When the two beams pass through the corresponding receivers' volumes, the difference in heat between the two chambers, due to the infrared absorption effect on the analyzed gas path, generates an higher pressure on one side of the diaphragm. The motion of the latter causes a variation of the capacitance of the system whose value represents the output signal measured to determined the concentration of  $\text{CO}$  or  $\text{CO}_2$ .

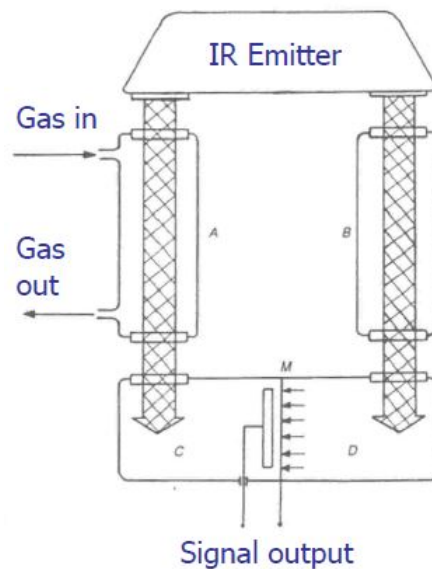


Figure 5.10: Schematic of a non-dispersive infrared analyzer for  $\text{CO}$  and  $\text{CO}_2$  measurement [7];

**POD (Paramagnetic Oxygen Detector)** Paramagnetic analyzer is used to quantify the concentration of oxygen in the sampled exhaust stream. This detector is endowed with permanent magnets positioned such that to generate an heterogeneous magnetic field. As schematized in figure 5.11, the instrument is provided with two quartz balls, filled with molecular nitrogen ( $N_2$ ), arranged in the form of a dumbbell which can rotate around a platinum wire.

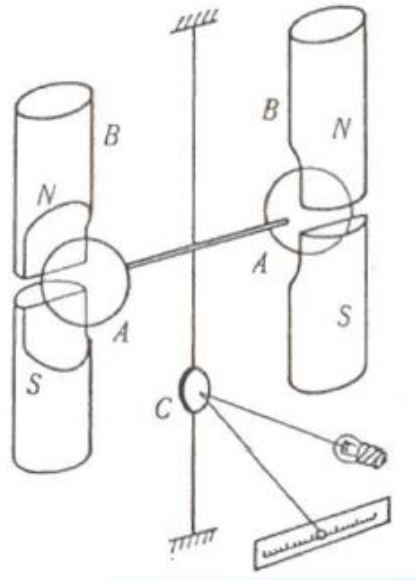


Figure 5.11: Schematic of a paramagnetic analyzer for molecular oxygen measurement [7];

Along the dumbbell centre line, a mirror, which reflects the light emitted by a source on a photoelectric cell, is placed. The presence of oxygen in the exhaust sample alters the system balance producing a force acting on the quartz balls due to its paramagnetic properties. This force is proportional to the  $O_2$  concentration and it acts in such a way to turn the dumbbell together with the mirror away from their original position. As a result of that, the intensity of the light reflected by the mirror detected by the photoelectric sensor changes. In order to bring the system to its initial state, a magnetic field generated by supplying current in a coil positioned around the balls. Therefore, the value of current furnished to obtain the same light intensity detection is a direct measure of the oxygen concentration in the exhaust sample analyzed.

### 5.2.6 PM measurement

The evaluation of particulate matter emissions necessitates of appropriate sampling filters and dilution systems meant to simulated the actual dilution occurring when PM are exhausted into the atmosphere. However, the achievable laboratory dilution always differs from the the actual ratio between air and PM, as a consequence, particle measurements are always affected by a certain error. Nevertheless, this particulate matter measuring systems must guarantee enough air dilution of the sampled exhaust gas in order to completely eliminate

water condensation along sampling line and to maintain a temperature not higher than 325 K (52 °C) of the diluted gas. Concerning filtering systems, they are constituted either by coated glass fiber filters or fluorocarbon membrane filters, whose specifications are defined by emission regulations. Finally, PM dilution and sampling system components which are in contact with raw and diluted gas must be designed to limit particulate deposition or chemical composition alteration.

### Smokemeter

During steady-state engine testing, particle matter emissions measurement is performed through the AVL 415S smokemeter, shown in figure 5.12. This device performs a fouling analysis of a paper filter through which the exhaust gas stream is driven, causing the trapping of carbonaceous solid particles on the paper. Thanks to a photo-electric instrument, the filter blackening degree can be determined by measuring the light intensity passing through the filter itself. The light intensity reduction reflected by the filter, even called smoke number (SN), is determined according to the linear Bosch scale which quantifies the amount of PM trapped from 0 to 10 or from 0 to 100.



Figure 5.12: AVL 415S smokemeter;

### Opacimeter

The AVL 439 opacimeter PM measuring instrument, reported in figure 5.13, is a device which determines the amount of particulate emissions by determining the opacity of the sampled exhaust gas. This machine is equipped with a measuring chamber of defined dimensions in which the exhaust gas is driven, and with a light source and a receiver utilized to evaluate the opacity of the gas sample, quantifying the loss of light intensity. This opacimeter is endowed with a temperature and pressure sensor so as to adjust the opacity measured value with reference to standard ambient temperature and pressure. Air purge operation should be

frequently performed in order to soot deposition removal from the light emitter and receiver, in order to guarantee correct instrument reading. In opposite way to the smokemeter PM measuring device, this instrument is typically employed to evaluate PM emissions during transient engine testing.



Figure 5.13: AVL 439 opacimeter;

## Chapter 6

# Cooled and uncooled EGR

In this chapter, the central theme of the thesis will be illustrated by depicting the employed experimental approach and the corresponding acquired results. Firstly, the main benefits and criticalities concerning engine layouts featuring uncooled and cooled exhaust gas recirculation are described referring to the experimental apparatus shown in chapter 5 and the combustion mode investigated (PCCI). Then, the adopted methodology regarding the testing campaign will be presented. Finally, the investigation's outcomes will be displayed and discussed in terms of intake charge characteristics, engine performance and combustion features, engine-out emissions and DOC efficiency.

### 6.1 Generalities

As already mentioned in chapter 4, the employment of a large amount of recirculated exhaust gases represents a mean to achieve low temperature combustion mode in diesel engine. Therefore, EGR quantity results to be one of the major parameters on which particular care has to be paid, in order to properly control PCCI combustion process. In similar fashion to diesel conventional case, when the engine runs under PCCI combustion, the EGR mass flow rate driven towards the intake manifold has to be correctly dosed considering the engine working regime in terms of load and speed, so as to obtain the right trade off between performance and pollutant emissions. Differently from today on-market diesel engine, PCCI engine applications could require EGR rates even higher than 30-40% [36, 37], to guarantee a sufficiently long ignition delay needed to realize a partially homogeneous mixture and to lower enough combustion flame temperature. As a result of that, traditional EGR circuit design has to be modified in order to provide heavy exhaust gas flow rate, for instance, by adopting partial throttling either on the exhaust side (as in the current layout) or on the intake side or both of them simultaneously. Nowadays, conventional diesel engine featuring external EGR strategies to abate  $NO_x$  emissions are characterized, in the majority of the case, by layouts with the presence of an EGR cooler utilized to cool down the recirculated gases. This practice further enhances their effectiveness in reducing combustion temperature and so nitrogen oxides as well as limiting the penalties in terms of volumetric efficiency and

PM emissions. Applying the same cooled approach in PCCI applications calls for devoted cooler design to assure suitable mechanical and thermal properties needed for EGR flow management.

The experimental investigation herein presented, has the aim to evaluate the main potentialities and criticalities given by operating the tested engine under PCCI mode when employing either cold or hot recirculated exhaust gases. Indeed, the study focuses on the analysis and comparison between performance parameters and emissions trends among the two engine configurations and, in particular, on the assessment of hot EGR influence on diesel PCCI combustion. The exploitation of a layout in which the exhaust gases guided back at the engine intake are not cooled, either by-passing them from the cooler or avoiding the cooler installation, could feature several advantages:

- A first benefit of employing a solution without exhaust gas cooler or with reduced exploitation of the latter regards the cooler fouling or clogging problematic [38, 39]. This issue is characterized by the accumulation of exhaust gas particles on the walls of the heat exchanger, forming an insulating layer which compromises its mechanical and thermal properties. Indeed, the layer formation is caused by PM and HC deposition which, as the cooler aging proceeds, is responsible for a noticeable pressure drop across the exchanger, resulting in flow reduction through the recirculating system and, at the same time, for heat transfer efficiency degradation. EGR system fouling represents not only one of the prevailing cause of its failure, but also a major problem to be faced at engine calibration level due to the drift in EGR level and its temperature. The absence of the cooling apparatus or its reduced use could surely attenuate this problematic on which engine researchers are working to find a solution to [40];
- Premixed combustion modes are all characterized by high level of HC and CO emissions due to the their intrinsic characteristics, as described in chapter 4. Therefore, diesel oxidation catalyst (DOC) plays a fundamental role in mitigating the engine-out emissions coming from PCCI applications. Being this combustion type based on low flame temperature, at low load and engine speed working points, exhaust gas temperature are not high enough to make the DOC reach its light-off temperature [39]. The utilization of hot EGR could allow to increase exhaust gas temperature with respect to the cooled case, thanks to the increase of the intake charge temperature. This could give the chance to achieve DOC light-off in the low load low speed working range so as to curb HC and CO engine-out emissions;
- Again considering the emissions side, investigations on the use of uncooled recirculated gas on PCCI engines revealed attainable engine-out unburned hydrocarbon and carbon monoxide emissions abatement compared to cooled EGR utilization [46, 47, 48].

However, the uncooled solution is also characterized by various drawbacks, some of which are common for conventional diesel engines as well:

- As said, EGR cooling is a mean to magnify the effect of the recirculated gas on ignition delay, combustion flame temperature and  $NO_x$  reduction. Avoiding the cooling stage results in a strict dependence between the EGR quantity and the intake charge temperature which increases as the recirculated flow rate raises. This has a direct impact on combustion temperatures, which inevitably rises, leading to an augmented production of nitrogen oxides;
- Considering cooled configuration, thermal throttling effect is fixed as the EGR outlet temperature from the heat exchanger is established. Conversely, when hot exhaust gas is exploited, the higher the EGR rate the higher the dilution due to thermal throttling and so the higher the penalties in terms of volumetric efficiency, which should be correctly compensated by the turbo-group, in case of turbocharged engines, in order to avoid fuel consumption penalties;
- EGR is one of the main engine parameters, together with injection timing, utilized to control PCCI combustion, therefore, changes in its characteristics lead to modification of mixture formation and reactivity patterns. Hence, prediction and control of auto-ignition and combustion phasing, already cumbersome in partially premixed combustion modes, is further complicated by using hot EGR and this calls for additional studies to be performed;
- Another drawback of the uncooled layout, still related to the increase of the intake charge temperature, is the additional limitation on the already restricted PCCI load range. This is due to the higher reactivity of the mixture due to the raised temperatures that results in a too advanced combustion and an increased combustion noise level for medium-high engine loads;
- As stated above, heavy EGR levels are required to obtain premixed charge combustion and this asks for new and more complex solutions in terms of EGR hardware layout and its control strategies. A solution in which the exhaust gases are not cooled could initially suggest a simplification of the EGR system, however, the constrained load application of hot EGR could not avoid the need of installing the cooler for PCCI operation at higher loads. As a results, a feasible solution would require to by-pass the recirculated gas during low load working conditions, i.e., an additional control logic has to be defined for the by-pass valve, which further complicates, the already difficult, engine calibration;

This investigation intends to inquire the above shortcomings and benefits regarding PCCI engines working with uncooled EGR and, if possible, provide additional understanding on the potentialities of this approach to mitigate the typical limits of low temperature combustion mode. The majority of the research studies concerning the employment of hot and cold EGR strategies regards conventional diesel engine while for those operating under premixed-charge mode limited material can be found in literature [41, 42, 43, 45, 46, 47, 48, 49]. These works

are characterized by diverse engine architecture (single cylinder, light duty, heavy duty), and they furnished cause for reflection for the current experimental analysis. As in some of the latter studies, the current analysis offers the chance to examine the potentialities of the hot EGR approach on a devoted PCCI engine architecture and for different fuel injection strategies.

## 6.2 Methodology

The experimental testing campaign was performed considering steady-state working conditions at two engine low load key points which were calibrated for PCCI cooled EGR operation in previous studies [39]. Engine uncooled EGR layout was realized by substituting the heat exchanger, seen in chapter 5, with an ad-hoc manufactured straight tube connecting the cooler inlet and outlet pipes. The tests were conducted for both hot and cold set-up by executing EGR sweeps at wide-open EGR valve while varying the exhaust flap position in order to portion the quantity of recirculated gas at the engine intake. Therefore, measurements gathered from this investigation will be characterized by a fixed position of the exhaust throttle valve and not from a fixed value of the EGR rate. Table 6.1 reports the values of the main engine calibration parameters manually set for the corresponding EGR layout and injection strategy utilized. Key points are displayed with values of engine spin speed in rpm and values of brake mean effective pressure in bar.

Table 6.1: Engine ECU parameters for the two key points

<b>Key points</b>	<b>EGR layout</b>	<b>Injection strategy</b>	<b>SOI<sub>1st</sub></b> [°bTDC]	<b>SOI<sub>2nd</sub></b> [°bTDC]	<b>q<sub>Pil</sub></b> [mm <sup>3</sup> /cyl]	<b>P<sub>Rail</sub></b> [bar]	<b>VGT position</b> [%]
<b>1400x1.1</b>	Uncooled	Single	22	-	-	800	30
	Uncooled	Double	22	7	5.5	800	30
	Cooled	Single	22	-	-	600	30
	Cooled	Double	22	7	5.5	600	30
<b>2000x2.3</b>	Uncooled	Single	26	-	-	1400	35
	Uncooled	Double	24	11	11	1400	35
	Cooled	Single	20	-	-	800	25
	Cooled	Double	20	9	11	800	25

The choice of the primary ECU quantities started from PCCI calibration under cooled EGR operation defined in previous works both for single and double injection patterns. Then, a judicious adjustment was performed to adapt them to hot exhaust gas recirculation mode without any optimization approach. PCCI double or split injection strategy was also explored in order to highlight its main benefits and penalties on performance and emissions as done in several researches [50, 51, 52, 53, 54, 55, 56], and above all to understand the effect of the EGR typology in presence of a pilot injection. The prime objective of this study is not to discuss the influence multiple or pilot injections on PCCI combustion characteristics, which will be nonetheless mentioned, but to comprehend principal dissimilarities caused by the diverse EGR approach on the premixed combustion mode here investigated.

## 6.3 Results and discussions

The results obtained from the test campaign on F1C PCCI engine will be illustrated by dividing them in terms of intake charge properties, performance and combustion features and engine-out emissions. Moreover, the corresponding trade-offs regarding the measured quantities will be proposed and finally DOC conversion efficiency will be also discussed. Graphs depicting emissions and fuel consumption trends are normalized with respect to F1C Euro VI version outcomes for confidentiality reasons. In similar manner noise level is shown as a dBA difference between the calibrated test bench value coming from F1C conventional diesel engine version and the conventional ones. Being the analysis based on exhaust recirculation sweeps, the measured quantities will be presented as a function of EGR quantity computed considering equation 3.4. Furthermore, visual distinction between cold and hot layouts is given by correspondingly utilizing cold and warm colors, whereas different symbols (triangles and diamonds) and lines (solid and dashed) are used to distinguish different key points or different injection patterns. Again engine working points were expressed in terms of engine spin speed in rpm and brake mean effective pressure in bar.

### 6.3.1 Intake charge analysis

The influence of the EGR approach on intake charge properties such as intake charge temperature, intake charge pressure and relative air fuel ratio, are here shown for single stage injection since no major qualitative differences are caused by a diverse injection strategy. Figure 6.1 (a) depicts EGR rate variation as the exhaust flap position changes and the corresponding rise of the recirculated exhaust gas temperature. As the exhaust throttle valve is closed the pressure downstream the turbine increases and for a fixed boost level the pressure differential between intake and exhaust manifold grows leading to higher quantity of EGR to be recirculated. When operating the engine with uncooled strategy, EGR temperature is not maintained constant at a desired level of 65 °C at 1400x1.1 and 85°C at 2000x2.3, therefore, the higher the degree of recirculation the higher the intake charge temperature and as a consequence the higher the EGR temperature.

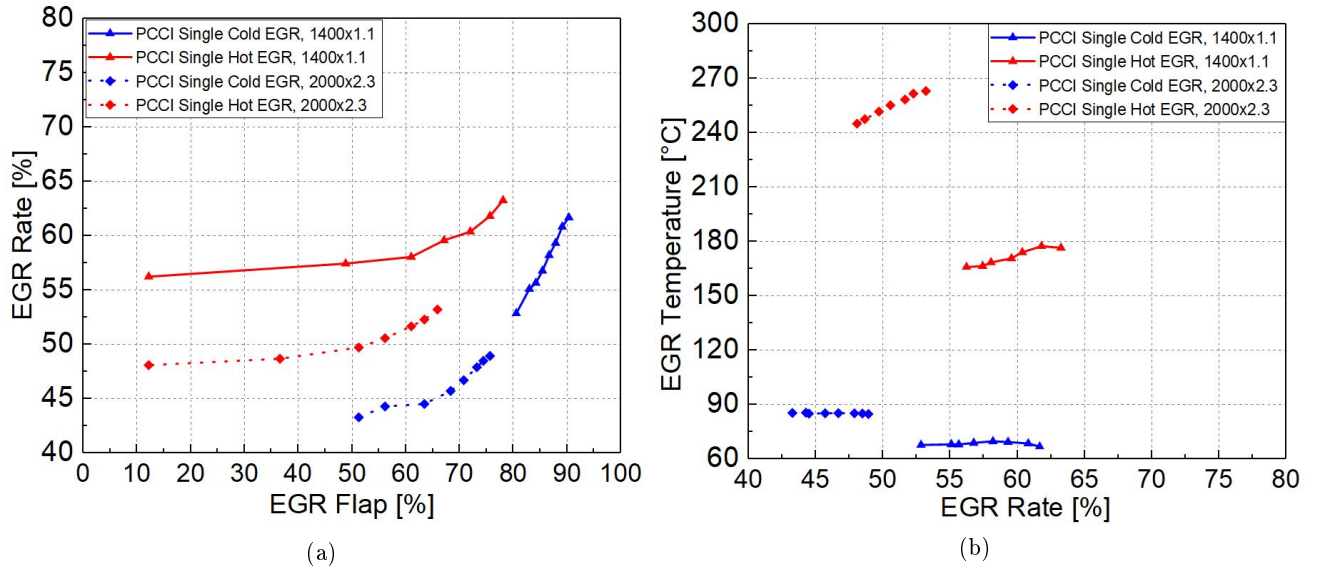


Figure 6.1: (a): EGR rate as a function of EGR flap opening , (b): EGR temperature at EGR cooler outlet as a function of EGR rate;

As a result of that, for a fixed position of the exhaust flap, an higher amount of EGR is recirculated with respect to the cooled case, because hotter and so more expanded exhaust gases are sent back to the intake manifold, or similarly when hot EGR is employed a certain quantity of that could be reached with a less closed position of the flap, which could be beneficial to reduce the associated pumping losses and so to improve fuel consumption. Another information which could be noticed from figure 6.1 (b) is the influence of the engine operating load on EGR level and temperature. In general, the EGR composition differs as load varies, and typically the higher the load the higher the amount of fuel burned which results in an increase of the exhaust gas temperature and a larger content of  $H_2O$  and  $CO_2$  in the EGR. The first effect of load variation can be obviously seen when hot EGR is employed, while the second one determines the necessity to work in different EGR range for the two key points and it can be observed even in cold case. Indeed, an augmented  $CO_2$  and  $H_2O$  concentration improve the effectiveness of the recirculation strategy on the abatement of  $NO_x$  and at the same time enhance combustion temperature reduction to allow PCCI mode.

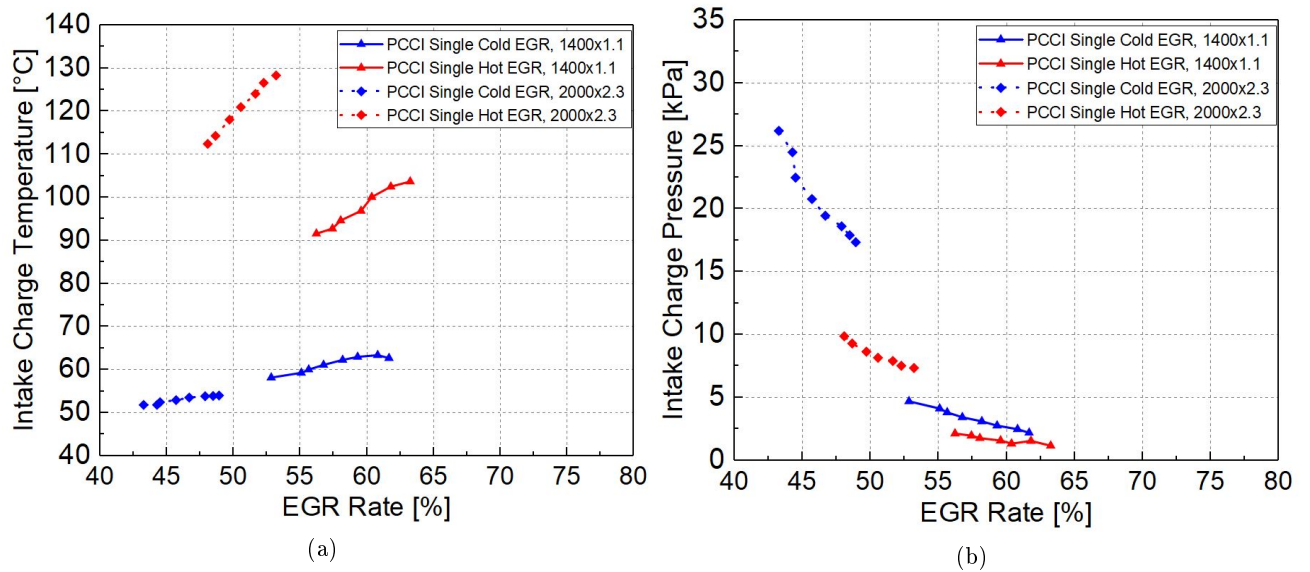


Figure 6.2: (a): Intake charge temperature as a function of EGR rate, (b): Intake charge pressure as a function of EGR rate;

An additional important difference between cooled and uncooled operation concerns the importance of the thermal throttling effect, defined in chapter 3, on the intake charge properties [44]. As seen in both layouts the EGR temperature is higher than that of fresh air, which is boosted and cooled to 22°C by the turbo-compressor and the intercooler, therefore, when mixing occurs the inlet charge temperature increases while the inlet charge pressure decreases for a fixed boost pressure, as shown in figures 6.2 (a) and (b). This behavior causes a reduction in the inlet charge density and so in the in-cylinder trapped mass due to the larger volume occupied by the charge. Considering the use of cooled EGR, thermal throttling is almost independent from the EGR quantity since the heat exchanger is always able to cool down the recirculated mass to the target temperature in any condition. Conversely, when hot exhaust gas recirculation is utilized the reduction of inlet pressure and the increase of inlet temperature are characterized by a linear dependence from EGR rate. The latter fact is justified by the increasing trend of recirculated exhaust gas temperature with EGR quantity. The modification of pressure and temperature of the inducted charge due to thermal throttling has an important effect on combustion features and it will be discussed in the following sections.

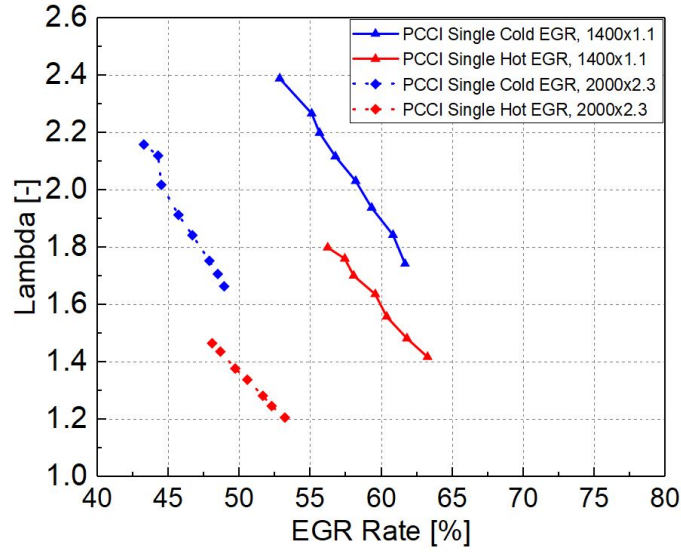


Figure 6.3: Relative air-to-fuel ratio as a function of EGR rate;

Figure 6.3 shows the variation of relative air fuel ratio as a function of the EGR rate. This graph put in evidence the different lambda working range, and so the different degree of dilution which is present when running the engine with the two EGR approaches. As the recirculated mass is increased, more and more fresh air is displaced by the exhaust gases, therefore, larger dilution is reached and oxygen concentration proportionally drops. When uncooled recirculation is adopted, for a certain EGR level, the higher temperature level results in a larger volume of gas driven back to the intake manifold, determining a wider displacement of fresh air and so an increased dilution level. This is the reason why comparing cooled and uncooled layout for a fixed recirculation rate different reduction in oxygen concentration are encountered.

### 6.3.2 Performance and combustion features

In this section, the effect of EGR approach on performance parameters such as brake specific fuel consumption (bsfc) and noise level, and combustion features such as heat release rate and mean in-cylinder pressure is described. The results are illustrated distinguishing between injection strategies and key working points, however, double injection results are reported together with single ones to offer a direct comparison among the two fuel injection approaches. In-cylinder pressure traces were experimentally acquired with a  $0.1^\circ$  crank angle degree resolution and were averaged over 100 consecutive engine cycles and between the 4 cylinders by using AVL Concerto software. The latter was also utilized to evaluate by means of a single zone analysis the average heat release rate trace. Brake specific fuel consumption and combustion noise were evaluated from AVL KMA 4000 fuel flow rate data and applying an opportune filtering procedure on the in-cylinder pressure signal, respectively.

## Single stage injection

Figures 6.4 depict the above-mentioned quantities for the engine working point 1400x1.1 (rpm x bar) with single injection strategy implemented. Considering this operating condition bsfc (figure 6.4 (a)) remains fairly constant with increasing EGR rate with the slight tendency to augment when larger EGR rates are applied for both recirculation typologies. Moreover, regardless of the recirculation approach bsfc was seen to be substantially higher than the conventional diesel case, as well. The introduction of EGR results in oxygen concentration diminution and the reduction of the average in-cylinder charge temperature due to the well-known dilution, chemical and thermal effects described in chapter 3. Both effects are typically responsible for the lengthening of the ignition delay due to a slower auto-ignition chemistry and a reduced burning rate which enlarges combustion duration. Therefore, as the EGR quantity increases combustion phasing retard takes place. During low load operation, the long ignition delay needed to achieve PCCI and the large content of oxygen give rise to an increase in over-mixed areas which are outside of the flammability limits. These conditions result in deterioration of combustion efficiency due to over-mixing and bulk quenching mechanisms both of which lead to incomplete combustion. Then, brake specific fuel consumption is strictly related to the previous two mechanisms and combustion phasing and the trend revealed by the tests could be attribute to a balance between a reduction of over-leaned areas due to oxygen substitution by EGR which can improve consumption and incorrect phasing of combustion that can worsen combustion completion. However, as it can be seen from the heat release rate curves in figure 6.4 (c) , for high  $X_{EGR}$ , either hot or cold, combined effect of oxygen shortening and low in-cylinder temperature significantly slow down fuel-air chemical kinetics leading to a too much retarded combustion, coinciding with a peak in fuel consumption.

Comparing the investigated EGR strategies, it is important to bear in mind that uncooled EGR implementation affects simultaneously inlet charge temperature and inlet charge dilution, i.e., relative air-fuel ratio values, whereas for the cooled strategy, being the recirculated exhaust gas cooled down, intake temperature is fixed and only the effect on lambda variation is obtained. Furthermore, as discussed in section 6.3.1, thermal throttling effect magnifies the reduction of fresh air trapped into the cylinders, that for hot EGR exploitation is  $X_{EGR}$  dependent, while for cold EGR this phenomenon is still present but independent from the amount of recirculated gas. As a consequence, lambda approaches less lean working range for the uncooled approach than cooled one. Then, considering again figure 6.4 (a) and similar amounts of EGR, hot recirculation featured an increase in fuel consumption of about 1-2% with respect to the cold case. This is thought to be related to the prevailing effect of intake dilution, and the consequent lower  $\lambda$  working window which deteriorates combustion, on the increase of intake charge temperature which was found to be beneficial to reduce overmixing and bulk quenching due to the higher burning temperature [46, 47]. Another possible explanation could be found considering combustion phasing, in fact, figure 6.4 (c) shows that for either low or high  $X_{EGR}$ , hot EGR phasing is slightly retarded with respect the cold one,

increasing the amount of fuel which does not complete combustion due to the sudden drop in temperature during the expansion stroke .

Again this could be a consequence of the oxygen deprivation effect which predominates on the higher in-cylinder temperature leading to an augmented combustion duration which negatively affects bsfc.

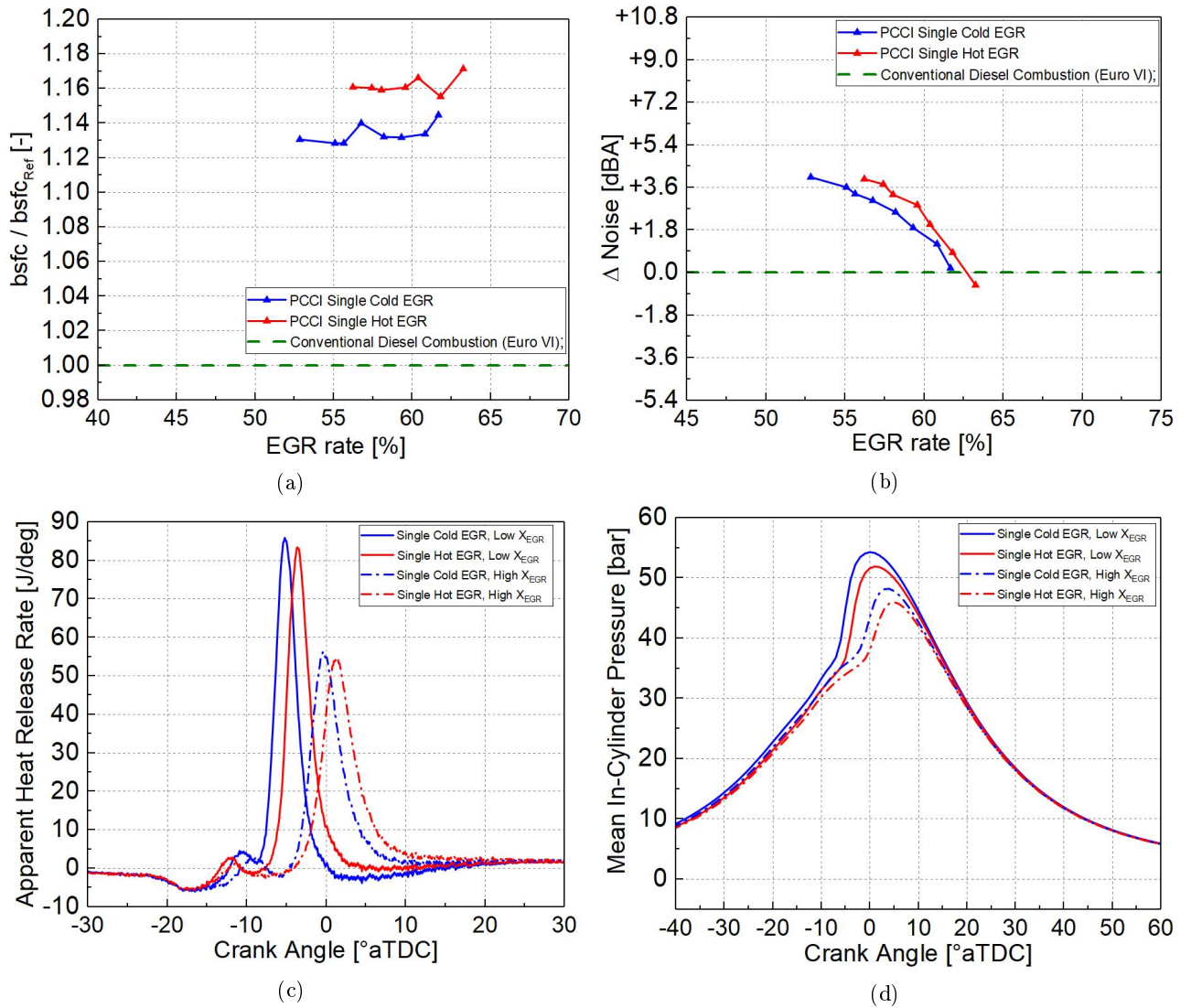


Figure 6.4: Engine working point 1400x1.1, Single injection: (a) Normalized brake specific fuel consumption as a function of EGR rate, (b) Noise level variation as a function of EGR rate, (c) Apparent heat release rate versus crank angle position for low and high EGR content, (d) Mean in-cylinder pressure versus crank angle position for low and high EGR content;

As far as the heat release rate is concerned, we can notice the typical two stage ignition behavior of diesel LTC for both EGR strategies. However, regardless of the low and high  $X_{EGR}$  when uncooled EGR is employed the low temperature oxidation (LTO) stage resulted

to be slightly advanced compared to the cooled case, as well as featuring a reduced HRR peak. This is thought to arise from the increased inlet charge temperature which anticipates the start of cool flames stage and from the reduced content of oxygen which limits burning rate and so the HRR. Regarding the high temperature oxidation (HTO) stage, there is no huge difference in terms of HRR peak and shape between the two EGR approaches. Nevertheless, due to the lower lambda values experienced and the reduced intensity of the LTO stage when implementing hot EGR, HTO stage of combustion results retarded compared to the cold case, giving raise to an augmented overall combustion duration. What could be inferred from figure 6.4 (c) is a noticeable crank angle difference during the negative temperature coefficient (NTC) phase among the two EGR strategies which seems to determine the consequent combustion lengthening.

Looking at figure 6.4 (b) combustion noise level as a function of EGR rate is represented. For either strategies, engine noise level tends to decrease as the amount of recirculated exhaust gas increases, and to remain above the conventional diesel value. As already discussed, the effect of exhaust gas recirculation of diminishing the average and peak combustion temperature together with the substitution of part of the fresh air entering the cylinder slow down the fuel oxidation process and produce the consequent diminution of the HRR peak. These factors influence the in-cylinder pressure build-up, i.e., the in-cylinder pressure rate rise (or pressure first derivative) as well as the value of the peak firing pressure. The latter quantities are indicators of the noise level and as shown in figure 6.4 (d) they are attenuated going from low to high EGR content, justifying the noise reduction. Comparing hot and cold EGR curves, they are both characterized by analogous values of engine noise. Despite that, taking into account a similar  $X_{EGR}$ , the utilization of hot EGR results in higher combustion noise level in the order of 1 dBA. This may be attributed to a prevailing effect of uncooled EGR on inlet charge temperature increase rather than the inlet dilution effect. This seems in contrast with the statements given for bsfc, but some considerations could be done looking at the mean in-cylinder pressure trace. Even though, they are not representative of the same EGR quantity, we can notice that the in-cylinder pressure rise in correspondence of the start of HTO stage results to be higher in the hot case with respect to the cold one. This could be due to a stronger hot flames combustion stage which could lead to increased value of pressure first derivative and so noise level.

Figures 6.5 show performance and combustion quantities for the engine working point 2000x2.3 (rpm x bar) with single injection strategy implemented. This engine key point is still representative of a low load working condition along the engine map, however, it features higher engine speed and almost twice the load of the previous investigated point. As a consequence, differences regarding the effect of hot EGR on combustion characteristics and performance are expected since the increase of the fuel injected leads to a simultaneous increase of the burned gas temperature due to the large heat released and of the equivalence ratio ( $\phi = \frac{1}{\lambda}$ ) approaching richer value, as described in section 6.3.1.

From the outcomes of these tests a comparison between cooled and uncooled approaches in terms of trend is done whereas there is no point in noting the differences considering the same level of EGR, because no sensible overlap is present. Figure 6.5 (a) reports brake specific fuel consumption versus  $X_{EGR}$ , and again different pattern for different EGR implementation can be observed as the EGR quantity increases. Particularly, when cooled EGR is adopted fuel consumption increase for large amount of recirculated gas while a more restrained growth is found for the uncooled case. Again this could be explained by the lowering of the in-cylinder temperature and of the oxygen concentration, whose consequence is to deteriorate combustion efficiency, worsen bulk quenching and change combustion phasing moving it toward the expansion phase so that the amount of fuel which fully oxides diminish.

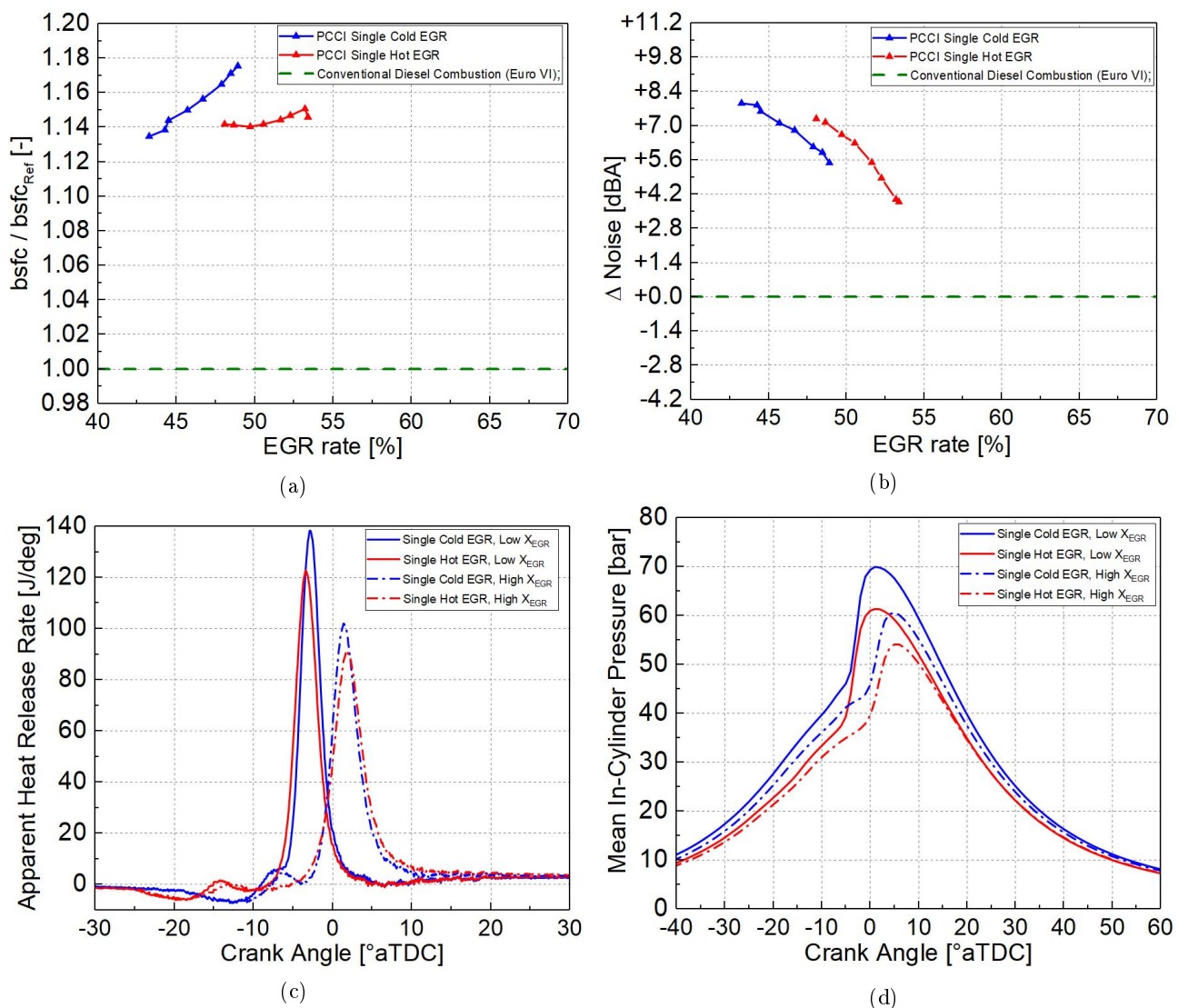


Figure 6.5: Engine working point 2000x2.3, Single injection: (a) Normalized brake specific fuel consumption as a function of EGR rate, (b) Noise level variation as a function of EGR rate, (c) Apparent heat release rate versus crank angle position for low and high EGR content, (d) Mean in-cylinder pressure versus crank angle position for low and high EGR content;

Instead, for hot EGR application, even if a larger intake dilution is present the increase in the inlet charge temperature effect seems to prevail, leading to a reduction of mechanisms such as over-mixing and bulk-quenching which could prevent a significant increase in fuel consumption. Either EGR strategies provided comparable value of bsfc and a better comparison will be presented in section 6.3.4 considering bsfc- $NO_x$  trade-off curve. Heat release rate curves for relatively low and high amount of EGR in cold and hot configuration are shown in figure 6.5 (c). HRR patterns do not present any significant difference with the aforementioned engine working point. Indeed, in similar fashion to 1400x1.1, hot EGR heat release rate trend is characterized by an advanced cool flames stage which is also accompanied by a reduced HRR peak. As already pointed out, these LTO stage characteristics, together with a larger inlet dilution effect due to thermal throttling, could be the main factors in having a long NTC period and so an enlarged combustion duration with hot EGR, overcoming the fastening effect of the increased initial charge temperature. Noise level variation as a function of  $X_{EGR}$  is depicted in figure 6.5 (b), and for either EGR configurations the common trend of combustion noise versus EGR quantity, which was previously discussed, can be noticed. Again, combustion noise results to be far higher than the conventional case, while analogous values of noise level among the two recirculation approaches can be observed and they will be better compared with noise- $NO_x$  trade-off graph in section 6.3.4. Finally, mean in-cylinder pressure traces for both EGR layouts and for different degree of recirculated exhaust gas are reported in figure 6.5 (d), as done for the previous key-point. Still, the usual reduction of pressure first derivative and peak firing pressure can be seen as the EGR quantity increases, justifying the diminution of noise level, regardless of the type of EGR implemented.

### Double stage injection

Figures 6.6 depict performance and combustion quantities for the engine working point 1400x1.1 (rpm x bar) with the adoption of double stage injection approach (dashed lines) together with the previously discussed single injection strategy outcomes (solid lines). As shown in figure 6.6 (a), going from a single stage to a double stage injection has a beneficial effect on fuel consumption for either EGR typologies. This is thought to be related with a better combustion phasing which means having a well distributed combustion event around TDC, i.e., reducing the negative work of the piston during compression stroke and enhancing the positive work during expansion phase. The double injection bsfc trends versus  $X_{EGR}$  are largely affected by EGR variation with respect to those of single injection, and this substantial increase of fuel consumption could still be attribute to the higher oxygen dilution and lower in-cylinder temperature which degrades combustion efficiency and moves combustion too much after TDC. Comparing hot and cold approaches considering similar EGR quantities, even for double injection the uncooled EGR tends to produce higher fuel consumption and this could be explained with the considerations done for single injection.

Looking at figure 6.6 (c), apparent heat release rate curves for double injection are shown and significant changes in the shape of the HRR could be noticed with respect the single injection pattern. It must be pointed out that the trend of the rate of heat release is highly influenced by the ratio between the quantities of fuel injected in the first and second injection and from their timings as well as the crank angle distance between them [53]. Being here these parameters fixed, the impact of EGR level and typologies can only be discussed. Regardless of the recirculation strategy, when low  $X_{EGR}$  is utilized two distinctive peak in the HRR trace after low temperature oxidation stage can be observed. This could be attributed to the fact that the second injection starts when the hot flame stage of the first injection is already initiated.

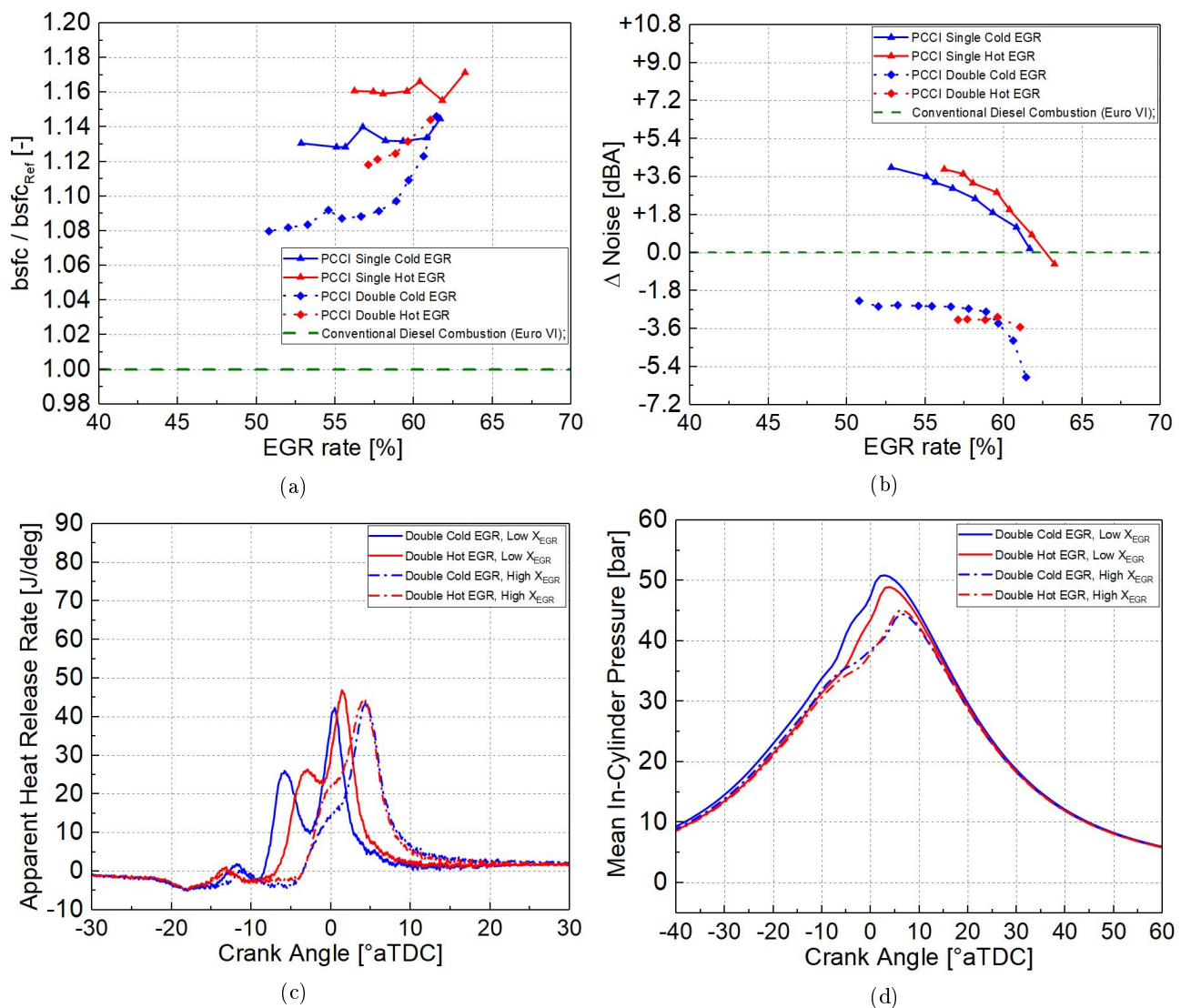


Figure 6.6: Engine working point 1400x1.1, Double injection: (a) Normalized brake specific fuel consumption as a function of EGR rate, (b) Noise level variation as a function of EGR rate, (c) Apparent heat release rate versus crank angle position for low and high EGR content, (d) Mean in-cylinder pressure versus crank angle position for low and high EGR content;

Moving toward high EGR level, reduction in oxygen concentration and in-cylinder temperature seems to significantly enlarge the NTC period retarding the start of HTO stage of the first injection. Therefore, when the second injection starts the combustion of the first one is not occurred yet. This results in HRR curve which approaches more the one typical of single injection. Considering combustion noise level, figure 6.6 (b) shows a substantial difference between single and double injection patterns. Particularly, double stage injection features lower noise level than single one for both hot and cold EGR. This could be attribute to fact that splitting the necessary amount of fuel injected to obtain the desired load, gives rise to a more gradual heat release process, resulting in a mitigated pressure rate rise as well as a reduced HRR and in-cylinder pressure peak. Moreover, combustion noise diminution as  $X_{EGR}$  increase results to be more attenuated with respect to the single stage case and comparable value of engine noise are encountered for both EGR approaches. In hot EGR case, the level of noise emitted by the engine tends to remain fairly constant until high exhaust gas quantities are recirculated for which a slight decrease can be observed. A possible explanation of this pattern could be found considering again the balancing effect of inlet charge temperature increase and charge dilution when uncooled EGR is implemented. In fact, these two factors influences fuel-air mixing and burning processes provoking changes in the in-cylinder pressure trace, as shown in figure 6.6 (d). Indeed, as EGR rate augments the inlet charge temperature increases speeding up combustion and pressure rise and so possibly increasing noise level, whereas the intake dilution increase slows down the fuel oxidation process, having the opposite effect.

In figures 6.7 are plotted performance and combustion quantities for the engine working point 2000x2.3 (rpm x bar) with the adoption of double stage injection strategy (dashed lines) together with the single stage injection outcomes (solid lines). Analyzing figure 6.7 (a) in which fuel consumption curve are reported, double stage injection trends are characterized by the already discussed increasing trend as a function of  $X_{EGR}$ . Comparing the two injection patterns, we can observe that a diminution of bsfc value is experienced for both cooled and uncooled case. Nevertheless, the extent of fuel consumption reduction is lower than the previous working point and this is particularly evident for hot EGR. A possible explanation for the latter fact could be found in a different interaction between the two injection shots for cold EGR, while for hot EGR the effect of having much higher intake charge temperature affects temperatures before and after the SOC which could substantially influence mixing and combustion phasing. As suggested, the split ratio between the injection and the corresponding timing plays a role, but they are not herein matter discussion. Figure 6.7 (c) illustrates apparent heat release rate trend associated with double stage injection with low and high content of EGR. It can be seen that there is a shape similarity with its corresponding single injection case, and a divergence with respect to double injection pattern obtained with the key working point 1400x1.1. This trend could be explained considering that the second injection

starts prior to the onset of the hot flames stage of the first injection [53] leading to the usual two peak shape typical of PCCI combustion. As a large amount of recirculation is introduced into the engine, again combustion duration increases and the HRR peak value diminishes, whereas no substantial shape variation occurs.

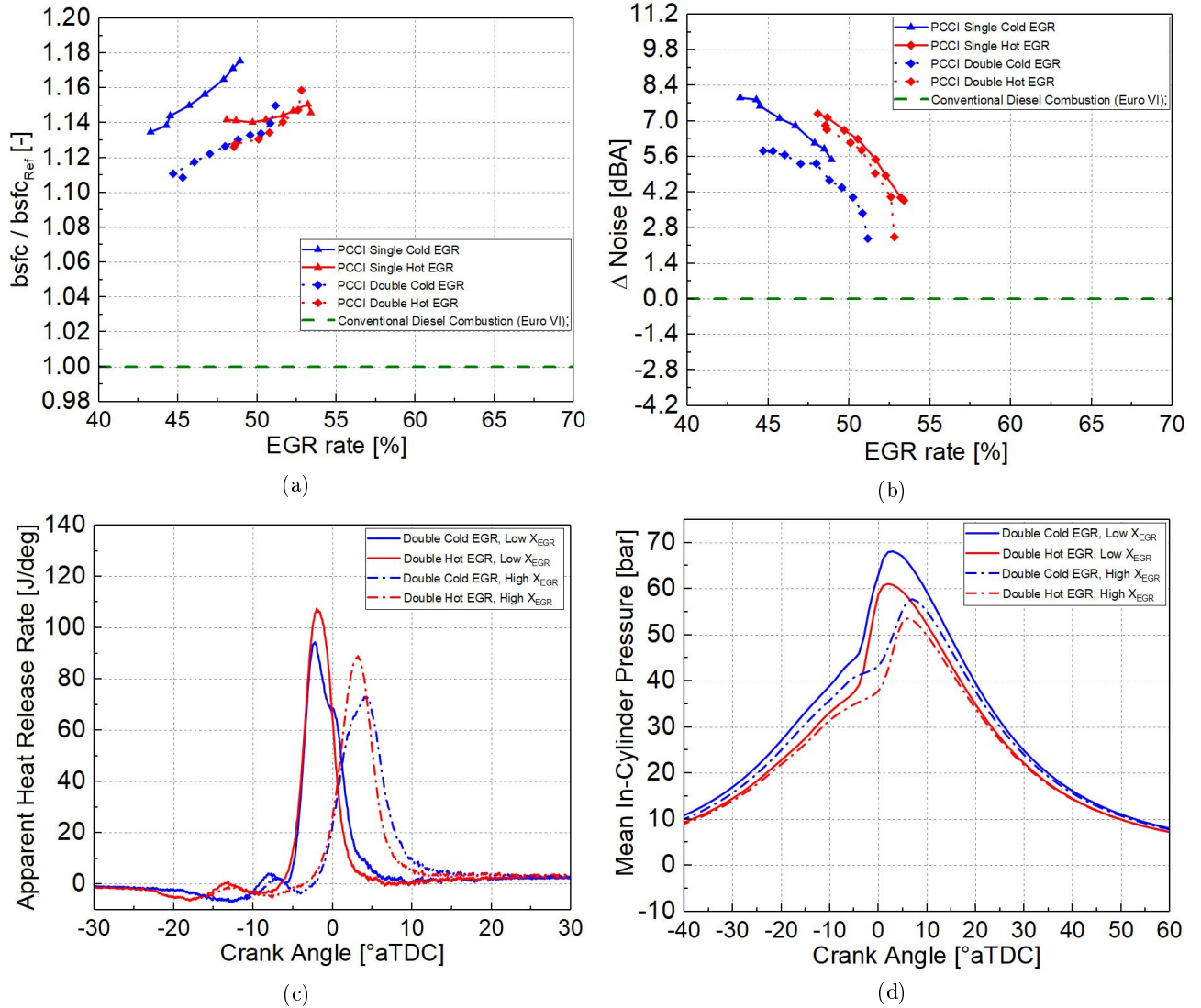


Figure 6.7: Engine working point 2000x2.3, Double injection:(a) Normalized brake specific fuel consumption as a function of EGR rate, (b) Noise level variation as a function of EGR rate, (c) Apparent heat release rate versus crank angle position for low and high EGR content, (d) Mean in-cylinder pressure versus crank angle position for low and high EGR content;

Noise level variation curves as a function of  $X_{EGR}$  for double injection are plotted in figure 6.7 (b). Comparing the two EGR approaches, similarly to the single injection case, analogous values of combustion noise can be observed and a more straightforward analysis will be done in section 6.3.4.

Instead considering different injection strategies, a reduction of noise level is experienced and it could be explained with the same reasoning done for the previous key-point. In comparison with the engine working point 1400x1.1, the achievable noise level damping with double stage injection is less intense and this could be attributed to the different HRR trends seen in these engine working points, which could affect the pressure first derivative and maximum in-cylinder pressure and so combustion noise. Considering uncooled EGR implementation, noise level diminution is farther mitigated and this was thought to be related to predominant effect of higher temperature of the inlet charge on inlet dilution. This could be responsible for an increased burning rate and so a faster pressure increase which leads to a less mitigated noise level. Finally, figure 6.7 (d) reports the variation of mean in-cylinder pressure for double injection pattern regarding working conditions with low and high EGR content, either cooled or uncooled. Again, going from low to high  $X_{EGR}$  produces the reduction of in-cylinder peak pressure as well as a smoother pressure build-up during combustion, in agreement with all the previously discussed configurations.

### 6.3.3 Engine-out emissions

This section illustrates the influence of cold and hot EGR implementation on raw engine-out pollutant emissions as soot, nitrogen oxides, carbon monoxide and unburned hydrocarbons. In similar manner to the previous section results are presented making a distinction between key working points and injection strategies. Pollutant emissions such as  $NO_x$ , HC and CO were measured utilizing AVL AMAi60 emission analyzer, whereas the steady-state measuring of soot emissions in the exhaust gases was performed by means of the AVL 415S smokemeter, both of them described in chapter 5.

#### Single stage injection

Figures 6.8 present pollutant emissions outcomes versus  $X_{EGR}$ , considering the engine key-point 1400x1.1 (rpm x bar) running under single injection strategy. Concerning soot emissions, reported in figure 6.8 (a), shows a near to zero level and it can also be observed that they are totally independent from the amount of recirculated exhaust gas either cooled or uncooled. As already pointed out in chapters 1 and 2, particulate matter formation is mixing and temperature related problem. PCCI combustion is characterized by long ignition delay due to the high amount of EGR employed and advanced injection timing resulting in low burning temperature which inevitably leads to almost soot free combustion. The increase of EGR level further enlarge the ignition delay enhancing mixture formation and so avoiding the formation of fuel-air rich pockets and this is true until the reduction in oxygen concentration is too high or temperatures are too low to allow soot oxidation reactions. The trends seen in figure 6.8 (a) are attributable to high degree of mixture homogeneity for whatever EGR level, and for hot EGR the increased inlet charge temperature and inlet charge dilution does not negatively influence the mixing process and so soot formation, as well.

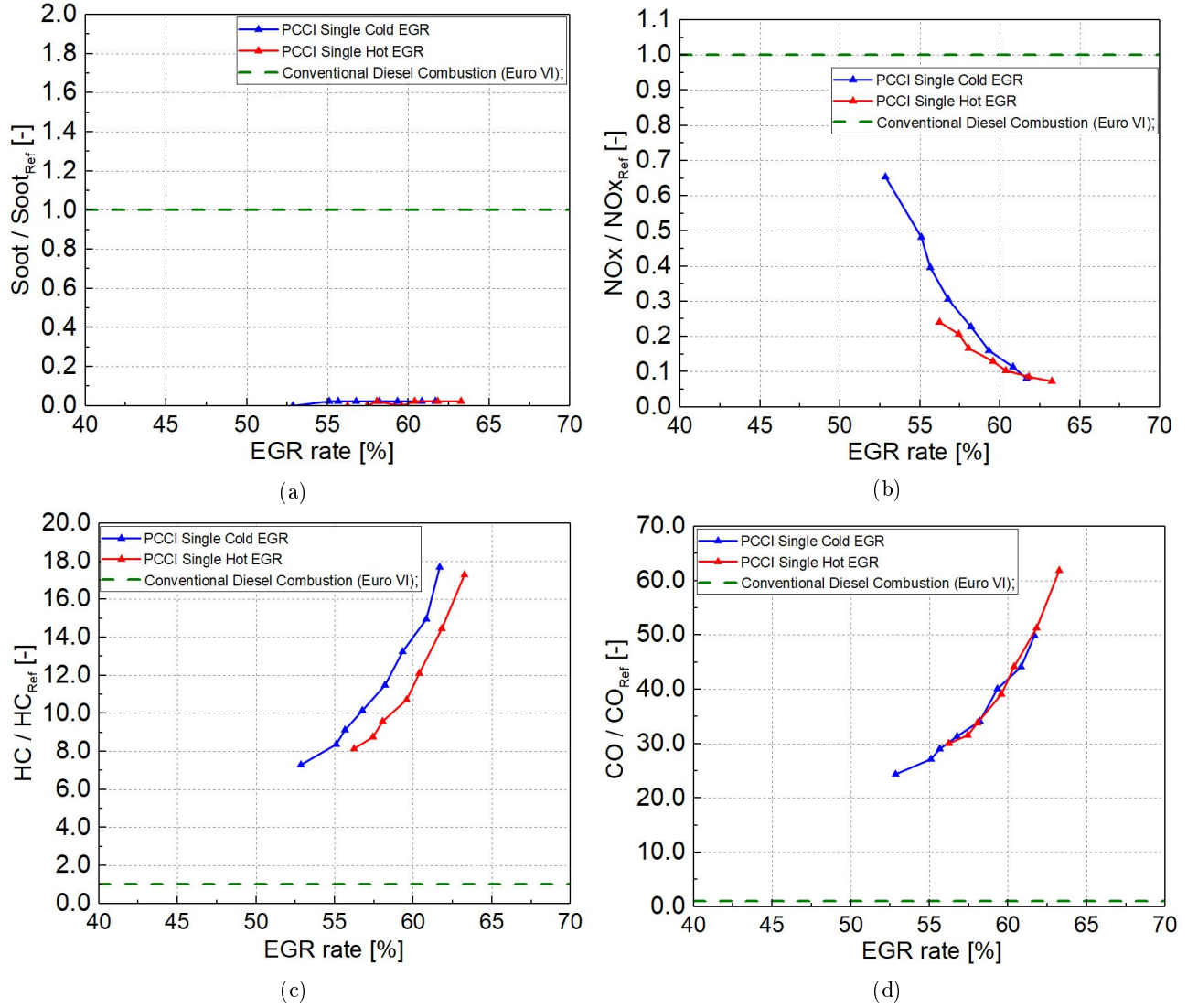


Figure 6.8: Engine working point 1400x1.1, Single injection: (a) Normalized soot emissions as a function of EGR rate, (b) Normalized  $NO_x$  emissions as a function of EGR rate, (c) Normalized HC emissions as a function of EGR rate, (d) Normalized CO emissions as a function of EGR rate;

Nitrogen oxides emission are reported in figure 6.8 (b), where the typical pattern of  $NO_x$  diminution as the  $X_{EGR}$  grows up can be observed due to the often mentioned EGR effects on peak combustion temperature and charge oxygen reduction which control oxides of nitrogen formation rate. From the same figure, we can notice that for a similar quantity of hot EGR is characterized by a slightly lower production of  $NO_x$  compared to cold EGR. This is thought to arise from the attenuated effect of the increase of intake charge temperature at such low load, with respect to the larger oxygen reduction due to thermal throttling effect which results in this minor emission abatement.

Regarding unburned hydrocarbons emissions, shown in figure 6.8 (c), either EGR strategies are characterized by a growing trend as larger EGR level is utilized. A possible explanation could be related to the worsening of mechanisms of bulk quenching and over-mixing as well as the fact that combustion is more and more retarded with higher level of  $X_{EGR}$  leading to a less complete fuel oxidation process. Comparing the uncooled and cooled EGR, in contrast to the increase in fuel consumption which has been seen in section 6.3.2, HC emissions tends to be lower in the hot case. The higher working temperature associated with the hot EGR strategies typically improves over-mixing and bulk-quenching phenomena [46, 47], resulting in simultaneous improvement of bsfc, HC and carbon monoxide emissions. However, being fuel consumption increased for this approach, the previous mechanisms could not be taken as responsible of HC diminution. A possible reason behind the minor reduction of HC could be found either in a mitigation of the wall impingement phenomenon (wall quenching) due to probable shorter fuel spray penetration, or to late oxidation reaction which may occur after the expansion stroke. The fact that other mechanisms than bulk quenching and over-mixing are involved in HC reduction, is sustained by the trend of CO emission, plotted in figure 6.8 (d), As it can be noticed, carbon monoxide emissions tends to overlap for the two EGR implementations. As discussed, CO typically forms due to incomplete oxidation of CO into  $CO_2$ , either at high temperature due to lack of oxygen (rich CO formation) or at low temperature in lean mixtures (low temperature CO). As EGR level increases more and more oxygen is displaced from the inlet charge and the average burning temperatures are lower and lower leading to the observed growing trend of CO emissions. Employing hot EGR could bring benefits in terms of in-cylinder working temperature leading to CO diminution, however it seems that , for this engine key point, the prevailing effect of intake dilution counterbalances that of temperature leading to comparable emissions for cooled and uncooled EGR.

Figures 6.9 show pollutant emissions results from EGR sweeps considering the engine key-point 2000x2.3 (rpm x bar) working with single injection strategy. In similar fashion to previous working point, figure 6.9 (a) still highlights the negligible dependence of soot emissions on EGR rate when correct fuel air mixing is reached under low temperature combustion mode. Nevertheless, being the operating engine load almost the double of the previous one, differences can be noticed on the extent to which EGR temperature and charge dilution affect nitrogen oxides, unburned hydrocarbons and carbon monoxide emissions. Concerning the latter pollutant emissions trends versus  $X_{EGR}$ , they resemble the already discussed patterns for both EGR strategies. As pointed out in 6.3.2, comparison between cooled and uncooled recirculation approach on a EGR level basis, on this engine working point, is limited by the small EGR range overlap, however, some points of reflection are proposed and the potentialities of hot EGR will be better seen in section 6.3.4. Considering the small window in which similar EGR quantity is recirculated, HC and CO emissions, respectively figure 6.9 (c) and 6.9 (d), result to be significantly reduced for uncooled strategy, whereas the opposite can be observed for  $NO_x$  emissions in figure 6.9 (b). This behavior is though to arise from the dominant influence that inlet charge temperature variation has on these emissions with

respect to inlet oxygen reduction when this working point at higher load is explored. Indeed, this fact could explain the improvement of HC and CO emissions due to the deterioration of over-mixing and quenching mechanism as well as the increase of nitrogen oxides production rate due to the higher peak combustion temperature.

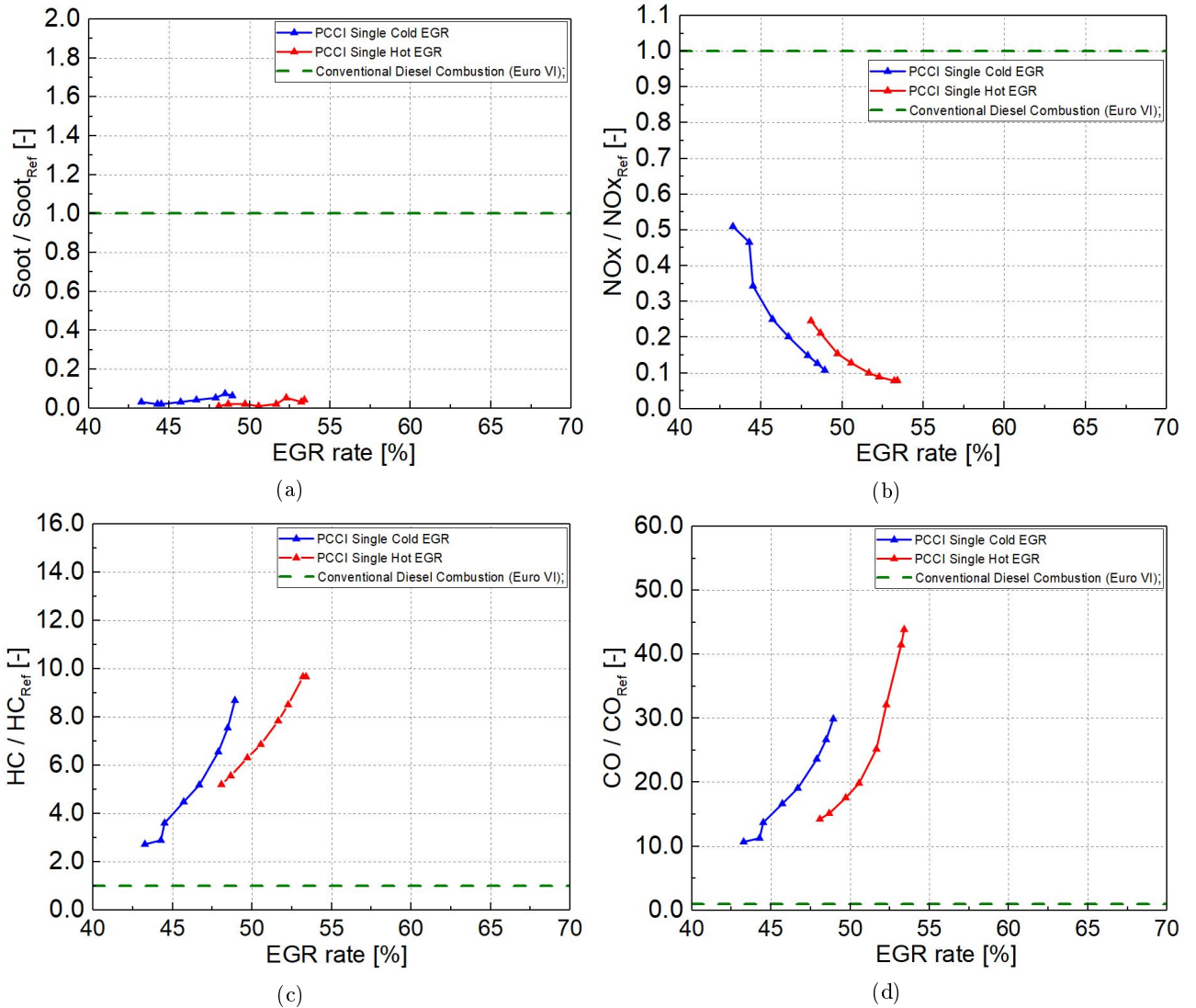


Figure 6.9: Engine working point 2000x2.3, Single injection: (a) Normalized soot emissions as a function of EGR rate, (b) Normalized  $NO_x$  emissions as a function of EGR rate, (c) Normalized HC emissions as a function of EGR rate, (d) Normalized CO emissions as a function of EGR rate;

### Double stage injection

Figures 6.10 present pollutant emissions outcomes as a function of EGR rate, considering the engine key-point 1400x1.1 (rpm x bar) running under double injection strategy.

As far as smoke emissions are concerned, figure 6.10 (a) shows an increased level of soot when double stage injection is implemented, which is particularly significant for uncooled EGR. This could be attributed to a deterioration of the mixing process due to the interaction between the two fuel injection shots. As seen in section 6.3.2, the HRR shape associated with this working condition was characterized by two distinctive peaks after cool flames oxidation stage.

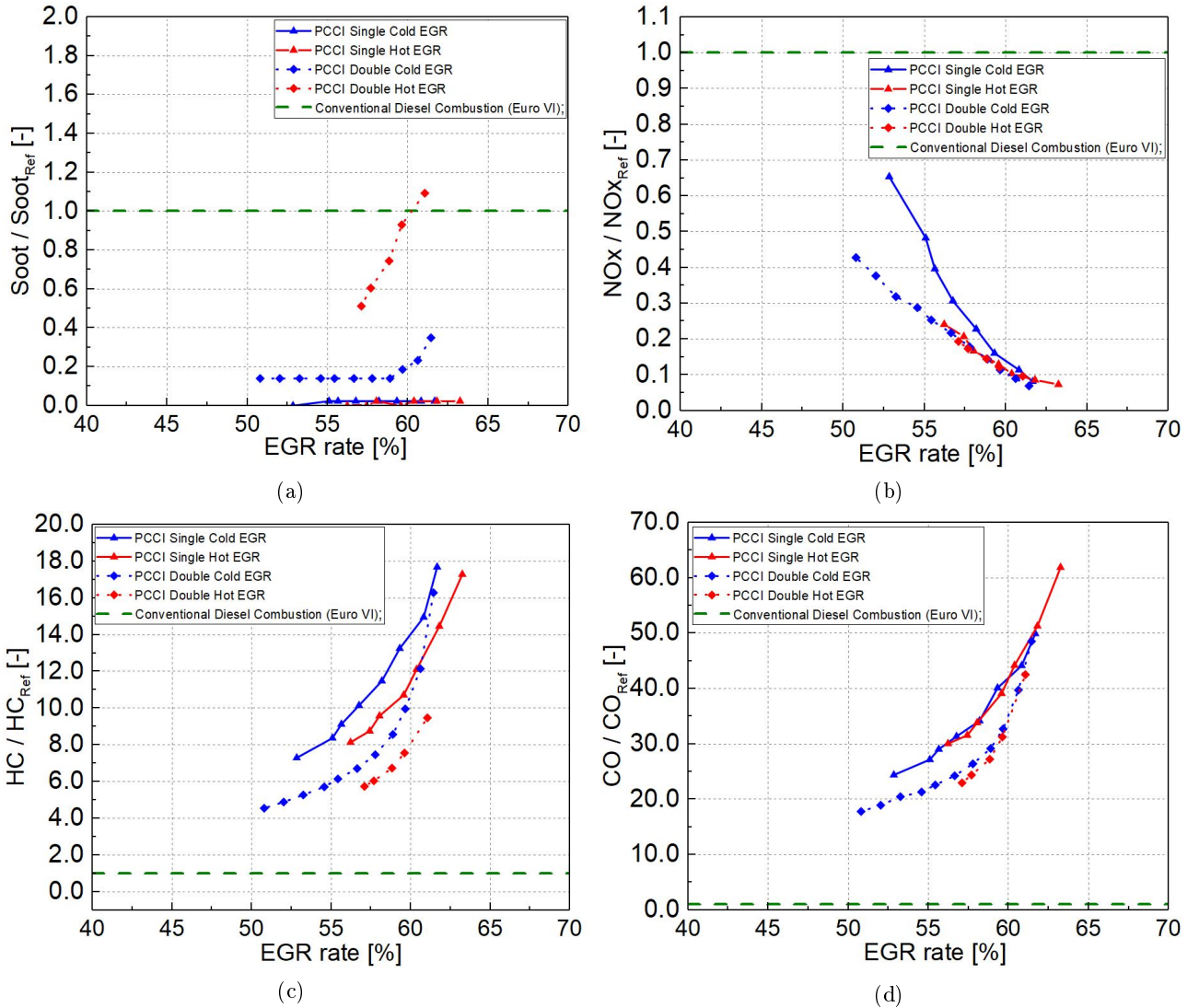


Figure 6.10: Engine working point 1400x1.1, Double injection: (a) Normalized soot emissions as a function of EGR rate, (b) Normalized  $NO_x$  emissions as a function of EGR rate, (c) Normalized HC emissions as a function of EGR rate, (d) Normalized CO emissions as a function of EGR rate;

This underlined the fact that the second injection occurs after the start of HTO stage of first one, which could result in a reduced mixing time for the foremost leading to an augmented

production of PM [53]. Considering hot EGR, the additional soot penalties could be justified by the higher intake temperatures which further enhances pyrolysis reactions and so soot production. With reference to figure 6.10 (b) where  $NO_x$  emissions versus  $X_{EGR}$  are reported, comparable level of nitrogen oxides can be observed for whatever strategy. Focusing the attention on double injection result for similar EGR level, we can notice that a reduction of this pollutant is only obtained from the cooled EGR configuration, whereas the uncooled EGR layout features an almost overlapping curve. The general purpose of a double injection strategy is to reduce  $NO_x$  by smoothing combustion [56] and so lowering the in-cylinder peak temperature. In fact, this has been seen in the HRR trace in section 6.3.2, where a more gradual rate of heat release was observed with respect the corresponding single injection. This behavior is true for both EGR approaches, however, in case of hot EGR, the increase in intake charge temperature could be detrimental to abate nitrogen oxides reaction rate and this could explain the coincident trend between the different injection pattern implemented. Figure 6.10 (c) and 6.10 (d) depict curve of HC and CO against EGR rate, and making a comparison in terms of EGR typology they show an analogous tendency to that of single injection, i.e., a reduction of HC and almost no difference for CO. Instead, comparing the injection strategies a significant diminution in unburned hydrocarbon and CO emissions can be noticed. This could be attributed to the simultaneous deterioration of over-mixing and bulk quenching as well as a better combustion phasing which, all together, could be responsible for CO and HC attenuation as well as the previously discussed improvement of fuel consumption. An additional effect of splitting the injection fuel is to mitigate the wall quenching phenomenon, because of the lower amount of fuel entering the cylinder with the first injection compared to a single injection event that diminished the quantity of fuel impinging on the piston top.

Figures 6.11 show pollutant emissions results versus EGR rate, considering the engine key-point 2000x2.3 (rpm x bar) working with double injection strategy. In different manner from the other engine working point, smoke emissions, displayed in figure 6.11 (a), remain unaffected by the adoption of a double stage injection in both EGR strategies. A possible reason behind this behavior could be found considering again the interaction between the two injection and the resulting HRR shape seen in section 6.3.2. As said, for this working point HRR trend for single and double injection resemble each other in opposite way to 1400x1.1 key-point. After LTO stage a single peak is present meaning that first injection hot flames stage do not occur before the second injection shot takes place. This could give an augmented amount of time for mixture formation since lower temperature and pressure are encountered by the fuel. Therefore, an enhanced fuel-air mixing is achieved playing a major role in preventing soot formation. Considering figure 6.11 (b),  $NO_x$  emissions for double injection results in similar trend versus  $X_{EGR}$  and no significant variation of their level for hot EGR, while, for cold EGR a little increase can be observed. The latter could be related to the variation of combustion phasing which, in similar fashion to what happens varying injection timing, could mitigate or magnify the combustion peak temperature.

As far as, HC emissions are concerned, figure 6.11 (c) shows an almost specular pattern between different injections strategies for both EGR approaches, and this could be justified with similar considerations done about single injection. Instead, concerning CO emissions in figure 6.11 (d), when implementing double injection stage a substantial abatement can be observed for cold EGR approach, while this is not the case for hot EGR. The latter fact could be explained comparing the heat release trend of single and double injection for the corresponding EGR strategies shown into figure 6.14 (a) in the following section. As it will be seen, for uncooled EGR, HRR is rather similar in terms of peak and shape for either injection patterns, while a substantial variation is encountered for cooled EGR.

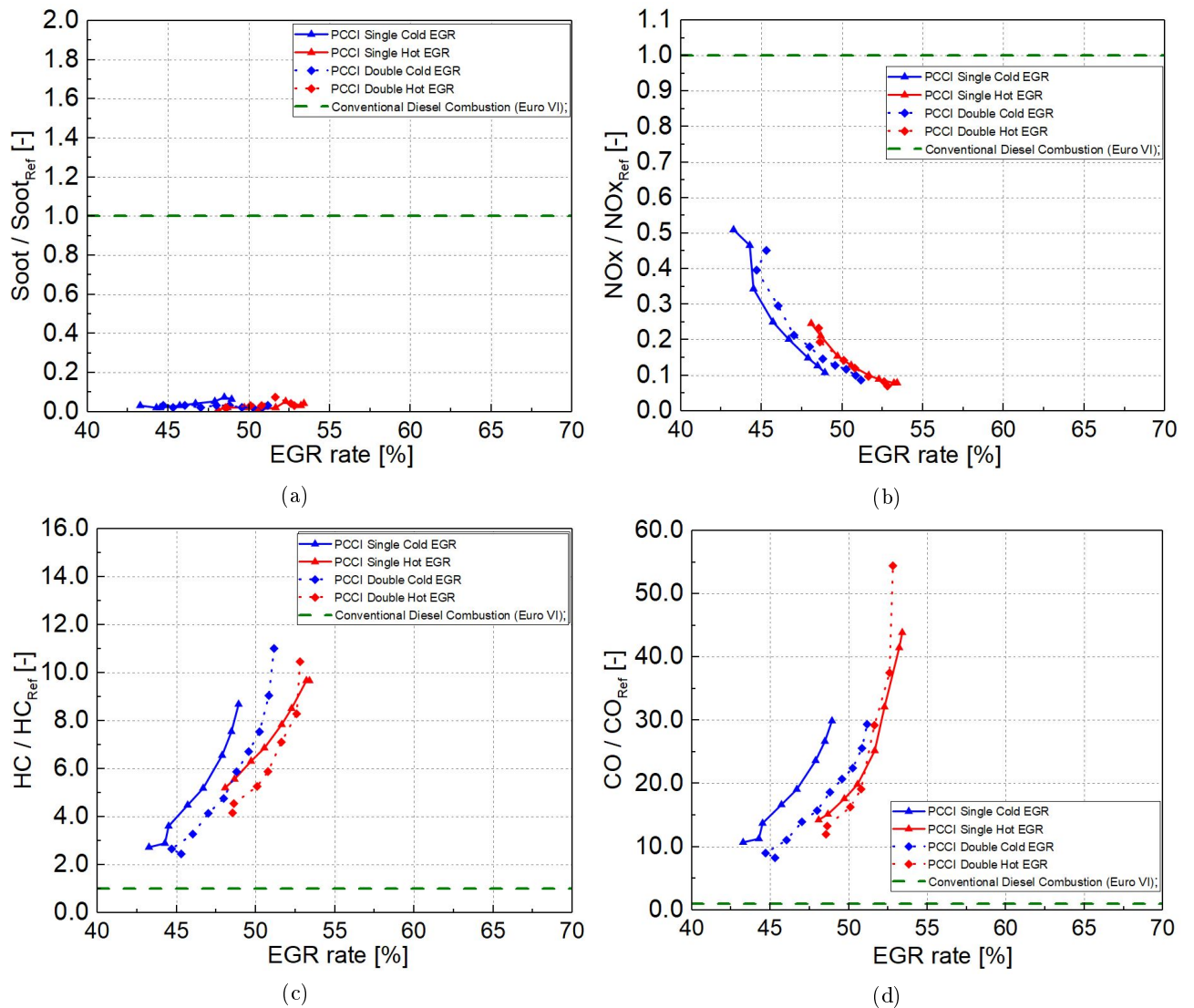


Figure 6.11: Engine working point 2000x2.3, Double injection: (a) Normalized soot emissions as a function of EGR rate, (b) Normalized  $NO_x$  emissions as a function of EGR rate, (c) Normalized HC emissions as a function of EGR rate, (d) Normalized CO emissions as a function of EGR rate;

### 6.3.4 Trade-offs

The current section presents EGR trade-off graphs regarding the previously discussed engine performance quantities and pollutant emissions. Results gathered on both engine key-points are illustrated giving a comparison between all the injection and EGR strategies implemented, so as to provide a complete picture on the achievable improvements in terms of performance and emissions, with particular focus to that brought by the uncooled and cooled EGR utilization. Since the herein experimental investigation concerns PCCI combustion on a devoted engine layout, together with the well-known conventional diesel EGR trade off curves bsfc- $NO_x$  and soot- $NO_x$ , carbon monoxide and unburned hydrocarbon trade-offs are reported. This choice was done considering the peculiar emissions characteristics of low temperature combustion modes which, differently from CDC, feature high amount of CO and HC emissions. Moreover, in section 6.3.3 it has been observed how there exists an EGR trade-off relationship between nitrogen oxides and the latter pollutants. Even though, combustion noise level has a decreasing trend versus EGR in similar fashion to nitrogen oxides, noise- $NO_x$  trade off graph is also illustrated to understand the influence of injection and EGR configurations on this performance parameter. Graphs of heat release rate and mean in-cylinder pressure corresponding to a judicious selection of optimal  $X_{EGR}$  for each working configuration are shown in order to furnish additional information on the analyzed trade-off trends. The comparison among the diverse approaches is obviously addressed considering the potential emissions reduction and performance improvements for a fixed level of  $NO_x$ .

#### Key-point 1400x1.1

Figures 6.12 and 6.13 depicts EGR trade-off curve for the engine key-point 1400x1.1 (rpm x bar). Looking at figures 6.12 (a) and (b), double injection results to be beneficial in terms of fuel consumption while the opposite occurs considering soot emissions. The reduction of fuel consumption due to double injection was previously justified with the change in combustion phasing which can now be visualized in figure 6.14. Among all the strategies, the choice of cold EGR double stage injection approach could give substantial advantages for bsfc and contained penalties regarding smoke emissions. Concerning CO and HC emissions trends in figure 6.12 (a) and (b), still double injection presents lower emissions levels in the same  $NO_x$  range, and hot EGR double injection configuration provides some additional benefits for HC emissions with respect the cold layout, whereas almost no difference is present for CO. As discussed, the effect of increased the inlet charge temperature brought from uncooled EGR seems not to be considerable for this working point, therefore not allowing a relevant attenuation of over-mixing and bulk quenching mechanisms. Moreover, this effect is counterbalanced from the larger inlet oxygen dilution, which carbon monoxide is very sensible to.

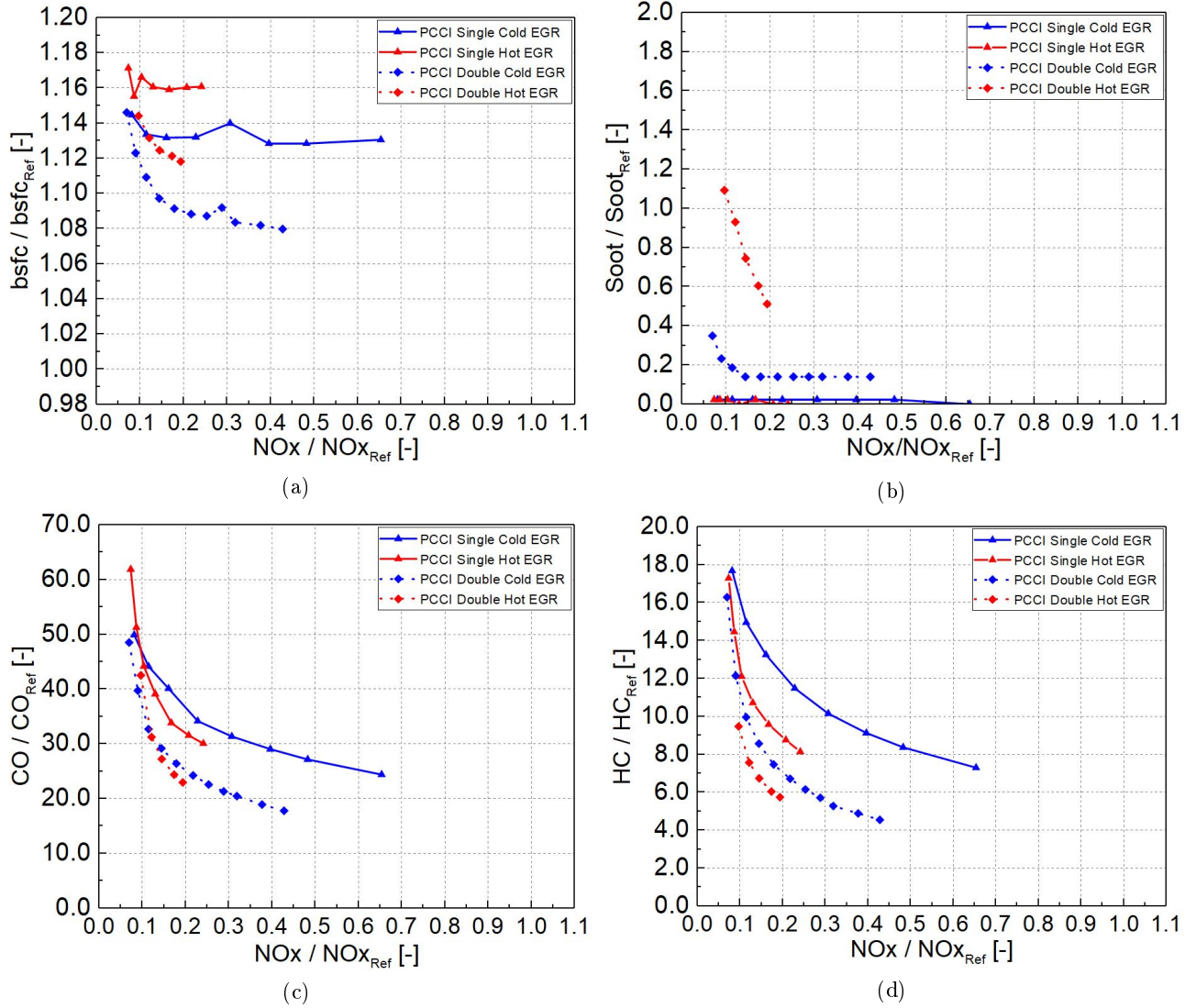


Figure 6.12: Engine working point 1400x1.1, Single-Double injection, EGR trade-off curves: (a) Normalized brake specific fuel consumption versus normalized  $NO_x$  emissions, (b) Normalized soot emissions versus normalized  $NO_x$  emissions, (c) Normalized CO emissions versus normalized  $NO_x$  emissions, (d) Normalized HC emissions versus normalized  $NO_x$  emissions;

In figure 6.13 noise- $NO_x$  trade off curves are plotted. Regardless of the EGR implementation, double injection strategy features an important noise level reduction, resulting from the smoother pressure increase and the diminished peak firing pressure, which could be seen in figure 6.14. The same figure could also justify the fact that looking for an optimal quantity of recirculated exhaust gas, hot EGR could provide a comparable or lower combustion noise level for reduced  $X_{EGR}$ , i.e., slightly higher  $NO_x$ .

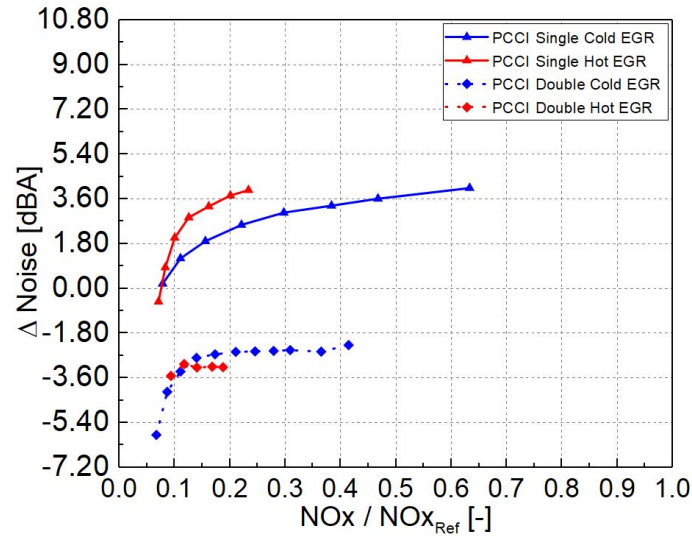


Figure 6.13: Engine working point 1400x1.1, Single-Double injection, EGR trade-off curve: Noise level variation versus normalized  $NO_x$  emissions;

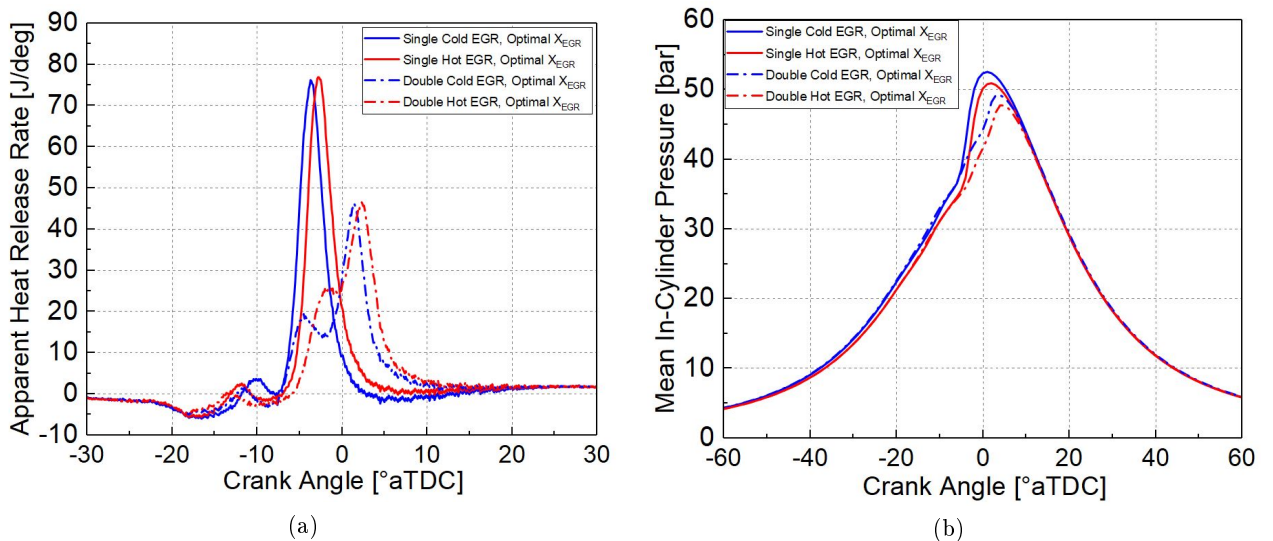


Figure 6.14: Engine working point 1400x1.1, Single-Double injection, Optimal trade-off points: (a) Apparent heat release rate versus crank angle position for optimal EGR quantity, (b) Mean in-cylinder pressure versus crank angle position for optimal EGR quantity;

### Key-point 2000x2.3

Figures 6.15 and 6.16 depict EGR trade-off curves for the engine key-point 2000x2.3 (rpm x bar). As described in sections 6.3.2, the implementation of double injection provides benefits in terms of engine fuel consumption for either EGR typologies, as shown in figure 6.15 (a), and this was attributed to the slightly retarded and improved combustion phasing which can now be visualized in figure 6.17. In choosing the most beneficial strategy no substantial bsfc value

difference is encountered among the EGR approaches resulting from double injection and both of them could be selected depending on the other trade-offs. As already pointed out in 6.3.3, on this engine working point, soot emissions resulted to be not influenced to any degree by the  $X_{EGR}$ , as depicted in figure 6.15 (b). In fact, they remained close to almost a zero level for all the working conditions analyzed, giving more freedom in the selection of the proper approach. Figure 6.15 (c) and 6.15 (d) report  $CO-NO_x$  and  $HC-NO_x$  trade-off, respectively. As it can be observed double injection hot EGR strategy is the most promising approach to simultaneously obtain carbon monoxide and unburned hydrocarbon reduction. This could put again in evidence how, when hot EGR is employed on this engine key-point, the effect of higher inlet charge temperature prevails on intake dilution leading to an enhancement HC and CO oxidation reactions with the least penalties in terms of  $NO_x$ .

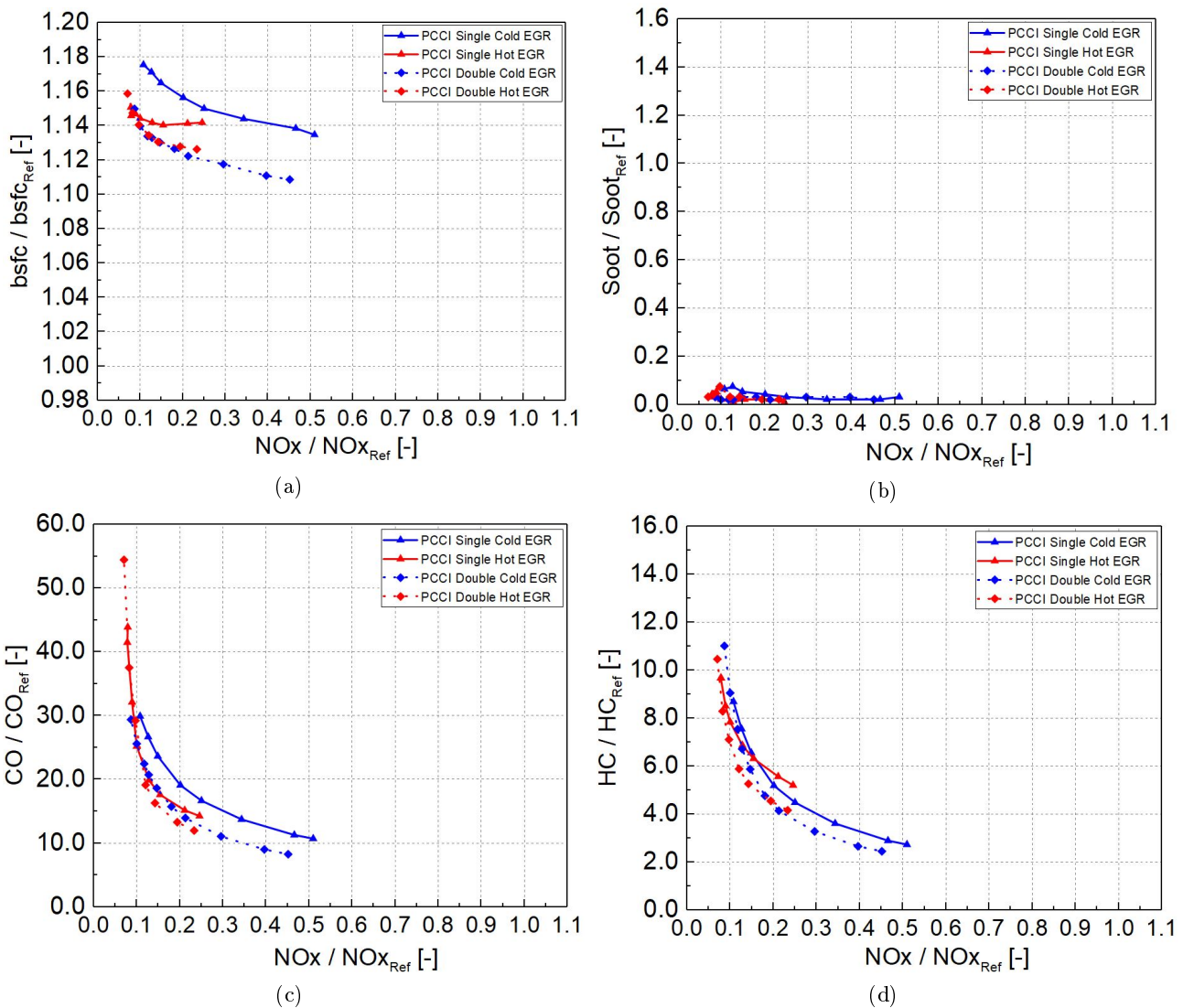


Figure 6.15: Engine working point 2000x2.3, Single-Double injection, EGR trade-off curves: (a) Normalized brake specific fuel consumption versus normalized  $NO_x$  emissions, (b) Normalized soot emissions versus normalized  $NO_x$  emissions, (c) Normalized CO emissions versus normalized  $NO_x$  emissions, (d) Normalized HC emissions versus normalized  $NO_x$  emissions;

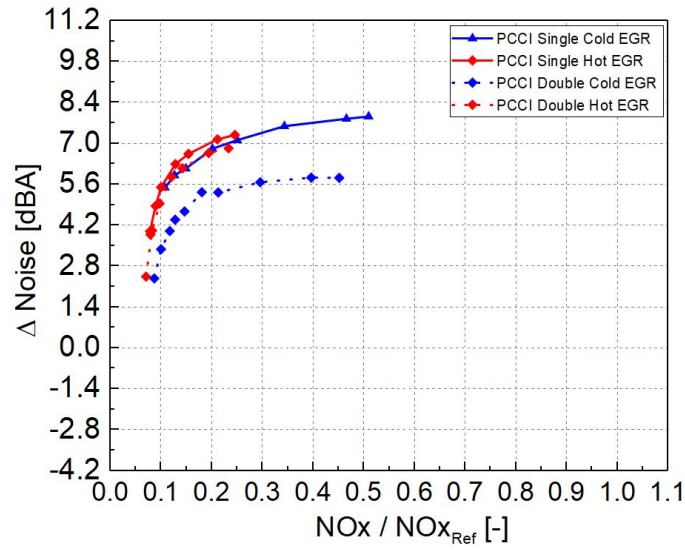


Figure 6.16: Engine working point 2000x2.3, Single-Double injection, EGR trade-off curve: Noise level variation versus normalized  $NO_x$  emissions;

Regarding combustion noise EGR trade-off curves in figure 6.16, a substantial reduction of noise level could be seen for double injection cold EGR with respect the corresponding single injection pattern. Instead, focusing the attention on hot EGR strategies the diminution is far more attenuated with respect to single injection and it fairly overlaps with it. Indeed, figure 6.17 (b) could confirm how similar their in-cylinder pressure trends are in terms of rate of pressure rise and peak firing pressure.

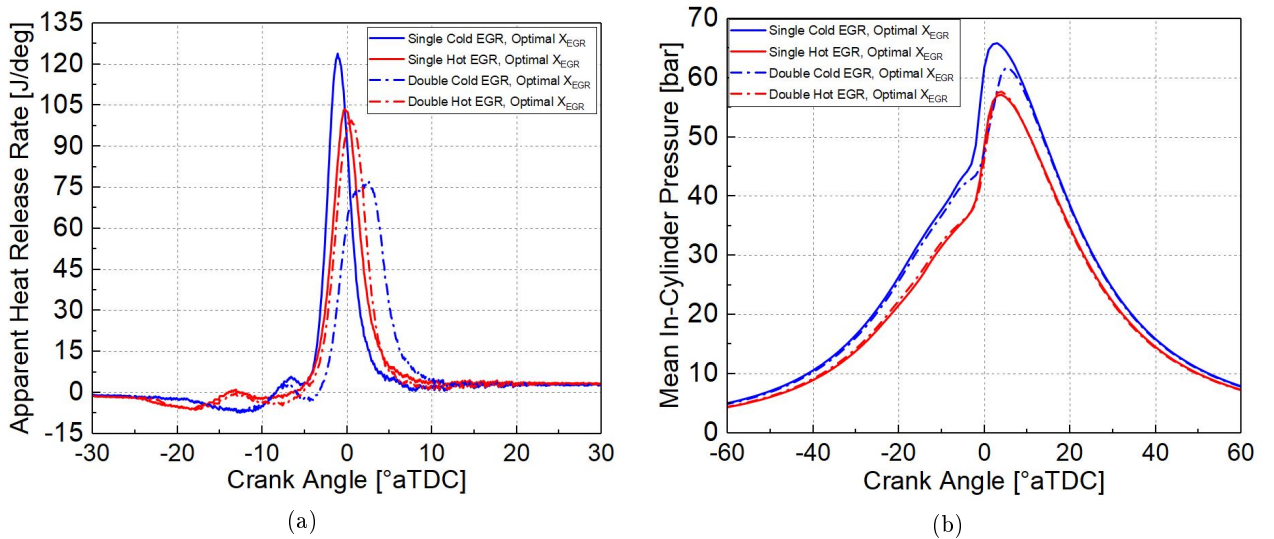


Figure 6.17: Engine working point 2000x2.3, Single-Double injection, Optimal trade-off points: (a) Apparent heat release rate versus crank angle position for optimal EGR quantity, (b) Mean in-cylinder pressure versus crank angle position for optimal EGR quantity;

### 6.3.5 DOC conversion efficiency

This last section wants to highlight how the uncooled EGR approach affects the performance of the diesel oxidation catalyst (DOC) installed in this experimental engine layout. The outcomes of the analysis will be presented by making a distinction between single and double injection strategies, while trends of the two investigated working points are reported separately for exhaust temperatures before and after DOC, and on the same graph for engine-out exhaust gas temperature and hydrocarbon conversion efficiency. The latter efficiency parameter was computed considering the following equation:

$$\eta_{HC} = \frac{[HC]_{in} - [HC]_{out}}{[HC]_{in}} \quad (6.1)$$

where  $[HC]_{in}$  is the unburned hydrocarbon concentration upstream the DOC (engine-out value) and  $[HC]_{out}$  represents the hydrocarbon concentration downstream the diesel oxidation catalyst (tail-pipe value).

Test data regarding CO emissions level downstream diesel oxidation catalyst could not be gathered due to a malfunctioning detected on the AVL AMAi60 emission analyzer train placed after the after-treatment device. In regard of that, previous research studies on DOC effectiveness proved comparable values of conversion efficiency between the two pollutants [57, 39], therefore, similar outcomes could have been expected even in this experimental investigation.

#### Single stage injection

In figure 6.18 (a) single injection engine-out exhaust gas temperature measured in exhaust runner of cylinder No.4 are reported as a function of  $X_{EGR}$  for two investigated engine key-points. Regardless of the analyzed engine working condition and of the EGR approach implemented, as the amount of recirculated gas is incremented the exhaust temperature tends to linearly increase. When cooled EGR is adopted, being the intake charge temperature maintained roughly constant by intercooler and EGR cooler, the observed increase in temperature could be justified from delayed combustion event which corresponds to higher temperature at the end of the expansion stroke. Instead, employing hot EGR means not only to have an higher range of temperature but also a more pronounced increase versus  $X_{EGR}$  with respect to the cold case. Being the recirculated gas not cooled, as seen in section 6.3.1, the intake charge temperature increases with the EGR level leading to higher in-cylinder and exhaust working temperature, moreover the effect of combustion phasing retard is still maintained, adding up its contribution to the increase of the exhaust gas temperatures. Figures 6.18 (b) and 6.19 (a) shows the variation of exhaust gas temperature before and after the diesel oxidation catalyst against EGR level variation for engine key point 1400x1.1 and 2000x2.3, respectively, and for the different EGR strategies.

The temperature increment of the exhaust gas stream downstream the DOC is an indication that the after-treatment is operational, i.e., exothermic oxidation reactions of HC and CO are taking place heating up the exhaust gas mixture.

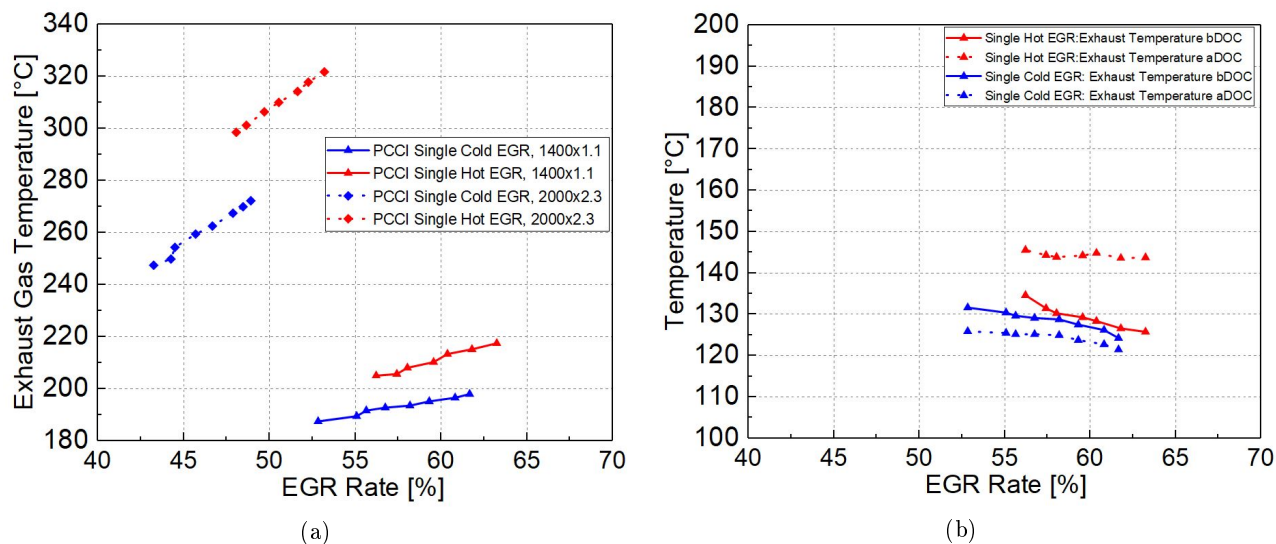


Figure 6.18: (a): Engine-out exhaust gas temperature (cylinder 4) as a function of EGR rate, (b): Exhaust gas temperature before and after diesel oxidation catalyst as a function of EGR rate at 1400x1.1;

This behavior can be observed when hot EGR is employed on both points of the engine map, whereas no relevant increase of temperature is seen when the recirculated exhaust gas are cooled. Moreover, focusing the attention on point 2000x2.3, when hot EGR is utilized the exhaust temperature downstream the oxidation catalyst featured an almost linear increase with EGR rate, which could be due to the larger amount of unburned hydrocarbons and carbon monoxide fed to the DOC. Figure 6.19 (b) reports the values of DOC conversion efficiency regarding HC. The trends confirm the indications given by the temperature data and put in evidence a significant aspect regarding the use of hot EGR to improve the DOC conversion efficiency. Considering point 1400x1.1, it can be seen that the catalyst is not able to provide any sensible HC reduction and efficiency approach the zero value. When the engine is running at the 2000x2.3 working point, the effect of higher working temperatures due to the augmented load, magnify the increase in inlet charge temperature when hot EGR is implement. As a consequence of that, during uncooled EGR operations the catalyst reaches its light-off temperature which causes conversion efficiency of about 95% with respect the 20% value reached with cooled EGR. Taking into account the typical high HC and CO emissions level coming from PCCI combustion, this could be one of the major benefits of hot EGR, which, nonetheless, seems to be engine load dependent.

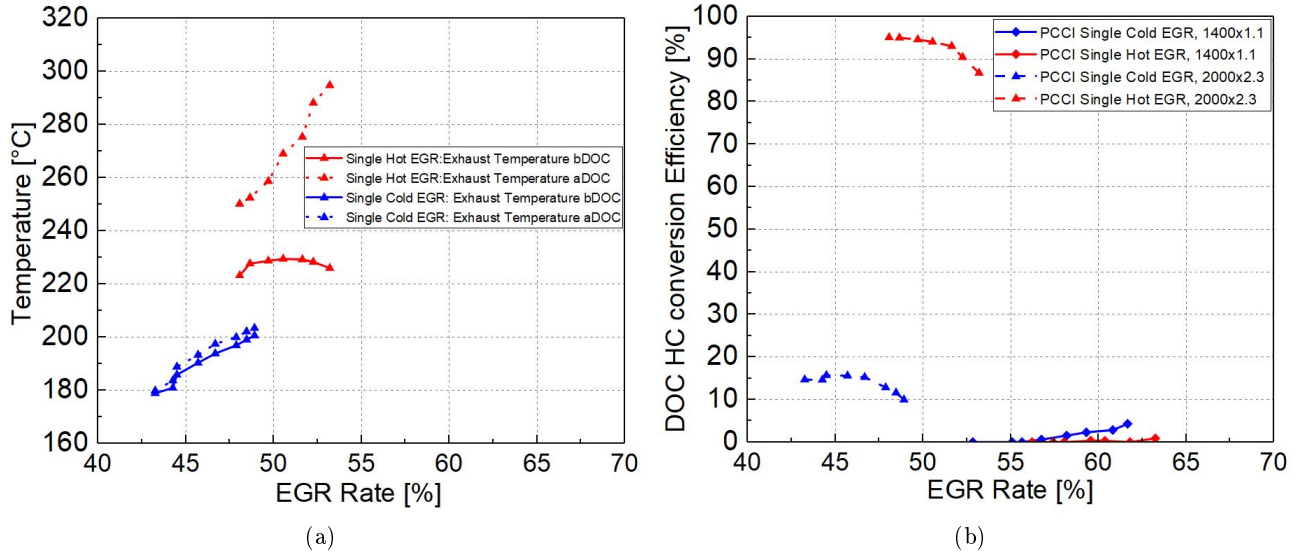


Figure 6.19: (a): Exhaust gas temperature before and after diesel oxidation catalyst as a function of EGR rate at 2000x2.3, (b): Diesel oxidation catalyst HC conversion efficiency as a function of EGR rate;

### Double stage injection

In figure 6.20 (a) double injection engine-out exhaust gas temperature measured in exhaust runner of cylinder No.4 are reported as a function of  $X_{EGR}$  for two investigated engine key-points.

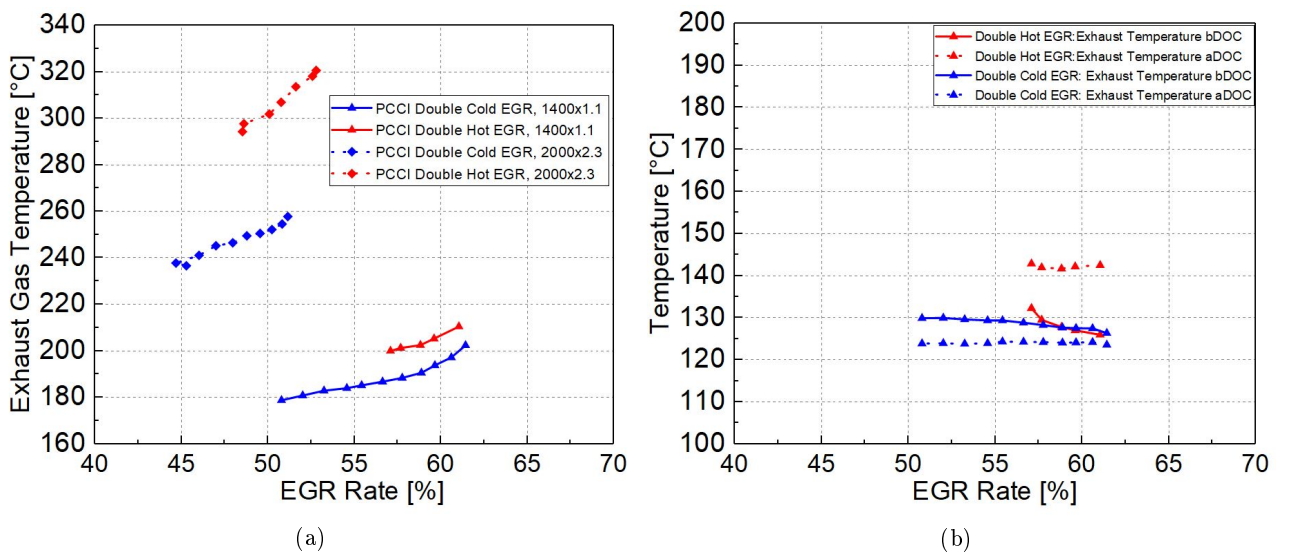


Figure 6.20: (a): Engine-out exhaust gas temperature (cylinder 4) as a function of EGR rate, (b): Exhaust gas temperature before and after diesel oxidation catalyst as a function of EGR rate at 1400x1.1;

With respect to the single injection results no variation in exhaust gas temperature trends is noticed, however, being combustion smoothed and HRR peak diminished by double injection, a minor range reduction in the achieved temperature could be found, except for point 2000x2.3 in hot configuration where the lowering is almost negligible. Looking at figures 6.20 (b) and 6.21 (a) in which curves of exhaust gas stream temperature before and after DOC are reported, we can observe that they follow the same pattern seen for single injection, i.e., a relevant increase in temperature after the catalyst is experienced just for uncooled configuration with point 2000x2.3. In similar fashion to the previous analyzed injection strategy, the conversion efficiency trends reported in figure 6.21 shows a correspondence between the temperature aDOC (after DOC) rise and the high value of DOC efficiency for both engine key points. Once again, the utilization of hot EGR is able to produce significant improvement in terms of tail pipe HC abatement with respect to the cooled approach only for an engine working point whose load level is not too low.

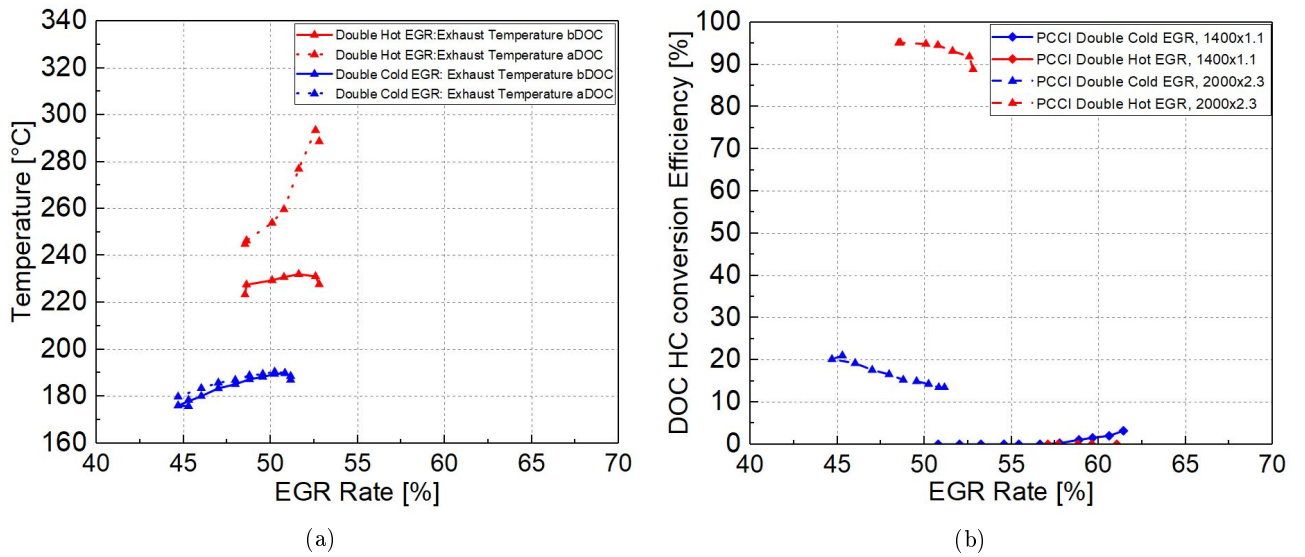


Figure 6.21: (a): Exhaust gas temperature before and after diesel oxidation catalyst as a function of EGR rate at 2000x2.3, (b): Diesel oxidation catalyst HC conversion efficiency as a function of EGR rate;

# Conclusion

This experimental investigation aims to comprehend the effect of exhaust gas recirculation strategy on the performance and the emissions, at steady-state conditions, on an FPT Industrial manufactured engine (F1C) with a modified layout to better suit PCCI low temperature combustion mode. The study concerned EGR sweep tests on two engine key points (1400x1.1 and 2000x2.3) with cooled and uncooled EGR engine configurations, involving with the installation of the EGR cooler or the substitution of the latter with a properly designed pipe, respectively. Moreover, the analysis was performed considering two different injection strategies, i.e., single stage and double stage injection both of which have been previously explored in other calibration activity. The main results coming from this research study are summarized as detailed below:

- bsfc was characterized by an engine point dependence, since the uncooled EGR approach was seen to be substantially beneficial in case of single injection 2000x2.3 engine key-point, whereas the opposite happens for 1400x1.1. In addition, double injection improved fuel consumption providing a reduction in a range of 2÷3 % and maintaining almost a specular trends to single injection case when operating with hot or cold EGR approaches. For the lower load working point, cold EGR layout with double injection resulted to be the most effective, while for the other engine key-point comparable bsfc values have been found among the two EGR strategies when the engine is operated with double injection approach;
- Uncooled EGR approach was noticed to be detrimental for combustion noise reduction, with the only exception for the engine key-point 1400x1.1 in which similar noise levels to those of cooled case have been experienced when the engine was run with double injection pattern.
- Particulate matter emissions were seen to be EGR approach insensitive and featuring almost soot-free emission levels for the engine working point 2000x2.3. This was not the case of 1400x1.1, in which the different injection strategy influenced the mixing process going from near to zero-level of PM emissions with single strategy to a substantial increase with double stage approach. In the latter operating mode, uncooled approach resulted to further worsen the mixing process leading to the highest emission values among all the implemented strategies;

- Hot EGR layout was able to bring noticeable benefits in terms of engine-out unburned HC and CO emissions since a simultaneous reduction of latter emissions were experienced for both engine working points regardless of the injection strategy, and, in particular, with a greater extent for the engine key-point 2000x2.3. Moreover, among the two injection patterns, in both engine speed and load tested conditions, double stage injection approach permitted to achieve larger HC and CO abatement;
- The values of hydrocarbon conversion efficiency of the installed DOC featured a 70% improvement when going from cold to hot EGR strategy for the engine key-point 2000x2.3 for both injection patterns. Instead, when a lower load was tested (1400x1.1) no beneficial effects came from the increased exhaust gas temperature achieved with uncooled approach, resulting in poor catalyst efficiency for all the operating strategies of the engine;

Future testing activity could be done with the idea of exploring a larger portion of the engine map, in order to gain further insight on the possible application of hot EGR approach for engines operating under PCCI combustion mode, with the purpose of partly attenuate the common shortcomings associated to them. Apart from that, trying to find the right EGR strategy and the corresponding EGR rate which are capable of providing a sufficient abatement of unburned HC and CO, as well as acceptable values fuel consumption and combustion noise, depends on the engine key-point and on the trade-off among the different targets (i.e. pollutant emissions, bsfc and combustion noise). Furthermore, a fundamental role in achieving emissions complaint and efficient engines is played by the possible synergy between combustion strategies and the after-treatment devices installed in the exhaust line, rendering the work of nowadays engine calibrators more and more challenging and complicated.

# Bibliography

- [1] J. G. V. Franco, F. P. Sánchez, and P. Mock. *Real-World Exhaust Emissions from Modern Diesel Cars: A Meta- Analysis of Pems Emission Data from Eu (Euro 6) and us (Tier 2 Bin 5/Ulev Ii) Diesel Passenger Cars*. The International Council on Clean Transportation, 2014.
- [2] A.K. Agarwal, A.P. Singh, R.K. Maurya. *Evolution, Challenges and Path Forward for Low Temperature Combustion Engines*. Elsevier, Progress in energy and combustion science 61, 1-56, 2017.
- [3] L. M. Pickett, D. L. Siebers. *Non-sooting, low flame temperature mixing-controlled DI diesel combustion*. SAE Technical Paper No. 2004-01-1399, 2004.
- [4] John B. Heywood. *Internal combustion engine fundamentals*. MC-GRAW HILL, 1988.
- [5] John B. Heywood. *Internal combustion engine fundamentals*. MC-GRAW HILL - Second Edition, 2018.
- [6] G. Ferrari. *Motori a combustione interna*. EDIZIONI Il Capitello, 2008.
- [7] Federico Millo. *Engine Emission Control*. MSc in Automotive Engineering, Politecnico di Torino, 2017.
- [8] Ezio Spessa. *Design of Engine*. MSc in Automotive Engineering, Politecnico di Torino, 2017.
- [9] G. M Faeth. *Current status of droplet and liquid combustion*. Prog. Energy Combust. Sci., Vol. 3, pp. 191-224, 1977.
- [10] John E. Dec. *A conceptual model of DI diesel combustion based on laser-sheet imaging*. SAE Technical Paper No. 970873, 1997.
- [11] Espey C. and John E. Dec. *Diesel engine combustion studies in a newly designed optical-access engine using high speed and 2-D laser imaging*. SAE Transactions, Vol. 102, Sec. 4, pp. 703-723, Paper No. 930971, 1993.
- [12] John E. Dec, C. Espey. *Ignition and early soot formation in a DI diesel engine using multiple 2D imaging diagnostics*. SAE Technical Paper No. 950456, 1995.

- [13] John E. Dec, E.B. Coy. *OH radical imaging in a DI diesel engine and the structure of the early diffusion flame*. SAE Technical Paper No. 960831 , 1996.
- [14] John E. Dec, C. Espey, T.A. Litinger, D.A. Santavicca. *Planar laser Rayleigh scattering for quantitative vapor-fuel imaging in a diesel jet*. Combustion and Flame No.109 , 1997.
- [15] P.F. Flynn, R.P. Durrett, G.L. Hunter, A.O. Zur Loye, O.C. Akinyemi, J.E. Dec, C.K. Westbrook. *Diesel combustion: An integrated view combining laser diagnostics, chemical kinetics, and empirical validation*. SAE Technical Paper No. 1999-01-0509, 1999.
- [16] John E. Dec, Robert E. Canaan. *PLIF imaging of NO formation in a DI diesel engine*. SAE Technical Paper No. 980147, 1998.
- [17] W. Addy Majewski, Hannu Jääskeläinen. *Exhaust particulate matter*. DieselNet technology guide, 2018.
- [18] David B. Kittelson. *Engines and nanoparticles: A review*. J. Aerosol Sci. Vol 29, No. 5/6, pp. 575-588, 1998.
- [19] Peter L. Kelly-Zion, John E. Dec. *The effects of injection timing and diluent addition on late-combustion soot burnout in a DI diesel engine based on simultaneous 2-D imaging of OH and soot*. SAE Technical Paper No. 2000-01-0238, 2000.
- [20] Dale R. Tree, John E. Dec. *Diffusion-flame/wall interactions in a heavy-duty DI diesel engine*. SAE Technical Paper No. 2001-01-1295, 2001.
- [21] N. Watson, M. S. Janota. *Turbocharging the internal combustion engine*. Palgrave - The Macmillan press, 1982.
- [22] H. Jääskeläinen, M. K. Khair. *Exhaust gas recirculation*. DieselNet Technology Guide, 2016.
- [23] N. Ladommatos, S. M. Abdelhalim, H. Zhao, Z. Hu. *The Dilution, Chemical, and Thermal Effects of Exhaust Gas Recirculation on Diesel Engine Emissions - Part 1: Effect of Reducing Inlet Charge Oxygen*. SAE Technical Paper No. 961165, 1996.
- [24] N. Ladommatos, S. M. Abdelhalim, H. Zhao, Z. Hu. *The Dilution, Chemical, and Thermal Effects of Exhaust Gas Recirculation on Diesel Engine Emissions - Part 2: Effects of Carbon Dioxide*. SAE Technical Paper No. 961167, 1996.
- [25] N. Ladommatos, S. M. Abdelhalim, H. Zhao, Z. Hu. *The Dilution, Chemical, and Thermal Effects of Exhaust Gas Recirculation on Diesel Engine Emissions - Part 3: Effects of Water Vapour*. SAE Technical Paper No. 971659, 1997.
- [26] N. Ladommatos, S. M. Abdelhalim, H. Zhao, Z. Hu. *The Dilution, Chemical, and Thermal Effects of Exhaust Gas Recirculation on Diesel Engine Emissions - Part 4: Effects of Carbon Dioxide and Water Vapour*. SAE Technical Paper No. 971660, 1997.

- [27] D. L. Siebers, B. Higgins, L. Pickett. *Flame Lift-Off on Direct-Injection Diesel Fuel Jets: Oxygen Concentration Effects*. SAE Technical Paper No. 2002-01-0890, 2002.
- [28] H. Jääskeläinen, M. K. Khair. *EGR systems and components*. DieselNet Technology Guide, 2019.
- [29] W. A. Majewski, M. K. Khair. *Diesel emissions and their control*. SAE International, 2006.
- [30] R. M. Wagner, J. B. Green, Jr., J. M. Storey, C. S. Daw *Extending Exhaust Gas Recirculation Limits in Diesel Engines*. Oak Ridge National Laboratory, 2000.
- [31] A. McIlroy, G. McRae, V. Sick, D. L. Siebers, C. K. Westbrook, P. J. Smith, C. Taatjes, A. Trouve, A. F. Wagner, E. Rohlfing, D. Manley, F. Tully, R. Hilderbrandt, W. Green, D. Marceau, J. O’Neal, M. Lyday, F. Cebulski, T. R. Garcia, D. Strong. *Basic research needs for clean and efficient combustion of 21st century transportation fuels*. U.S. Department of energy - office of scientific and technical information ,935428, 2006.
- [32] John E. Dec. *Advanced compression-ignition engines - understanding the in-cylinder processes*. Elsevier, Proceedings of the combustion institute 32, 2727-2742, 2009.
- [33] Mark P.B. Musculus, Paul C. Miles, Lyle M. Pickett. *Conceptual models for partially premixed low-temperature diesel combustion*. Elsevier, Progress in energy and combustion science 39, 246-283, 2013.
- [34] FPT Industrial. *F1C User Handbook*. 2013.
- [35] AVL. *AMAi60 emission test system User’s Guide*. 2008.
- [36] W. L. Hardy, R. D. Reitz. *A study of the effects of high EGR, high equivalence ratio, and mixing time on emissions levels in a heavy-duty diesel engine for PCCI combustion*. SAE Technical Paper No. 2006-01-0026, 2006.
- [37] S. d’Ambrosio, A. Ferrari. *Effects of exhaust gas recirculation in diesel engine featuring late PCCI type combustion strategies*. Elsevier, Energy conversion and management, Volume 105, 2015.
- [38] J. Hoard, M: Abarham, D. Styles, J. M. Giuliano, C. S. Sluder, J.M.E. Storey. *Diesel EGR Cooler Fouling*. SAE Technical Paper No. 2008-01-2475, 2008.
- [39] D’Ambrosio S., Gaia F., Iemmolo D., Mancarella A. et al. *Performance and Emission Comparison between a Conventional Euro VI Diesel Engine and an Optimized PCCI Version and Effect of EGR Cooler Fouling on PCCI Combustion*. SAE Technical Paper No. 2018-01-0221, 2018.
- [40] M. Abarham, J. Hoard, D. Assanis, D. Styles, E. W. Curtis, N. Ramesh. *Review of Soot Deposition and Removal Mechanisms in EGR Coolers*. SAE Technical Paper No. 2010-01-1211, 2010.

- [41] R. Kiplimo, E. Tomita, N. Kawahara, S. Yokobe. *Effects of spray impingement, injection parameters, and EGR on the combustion and emission characteristics of a PCCI diesel engine*. Applied Thermal Engineering, Volume 37, Pages 165-175, 2012.
- [42] S. Kook, C. Bae, P.C. Miles, D. Choi, L.M. Pickett. *The Influence of Charge Dilution and Injection Timing on Low- Temperature Diesel Combustion and Emissions*. SAE Technical Paper No. 2005-01-3837, 2005.
- [43] Yuwei Zhao, Ying Wang, Dongchang Li, Xiong Lei, Shenghua Liu. *Combustion and emission characteristics of a DME (dimethyl ether)-diesel dual fuel premixed charge compression ignition engine with EGR (exhaust gas recirculation)*. Elsevier, Energy, Volume 72, Pages 608-617, 2014.
- [44] N. Ladommatos, S. M. Abdelhalim, H. Zhao, Z. Hu. *The Effects on Diesel Combustion and Emissions of Reducing Inlet Charge Mass Due to Thermal Throttling with Hot EGR*. SAE Technical Paper No. 980185, 1998.
- [45] S. Simescu, T. W. Ryan III, G- D. Neely, A. C. Matheaus B. Surampudi. *Partial Pre-Mixed Combustion with Cooled and Uncooled EGR in a Heavy-Duty Diesel Engine*. SAE Technical Paper No. 2002-01-0963, 2002.
- [46] Shim E.J., Park H., Bae C. *Effects of Hot and Cooled EGR for HC Reduction in a Dual-Fuel Premixed Charge Compression Ignition Engine*. SAE Technical Paper No. 2018-01-1730, 2018.
- [47] S. Zeraati-Rezaei, Y. Al-Qahtani, H. Xu. *Investigation of hot-EGR and low pressure injection strategy for a Dieseline fuelled PCI engine*. Fuel, Volume 207, Pages 165-178, 2017.
- [48] M. D. Boot, C. C. M. Luijten, L. M. T. Somers, U. Eguz and D. D. T. M. van Erp, A. Albrecht, R. S. G. Baert. *Uncooled EGR as a Means of Limiting Wall-Wetting under Early Direct Injection Conditions*. SAE Technical Paper No. 2009-01-0665, 2009.
- [49] Zhou L., Liu Y., Sun L., Hou H. et al. *Effect of Hot Exhaust Gas Recirculation on the Combustion Characteristics and Particles Emissions of a Pilot-Ignited Natural Gas Engine*. SAE Technical Paper No. 2013-01-1341, 2013.
- [50] A. Jain, A. P. Singh, A. K. Agarwal. *Effect of split fuel injection and EGR on NOx and PM emission reduction in a low temperature combustion (LTC) mode diesel engine*. Elsevier, Energy, Volume 122, Pages 249-264, 2017.
- [51] A.J. Torregrosa, A. Broatch, A. García, L.F. Mónico. *Sensitivity of combustion noise and NOx and soot emissions to pilot injection in PCCI Diesel engines*. Elsevier, Applied Energy, Volume 102, Pages 149-157, 2013.

- [52] G. D. Neely, S. Sasaki, J. A. Leet. *Experimental Investigation of PCCI-DI Combustion on Emissions in a Light-Duty Diesel Engine*. SAE Technical Paper No. 2004-01-0121, 2004.
- [53] N. Horibe, S. Harada, T. Ishiyama, M. Shioji. *Improvement of premixed charge compression ignition-based combustion by two-stage injection*. International Journal of Engine Research, 2009.
- [54] Korkmaz M., Zweigel R., Niemietz K., Jochim B. et al. *Assessment of Different Included Spray Cone Angles and Injection Strategies for PCCI Diesel Engine Combustion*. SAE Technical Paper No. 2017-01-0717, 2017.
- [55] T. Fuyuto, M. Taki, R. Ueda, Y. Hattori, H. Kuzuyama, T. Umehara. *Noise and Emissions Reduction by Second Injection in Diesel PCCI Combustion with Split Injection*. SAE Technical Paper No. 2014-01-2676, 2014.
- [56] Y. Park, C. Bae. *Influence of EGR and Pilot Injection on PCCI Combustion in a Single-Cylinder Diesel Engine*. SAE Technical Paper No. 2011-01-1823, 2011.
- [57] S. Katare, P. Laing. *Hydrogen in Diesel Exhaust: Effect on Diesel Oxidation Catalyst Flow Reactor Experiments and Model Predictions*. SAE Technical Paper No. 2009-01-1268, 2009.